STUDIES ON THE PERFORMANCE OF OUTDOOR OPTICAL WIRELESS SYSTEMS UNDER DIFFERENT ATMOSPHERIC CONDITIONS

A Thesis Submitted
In Partial Fulfillment of the Requirements
for the Degree of
Master of Technology

by

MANOJ SATLE

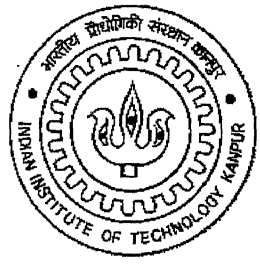

to the

DEPARTMENT OF ELECTRICAL ENGINEERING
INDIAN INSTITUTE OF TECHNOLOGY
KANPUR

JUNE 2004

CERTIFICATE

This is to certify that the thesis work entitled **"STUDIES ON PERFORMANCE OF OUTDOOR OPTICAL WIRELESS SYSTEMS UNDER DIFFERENT ATMOSPHERIC CONDITIONS"** submitted by Manoj Satle (Roll No.- Y210420) has been carried out under my supervision and the same has not been submitted elsewhere for a degree.

June, 2004

(Dr. Joseph John)
Professor
Department of Electrical Engineering
Indian Institute of Technology
KANPUR-208016

ABSTRACT

An optical wireless system is an alternate wireless system for high speed data transfer to combat the highly congested RF spectrum. Outdoor optical wireless systems are becoming more popular and gaining market acceptance as a functional wireless tool, because of their advantages such as, unlimited and unregulated spectrum, low cost, etc. One barrier which still exists in the acceptance for wide acceptance of OWC systems is the effect of weather on such systems. The performance of these systems are very much affected by the atmospheric attenuation due to non-stationary weather conditions viz. fog, haze, rain, etc. Of particular interest is the effect of fog as it causes absorption and scattering losses thereby giving higher optical power attenuation.

In this work a comprehensive review of the outdoor optical links is done and their major factures compared. Atmospheric attenuation is theoretically calculated using present models and is compared with experimental results under different fog conditions. An experimental outdoor optical link with 10Mbps data rate and length up to 60m is designed, implemented and tested. The transmitter uses a low cost laser diode and a TTL driver IC. The receiver uses BPX65 PIN photodiode with a JFET frontend preamplifier. Receiver uses a focusing lens to focus the laser light on the detector aperture.

ACKNOWLEDGMENTS

I am very much grateful to my Thesis Supervisor, **Dr. Joseph John**, for dedicating his valuable time and advice that he has given me while I have been at IIT, without whom, this dissertation would have not been possible. He has provided a solid basis for my studies.

I am especially thankful to my friend A.Sivabalan, for his excellent company and support during my work.

I would like to thank Mr. S. K. Kole and the staff of the PCB lab for making the PCBs on time.

I am also indebted to the authorities of Doordarshan, my parent Organization, who gave me nice opportunity to pursue M.Tech. Programme from IIT, Kanpur.

Finally, I would like to thank my parents for providing an example in life that is worthy to be followed.

- Manoj Satle

CONTENTS

CHAPTER 1

INTRODUCTION

Since the invention of radio, more and more of the electro-magnetic frequency spectrum has been used for business, the military, entertainment broadcasting and telephone communications. The radio spectrum is becoming severely overcrowded. There is little room left in the radio frequency spectrum to add more information transmitting channels. Moreover all the restrictions and regulations governing the transmission of information by radio have frustrated the companies and individuals. For this reason, many companies turned up toward light as a way to provide the needed room for communications expansion. By using modulated light as a carrier instead of radio, an almost limitless, and unregulated, spectrum becomes available. High modulation rate has fulfilled all of the typical radio, TV and business communications needs. However, with the addition of more light sources, each at a different wavelength, even more information channels could be added to the communication system without interference. Such an enormous information capacity is impossible with radio. A point-to-point outdoor optical link is shown in Fig.1.1.

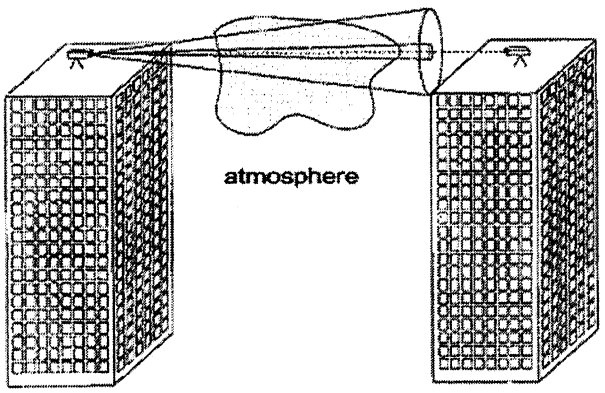

Figure 1.1 ***An example of optical wireless link***

Although light can be efficiently injected into tiny glass fibers (fiber optics) and used like copper cables to route the light information where it might be needed, there are many applications where only the space between the light information transmitter and the receiver is needed. This "freespace" technique requires only a clear line-of-sight path between the transmitter and the distant receiver to form an information link. No cables need to be buried, no complex network of switches and amplifiers are needed and no right-of-way agreements need to be made with landowners. Also, like fiber optic communications, an optical wireless technique has a very large information handling capacity. Very high data rates are possible from multiple color light sources. In addition, systems could be designed to provide wide area communications, stretching out to the distances of the kilometer order.

The only disadvantage of OWC systems over fiber is that laser power attenuation through the atmosphere is variable and difficult to predict, since it is weather dependent. This factor limits the link distance of free space optical systems. Using historical weather data collected at airports, the link availability as a function of distance can be predicted for many free space optical systems.

Atmospheric effects on laser beam propagation can be broken down into two categories: attenuation of the laser power and fluctuation of laser power due to laser beam deformation. Attenuation consists of absorption and scattering of the laser light photons by the different aerosols and gaseous molecules in the atmosphere. Atmospheric attenuation is typically dominated by Fog, Clouds, Rain, Snow, Smoke and dust. The attenuation due to rain and snow is generally significantly less. In case of transmission through Fog and cloud, it is clear that at some attenuation level the optical wireless communication system will cease to operate .Laser beam deformation occurs because of small-scale dynamic changes in the index of refraction of the atmosphere. This causes laser beam wander, laser beam spreading, and distortion of the wavefront or scintillation.

1.1 APPLICATIONS OF OPTICAL WIRELESS COMMUNICATIONS

Optical wireless communication can bridge the gap by enabling connection with offices, business facilities, and other targeted locations without relinquishing the performance parameters offered by Radio communication. Some of the short range, long range, and wide area applications are listed below.

Short Range Applications

- Industrial controls and monitors
- Museum audio; walking tours, talking homes
- Garage door openers
- Lighting controls
- Driveway annunciators
- Intrusion alarms
- Weather monitors; fog, snow, rain using light back-scatter
- Traffic counting and monitoring
- Medical monitors

Long Range Applications

- Deep space probe communications; distances measured in light-years
- Building to building computer data links; very high data rates.
- Ship to ship communications; high data rates with complete security.
- Telemetry transmitters from remote monitors; weather, geophysical.
- Electronic distance measurements.
- Optical radar; shape, speed, direction and range.
- Remote telephone links; cheaper than microwave

Wide Area Applications

- Campus wide computer networks
- City-wide information broadcasting
- Inter-office data links
- Computer to printer links
- Office or store pagers
- Cloud bounce broadcasting

- Cloud bounce broadcasting

1.2 LIMITATIONS OF OPTICAL WIRELESS COMMUNICATIONS

In spite of the numerous advantages of OWC systems, there are some atmospheric factors imposing limitations on the performance of OWC systems. Some of the limitations of OWC systems are as follows.

- The main factor that can influence the ability of an optical communications system to send information through the air is weather. Fog, heavy rain and snow block the light path or attenuate the light power and thus affect the communication. Some infrared wavelengths are able to penetrate poor weather much better than visible light. Also, for short distances, systems can be designed with sufficient power to go through most weather conditions.
- Another limitation of light beam communication is the inability of light to penetrate trees, hills or buildings. A clear line-of-sight path must exist between the light transmitter and the receiver.
- A third limitation is the position of the sun relative to the light transmitter and receiver. Such a condition where direct sunlight is falling on the detector surface may damage some components and must be avoided.

1.3 OBJECTIVE OF THESIS

Many researchers and engineers are currently involved in the development of systems for information transfer by optical radiation propagating through the atmosphere. A well-known disadvantage of OWC, as compared to fiber optic communication, is their sensitivity to weather conditions primarily due to fog ,haze, rain, etc., causing substantial loss of light power over the communication path. The main objective of this thesis is to study some of these atmospheric losses, especially Fog and haze. This involves the following tasks.

- Review of the subject and thorough understanding of the various aspects of outdoor optical communication under the different atmospheric conditions
- Design and implementation of a Laser-PIN transmitter and receiver
- Establishing an experimental outdoor link
- Theoretical calculations of various atmospheric losses
- Graphical representation of various atmospheric losses with different link design parameters.
- Experimental verification

1.4 ORGANIZATION OF THESIS

Chapter 2 gives a review of the outdoor optical wireless links. A comparison of presently available systems is also given.

Chapter 3 reviews the propagation of Gaussian beam. The effect of various weather conditions on the laser beam propagation is discussed. The effect of fog is discussed and the atmospheric attenuations for different fog conditions are calculated. Variation of atmospheric attenuation with visibility is plotted. The effect of fog on the bit error rate is also discussed in this chapter.

Chapter 4 deals with the design of outdoor optical wireless link.

Chapter 5 discusses the implementation of transmitter and receiver circuit and PCB fabrication. It also includes experiments in indoor and in outdoor situation under various weather conditions.

Chapter 6 concludes the thesis with the major results and gives suggestions for further work in this area.

CHAPTER 2

REVIEW OF OUTDOOR OPTICAL WIRELESS LINKS

2.1 INTRODUCTION

Outdoor optical wireless communications (OWC) systems use light to communicate through the air, and require clear line of sight between the units. Modern systems typically use lasers and photo diodes at the receiver to detect the incoming light, and send an appropriate signal for processing. Outdoor OWC systems are used, mostly for high-bandwidth applications needing data transfer of hundreds of megabits per second. Recent developments are bringing such inexpensive OWC consumer products.

2.2 FREE SPACE OPTICAL COMMUNICATION (PRESENT STATUS)

Optical communications is one of the cornerstones of today's revolution in information technology. With the drive towards portable and multimedia communications, we are increasingly faced with the challenge of bringing the capacity of our communication infrastructure directly to the user, providing seamless access to huge quantities of information, anywhere and anytime. Whether it is the transfer of an image from a digital camera to a laptop computer or the communication of data within a massively parallel computer, there is an urgent need to develop new methods of high speed data communications. Light offers many advantages as a medium for communication. Whether traveling through free space or through optical fiber, light provides large channel bandwidth and data rates in the terabits per second. This immense capacity is due to the nature of the photons that constitute an optical signal. Unlike electrons, photons react weakly to their environment and to one another. As such, optical signals neither generate nor are sensitive to electromagnetic interference (EMI), parasitic coupling, and other problems faced by electrical signals. Due to their advantages, optical wireless links

are becoming more popular into application areas as compared to traditional Radio and fiber-optic. Some of the worldwide industries manufacturing outdoor Optical Wireless Systems and their products are given below [17].

- *Air Fiber Inc.* - Wireless optical network technology providing a 2-4 independent 622Mbps mesh-based ATM connections over 200-500m between buildings .

- *AMSKAN Ltd.* - Low data rate, point-to-point infrared links for data transfer from vehicles as the refuel or at highway speeds. Typical application is for toll-ways .

- *Cablefree Solutions* - Offer a range of point-to-point wireless optical links from 155Mbps over 4km to 1.5Gbps over 1km. For use in enterprise networks and CCTV applications among others.

- *Canon USA* - Canobeam Optical beam transmitter - Point-to-point infrared links for video feed applications as well as data comm. Advanced autotracking system to ensure link robustness. 622Mbps over 1km or 156Mbps over 2km.

- *Digital Atlantic* - A hybrid communication system with short (approx. 100m) wireless optical links in cascade with fiber links using Gigabit Ethernet standard.

- *Efcon* - Systems for collecting tolls on highways without requiring vehicles to stop using scannig laser beams. Also a series of smart IR cards to be used for simplifying collection of public transit fares and parking fees.

- *fSONA Communications* - provide links at data rates from Fast Ethernet/OC-3 through 1.25 Gbps at eye-safe 1550nm wavelengths at distances from 500m to 4km. A robust tracking system is used to improve availability.

- *GoC mbH* - Wireless optical links of up to 155Mbps over 500m at 850nm (class 3A), 10Mbps over 300m with a compact transmitter or 155Mbps over a 2km range.

- *Holoplex Technologies* - Free-space links over 2 or 4km at 155 or 622Mbps operating at Class 1 eyesafe levels.

- *Infrared Acropolis* - Free-space optical links at maximum rate of 100Mbps over 1km using 4 channels.

- *Infrared Communication Systems Inc.* - Provide broadband wireless high-speed laser communication systems for voice and data transmission systems over point-to-point line-of-sight, links from T-1 1.544 Mbps over 6km to 622 Mbps OC-12 over 1km.

- *iRLan* - Indoor and outdoor free-space optical links. Provide a 10Mbps full-duplex link over 200m for outdoor operation.

- *LASE Industrielle Lasertechnik GmbH* - Wireless optical links at a maximum rate of 155Mbps over 5km for video and networking.
- *Lightec* - Terrestrial free-space optical communications. One project mentioned for the Naval Air Warfare Center for secure laser communication between aircraft carrier and aircraft.

- *LightPointe* - High-speed free-space optical for a variety of applications from 850nm, 1.25Gbps over 4km, to 2.5Gbps at 1550nm over 1km range.

- *LSA Photonics* - Protocol independent free-space links of rates up to 155Mbps over 4.5km.

- *Olencom Electronics* - Free-space optical links at 870nm wavelength supplying solutions at 1.55Mbps over 2km to 100Mbps over 300m.

- *Optical Access* - Terrestrial free-space optical T1/E1, 10/100/1000 Ethernet, OC-3, and OC-12 links at rates up to 1.25Gbps over 500m to 2Mbps over 5km.

- *Optical Crossing* - Single channel free-space optical transceiver operating at 2.5Gbps over 2km.

- *Optel Communication* - Single and dual channel free-space products operating at a maximum of 155Mbps over a 4km range. See image gallery of installations including some 3-D models.

- *OrAccess* - Developers of DWDM technology over the air, supporting 10Gbps at 1310nm and 1550nm wavelengths.

- *PAV Data Systems a division of Conversant Communications* - Point-to-point free-space links for base station controllers (2Mbps over 6km), network extension (10Mbps over 6km) and wireless video applications (270Mbps over 500m) at 750-950nm wavelengths.

- *Plaintree Systems Inc.* - Provide eyesafe, point-to-point free-space optical links from E1/T1 levels to 155Mbps for up to 2km distance. Also provide wireless optical solutions to connect GSM basestations to microcells at E1/T1 rates at distances of up to 3km. Also provide indoor 10Mbps point-to-point optical links.

- *Silcom Technology* - Protocol independent free-space links at maximum data rate of 155Mbps over 2km with 1300nm optical wavelength or up to 155Mbps over 750m using 780nm wavelength.

- *SVE TEHS* - Wireless optical link to extend 10Mbps network over 300m at 785nm wavelength.

- *TeraBeam* - Provide free space links for last mile solutions at rates of 5,10 100 and 1000 Mbps operating in the 1550nm band. For use as a replacement for high speed data communication when fiber is not available.

2.3 A BASIC OUTDOOR OPTICAL WIRELESS LINK

Fig 2.1 shows the basic elements of an outdoor optical link. On the transmitter side, an information source produces a data stream that is encoded and sent to the appropriate drive circuitry used to modulate the optical signal generated by a laser. Optical transmitter emits P_t watts of power into a solid angle of Ω_t steradians. The signal propagates through free space until it reaches the photodetector on the receiver end. The optical receiver has a collection aperture area of A_r m^2. The distance Z between the transmitter and the receiver can range from a few tens of meters (for inter building links), through several tens of thousands of kilometers (for intersatellite links), to several astronomical units- and possibly even farther- in deep-space applications. The photodetector converts the optical signal into an electric current that is sensed by the optical preamplifier and regenerated to a sufficiently strong voltage signal from which the original data can be recovered by the demodulator.

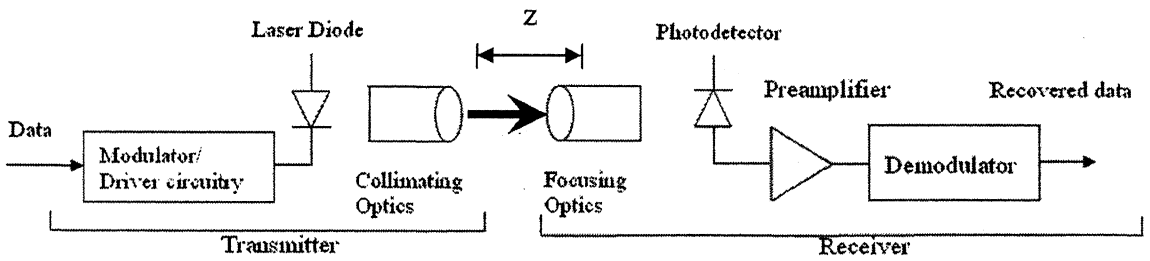

Fig 2.1 Basic Optical link

In addition to the transmitter and the receiver, outdoor optical communication systems include subsystems to perform functions such as beam manipulation, viz. acquisition and

tracking. In an outdoor optical communication link, assuming ideal conditions, viz. perfect alignment of transmitter and receiver, lossless optical components and detectors, the received power, P_r is determined by the formula [4]

$$P_r = P_t \frac{A_r}{\Omega_t Z^2} \quad \ldots (2.1)$$

When the real life conditions are taken into account, the right hand side of equation 2.1 has to be multiplied by several inefficiency factors, such as mis-pointing errors, receiver optical losses, geometrical spreading loss, atmospheric attenuation and scintillation (atmospheric turbulence).

Outdoor optical links require the transmitter and receiver to be spatially aligned in order to maintain communication. Thus an important step in establishing the link involves the process of beam acquisition. The transmitted beam has to be pointed in the direction of the receiver. A beacon source operating at a different wavelength from that of the transmitter at or near the receiver is often used to designate the correct direction. Alternately, in duplex systems each transmitter can serve as a beacon to the other terminal. The optical receiver has to be pointed in the approximate direction of the transmitter, and then some scanning has to be done until the transmitted beam is within the field of view of the tracking detector. Most receivers employ separate detectors to assist in the beam manipulation functions. These detectors usually have a larger field of view and a lower sensitivity than the optical detector that detects the information signal. Beam acquisition can be simplified by using detector arrays with a large number of elements (e.g. CCD with or without light amplification stages) that can stare into a large field of view. Once the beam is acquired, the alignment is maintained using the spatial information derived from the tracking detector.

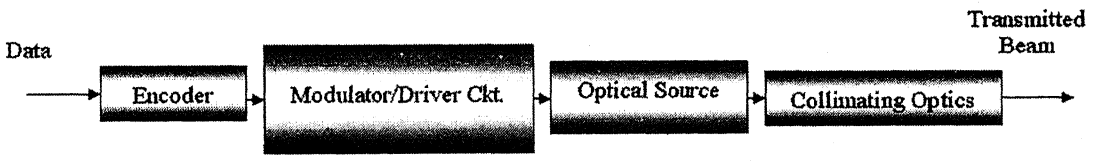

Fig. 2.2 ***A typical Transmitter***

2.4 TRANSMITTER

The basic role of a transmitter is to convert the electrical data to a corresponding optical signal. In almost all systems the light intensity of the Laser is changed in accordance with the electrical signal.

2.4.1 System Requirements

The transmitter consists of an encoder, followed by a modulator or driver circuitry. Fig. 2.2 shows a typical transmitter. A property of the light is modulated with the information signal. This property may be intensity, frequency, phase or polarization (direction). Either Intensity Modulation (IM)/Direct Detection (DD) schemes or Coherent optical communication system can be employed for this purpose. Intensity Modulation (IM) is preferred due to its

simplicity. The modulated beam is finally collimated.

Intensity modulation is easy to implement with the electro luminescent sources available at present (LEDs and injection lasers). The devices can be directly modulated simply by variation of their drive currents at rates up to several gigahertz. However, considering the recent interest in integrated optical devices, it is likely that external optical modulation may be utilized more in the future in order to achieve greater bandwidth and to allow the use of non-semiconductor sources.

2.4.2 Optical Sources

A wide variety of optical sources can be used for free space optical communications. The performance of an optical communication system depends to a large extent on the optical source used. The light source should be chosen based on the type of information that

needs to be transmitted and the distance to be covered to reach the optical receiver. In all cases the light source must be modulated to transmit information. The modulation rate will determine the maximum rate information can be transmitted. We may have to make some tradeoffs between the modulation rates needed, the distance to be covered and the cost.

For intensity modulated optical transmitters, two semiconductor devices-light emitting diodes (LEDs) and injection laser diodes are suitable in terms of size, speed, efficiency, and electrical characteristics. But semiconductor lasers offer narrow spectral width (<10 nm) and hence are suitable for long distance, high bit rate applications. And because of the broad spectral width (50-150 nm full width at half maximum amplitude) of LEDs, they are generally used only for short distance, and lower bit rate applications. Hence LEDs are not suitable for outdoor applications.

Lasers

Lasers produce intense beams of light that are monochromatic, coherent, and highly collimated. The wavelength (color) of the laser light is extremely pure (monochromatic) when compared to other sources of light, and all of the photons (energy) that make up the laser beam have a fixed phase relationship (coherence) with one another. This causes the light to form a beam with a very low rate of expansion (highly collimated) that can travel over great distances, or can be focused to a very small spot with a brightness that can approximate that of the sun. Because of these properties, lasers are used in a wide variety of applications.

Over the four decades since the first ruby laser was first tested in 1960, literally hundreds of different lasers have been invented. Nevertheless, only a handful have found general acceptance for use in volume OEM applications as well as in the laboratory. The helium neon (HeNe) laser, air-cooled ion laser (argon, krypton, or mixed gas), and the solid state lasers have been the omnipresent lasers. Recently, diode-pumped solid-state (DPSS) lasers and helium cadmium (HeCd) lasers have been used successfully in many OEM systems.

Helium Neon (HeNe) lasers

Helium Neon (HeNe) lasers were the first to be used in volume applications. The key to the HeNe's success has been its low cost, small size, long operating life, and beam quality. HeNe lasers produce milliwatts of output power and are available in a variety of wavelengths ranging from 543 nm (green) to 3.39 μm (infrared). The most common wavelength is the familiar red (633 nm). The lasers are small, convection cooled, and can be operated from ordinary household power services, or even from batteries. Metrology, reprographics, and bar-code scanning are a few of the many applications in which the HeNe laser has found wide acceptance. They are used as alignment and pointing devices in surgical systems, as precision light sources in clinical and analytical applications such as cell sorting, as wavelength references in industrial measurement and positioning systems, and as large-depth-of-field holography sources.

Solid State Lasers

Improvements in semiconductor fabrication techniques has made it possible to fabricate smaller, more complex diode lasers with greatly increased reliability and extended lifetime and it is possible to develop diode lasers having shorter wavelengths, greater power output, more consistent beam quality, and greatly increased life. Telecommunication and digital optical signal storage and retrieval are probably the best known fields in which diode laser technology has played an integral role.

Diode laser has all the general advantages and convenience of semiconductors and solid-state devices. They are compact, efficient, cost effective, amenable to mass production, and in many ways superior to non-solid state counterparts. Currently the smallest lasers, a diode laser mounted complete with heat sink, photodiode detector, and protective window can measure as little as $50mm^2$ yet deliver as much as 100mW of continuous power. Their efficiency far exceeds that of most other types of laser with typically 20%of input power being converted into laser radiation, compared to < 2% for a HeNe or a Nd-YAG laser. Above lasing threshold, typically greater than 80% of the additional input power is converted to laser radiation in a diode laser.

Since they are small solid-state devices, diode lasers can respond fast to changes in the driving current. The output of a diode laser can therefore be modulated at very rapid rates when accurately slaved to complex high frequency waveforms. Most laser diodes are fabricated from the third and fifth group compounds (such as gallium arsenide, InP, InAs, and more complex compounds). The most important materials are GaAs and its derivatives, which lase at wavelengths from 660-900nm, and InP -based compounds which are used for diode lasers in the 1300-1550 nm windows.

The diode lasing principle was first demonstrated in 1962, but these small devices did not come into common use until the 1980s with the advent of the audio-disk player. Since then, there has been a continuous push for higher power, longer lifetime, and different wavelengths. Today, diode lasers are readily available at wavelengths varying from 630 nm to 1.6 μm and above, and at output power ranging from a few milliwatts to several watts. Because of their small size and exceptional efficiency, diode lasers have replaced the HeNe laser in many applications, particularly in those where beam quality, wavelength stability, and unit-to-unit repeatability are not critical. The typical diode laser is an edge-emitting device with a Fabry-Perot lasing cavity processed into the length of the semiconductor. Because of the small size and rectangular configuration of the cavity, the resulting beam diameter is very small (~1 μm), beam divergence is quite high (20-40 degrees), and the beams are astigmatic and elliptical (typically 3:1 or greater). These drawbacks can be reasonably corrected with appropriate collimating and anamorphic beam-conditioning optics, but it is important to recognize that these parameters can vary significantly from laser to laser, placing constraints on unit-to-unit repeatability with a standard optic set. Diode-laser wavelength can vary several nanometers with changes in substrate temperature, thus requiring tight temperature control for stable operation.

2.4.3 Eye Safety Considerations

Optical wireless systems like their radio counterparts, can pose a hazard if operated incorrectly. Therefore a laser safety standard has been established in which optical sources have been classified in accordance with their total emitted power. The principal

classifications are summarized in Table 2.1 for a point source emitter such as a semiconductor laser [1].

Out door point-to-point systems, generally use high power lasers that operate in the class 3B band to achieve a good power budget. The safety standard recommends that these systems should be located where the beam cannot be interrupted or viewed inadvertently by a person. Roof top locations or high walls are usual for this type of systems. The wavelength band between about 780 and 950 nm is presently the best choice for most applications of infrared wireless links, due to the availability of low cost laser diodes (LDs), and because it coincides with the peak responsivity of inexpensive, low capacitance silicon photodiodes. The primary drawback of radiation in this band relates to the eye safety; at this wavelength the radiation can pass through the human cornea and be focused by the lens on to the retina, where it can potentially induce thermal damage. The cornea is opaque to radiations beyond 1400nm, considerably reducing potential ocular hazards, so that it has been suggested that the 1550 nm band may be better suited for infrared links.

Wavelength	**650nm**	**880nm**	**1310nm**	**1550nm**
Class1	Up to 0.2mW	Up to 0.5mW	Up to 8.8mW	Up to 10mW
Class2	0.2-1mW	N/A	N/A	*N/A*
Class3A	1-5mW	0.5-2.5mW	8.8-45mW	10-50mW
Class3B	5-500mW	2.5-500mW	45-500mW	50-500mW

Table 2.1 Laser safety classifications for a point source emitter

2.4.4 Problems Associated With Lasers

As discussed, LDs are the best choices for optical sources in outdoor optical links. However, there are several problems associated with LDs, which must be borne in mind while using them.

***Facet Damage*:** Attempts to operate semiconductor lasers at high powers can result in gross damage to the cleaved facets that act as mirrors. This is believed to be due to a high surface state recombination rate which prevents the facet surface from being inverted, thus causing absorption of laser light. This can either melt the mirror surface in a catastrophic manner or propagate dark lines and other defects into the active region. The critical peak optical power density for catastrophic mirror damage is approximately 10^6 W/cm^2 for CW operation and about 10^7 W/cm^2 for pulsed operation with very short pulses (<100 ns). Interestingly, the longer wavelength InGaAsP semiconductor laser does not seem to have a limit on the optical power density at the facet. This may be due to the lower recombination rate at the surface of InGaAsP.

***Ohmic Contact Degradation*:** This problem is common to all semiconductor devices and is observed under certain conditions in transistors, rectifiers, and other components subjected to either high current densities or high temperatures. Because the threshold current of laser diodes is fairly temperature dependent, an increase in thermal and/or electrical resistance affects the laser performance. In laser diodes, the thermal resistance of the contact between the laser chip and the heat sink tends to increase with time. This degradation process depends on the solder used, the current density through the contacts, and the temperature. The increase in thermal resistance of the contact produces an increase in the junction temperature for a given operating current. Thus it is possible to observe a decrease in the CW output of a laser operated at a constant current that is directly caused by this effect.

***Internal Damage*:** Internal damage in the laser often appears as dark line defects (DLD). A DLD is a network of dislocations that can form during laser operating in the region of

the active cavity. Once started, it can grow extensively in a few hours. The initiation of DLD can take much longer. The DLD produces relatively high absorption and is a region with a high density of nonradiative recombination centers. The growth of DLD is accompanied by an increase in the threshold current and a decrease in the external differential quantum efficiency.

Modal Partition Noise: When operated continuously (CW) above threshold, multilongitudinal mode lasers show a spectrum characterized by several wavelengths (modes) spaced according to the dimension of the Fabry-Perot cavity. When the diode forward current is modulated at high frequencies, many multilongitudinal mode lasers develop additional modes. In addition to resulting in a wider spectrum, the modes have a probability of exchanging power with each other. Whether or not additional modes appear, modulation induces 'noisy' statistical power fluctuations (modal partition noise or MPN) among the modes already present. Because these fluctuations in amplitude and wavelength are chromatically time-dispersed during transmission, jitter and eye closure are observed at the receiver, leading to a sensitivity penalty.

Chirp: Fast changes in laser current also induce unwanted spectral effects by modulating the refractive index of the cavity. The resulting 'chirp' of the emitted wavelength is chromatically dispersed, leading again to power penalties at high bit rates.

Delay: For digital applications, it is important to maximize the energy in the 1 or mark level and minimize the energy in the 0 or space level. The ratio of these two intensities is the extinction ratio or contrast ratio γ. High values of γ cannot be obtained arbitrarily, since the 1 level is usually subject to peak power limitations of the laser set by reliability considerations, and the 0 level is determined by the laser turn on dynamics or spontaneous emission near threshold. Suppose a laser initially has a zero bias (current or voltage) applied to it. If the current is now rapidly increased to a level corresponding to the desired power for the 1 state, a delay between the leading edge of the current pulse

and the light output is observed. The delay is accompanied by a transient overshoot (ringing) in the light output, again arising from the dynamics of the coupled carrier and photon populations in the cavity. This delay t_d is given by [10]

$$t_d = \tau_{th} \ln \frac{I}{I - I_{th}} \qquad \ldots(2.2)$$

where I is the magnitude of the current pulse, I_{th} is threshold current and τ_{th} is the carrier recombination lifetime at threshold (usually 2-5ns). The delay can be reduced by making the drive current large with respect to threshold. Then

$$t_d = \tau_{th} \frac{I}{I - (I_{th} - I_{bias})} \qquad \ldots (2.3)$$

where I_{bias} is the dc biasing current. When $I_{bias} = I_{th}$, $t_d = \tau_{th}$. The amplitude of the overshoot or ringing (whose frequency is nearly equal to the laser resonance frequency and whose damping time constant is twice the recombination lifetime), becomes small as the laser is biased near threshold. Therefore, to minimize delay and overshoot, both of which cause serious pattern dependant distortion, a near threshold dc bias (I_{bias}) is added to the pulse current. This bias, however results in a nonzero '0' light level, reducing the extinction ratio and incurring a sensitivity penalty at the receiver. Therefore the bias current used must be optimum for the application in mind and chosen carefully. It is also important that the transmitter circuit to maintain this bias at the optimum point under all operating conditions.

2.5 RECEIVER

The optical receiver is a critical element of an optical communicating system since it often determines the overall system performance.

2.5.1 System Requirements

The receiver essentially consists of an **optical detector** which converts the received optical signal into an electrical current, **a pre-amplifier** where initial amplification is performed without additional noise corrupting the received signal, **a post amplifier** for providing additional low noise amplification of the signal, **an equalizer** for compensating the distorted input signal and to provide suitable signal shape, and a **filter** to maximize the received signal to noise ratio while preserving the essential features of the signal. A block diagram of the receiver is shown in Fig. 2.3.

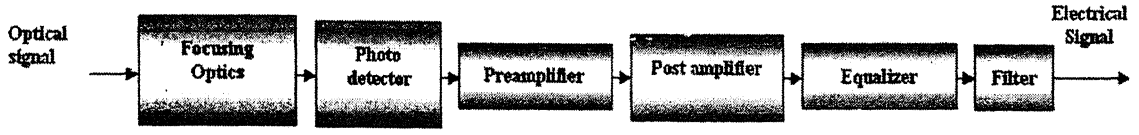

Fig. 2.3 ***Block diagram of the receiver***

The sensitivity of the receiver depends upon the detector type (i.e. whether it is p-i-n or avalanche photodiode) and also on the characteristics of the pre-amplifier.

2.5.2 Optical Detector

In optical communications a light source forms the carrier and must also be modulated to transmit information. Virtually all present optical communications systems modulate the intensity of the light source. Usually the transmitter simply turns the light source on and off. To decode the information from the light pulses, some type of light detector must be employed. The detector's job is to convert the light signals, collected at the receiver, into electrical signals. The electrical signals produced by the detector are much easier to demodulate than light signals.

PIN Photodiodes

PIN photodiodes are generally used for detecting the light of longer wavelengths. At longer wavelength the light penetrates more deeply into the semiconductor material for this a wider depletion region is needed. So a intrinsic semiconductor layer is added between a p layer and an n layer. This creates a PIN photodiode

Silicon PIN Photodiode

Silicon "PIN" photodiode has the speed, sensitivity and low cost to be a practical detector. This device is made of "P" and "N" semiconductor layers with a middle

intrinsic or insulator layer. Most PIN photodiodes are made from silicon. Figure2.4 shows specific response curve [11]. The device is most sensitive to the near infrared wavelengths around 900 nm. The response falls off sharply beyond 1000 nanometers, but has a more gradual slope toward the shorter wavelengths, including the entire visible portion of the spectrum. In addition, note that the response drops to about half of its peak at the visible red wavelength (640 nm). It should therefore be obvious that if we want to maximize the device's conversion efficiency we should choose an information transmitter light source which closely matches the peak of the silicon PIN photodiode's response. The 'Responsivity', which is essentially the transfer characteristics (the current output for a given optical input power expressed as A/W) is the most important characteristic of the PIN photodiode.

InGaAs PIN Diode

Though silicon is the most popular material for optical detectors, there are other materials as well for solid-state light detectors. Photodiodes made from Germanium, InGaAs, and others work well at longer infrared wavelengths than silicon devices. These devices have been used for many years in optical fiber communications systems, which rely on longer wavelengths. Glass optical fibers operate more efficiently at these longer wavelengths. The curve shown below is the typical response for a InGaAs device but peak can be shifted slightly as needed.

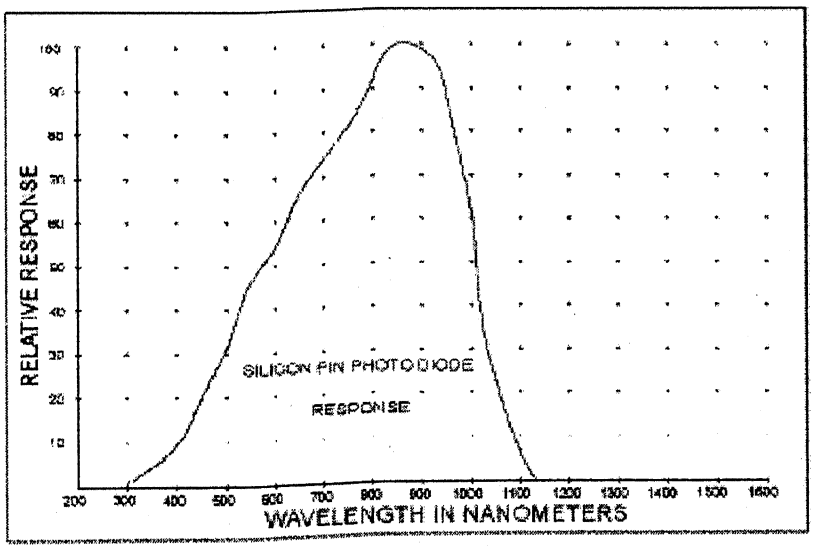

Fig. 2.4 ***Response of silicon PIN photodiode***

As shown in the Fig.2.5 [11], an InGaAs photodiode's response includes only some of the wavelengths that a silicon photodiode covers. However, most of the devices made are designed for optical fiber communications and therefore have very small active areas. They are also much more expensive. Some of the parameters of interest in PIN photodiodes are briefly discussed below.

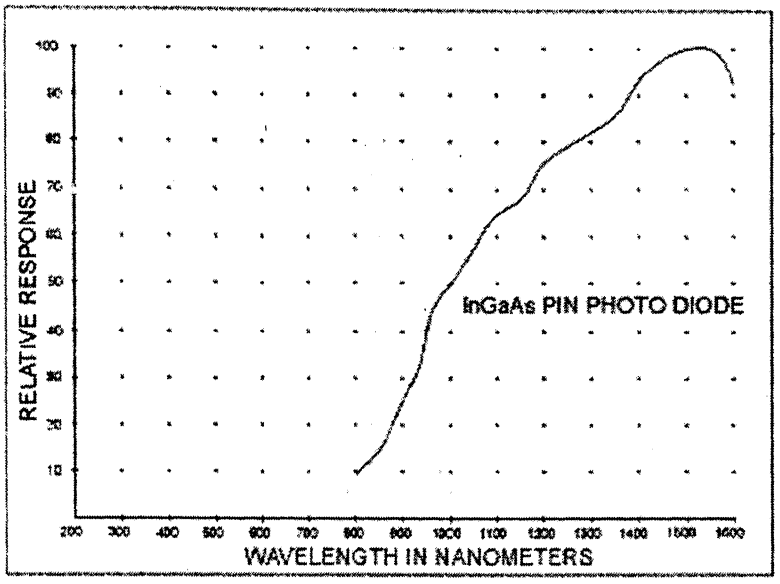

Fig.2.5 ***Response of InGaAs PIN photodiode***

Active Area

This corresponds to the size of the actual light sensitive region, independent of the package size. PIN Diodes with large active areas will capture more light but will always be slower than smaller devices and will also produce more noise. However, if a small device contains an attached lens it will often collect as much light as a much larger device without a lens. However, the devices with attached lenses will collect light over narrower incident angles (acceptance angle). Flat surface devices are usually used if light must be detected over a wide area. For most applications either style will work. For high speed applications a device with a small active area is always preferred. However, there is a tradeoff between device speed and the active area. For most long-range applications, where a large light-collecting lens is needed, a large area device should be used to keep

the acceptance angle from being too small. Smaller acceptance angles can make it nearly impossible to point the receiver in the right direction to collect the light from the distant transmitter.

Response Time

This defines the time the device needs to react to a short pulse of light; smaller the response time, faster the device. Large area devices will always be slower and have longer response times. A slow device will respond to a short light pulse by producing a signal that lasts much longer than the actual light pulse. It will also have apparent lower conversion efficiency. The detector should have a response time that is smaller than the maximum needed for the detection of the modulated light source .The response time may also be linked to a specific reverse bias voltage. In general, all devices respond faster when a higher bias voltage is used.

Capacitance

When choosing a suitable light detector from a manufacturer, their data sheets may also list a total capacitance rating for the PIN device. It is usually listed in picofarads. There is a direct correlation between the active area and the total capacitance, which has an effect on the speed. However, the capacitance is not a fixed value. The capacitance will decrease with higher reverse bias voltages. Large area devices will always have a larger capacitance and will therefore be slower than small area devices.

Dark Current

All PIN diodes have dark current ratings. This rating corresponds to the residual leakage current through the device, in the reversed biased mode, when the device is in complete darkness. This leakage current is usually small and is typically measured in nanoamps. Large area devices will have larger dark currents than smaller devices.

Package

PIN silicon photodiodes come in all sizes and shapes. Some commercial diodes are packaged in special infrared (IR) transparent plastic. The plastic blocks most of the

visible wavelengths while allowing the IR light to pass . Some of these packages also place a small plastic lens in front of the detector's active area to collect more light. As long as the modulated light being detected is also IR, either the filtered or the unfiltered devices will work.

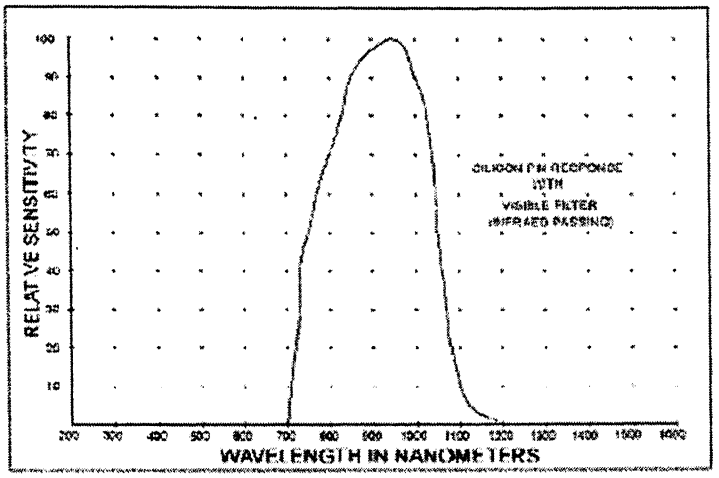

Fig.2.7 ***Sensitivity of PIN photodiode***

Avalanche Photodiodes

An APD is a special light detecting diode that is constructed in much the same way as a PIN photodiode. Unlike a PIN diode that only needs a bias of a few volts to function properly, an APD is biased with voltages up to 450 volts. When light strikes the device it produces current in much the same way as a typical PIN diode, but at much higher levels. Unlike a PIN diode that may produce, say only one microamp of current for two microwatts of light (i.e. a responsivity of 0.5 A/W), an APD can produce as much as 100 microamps for each microwatt (x100 gain, or a responsivity of 100 A/W). This gain factor is very dependent on the bias voltage used and the APD's operating temperature. Some systems take advantage of these relationships and vary the bias voltage to produce the desired gain. When used with narrow optical band pass filters and laser light sources, APDs could allow a OWC system to have a much higher light sensitivities and thus longer ranges than might otherwise be possible with a standard PIN device. However, in systems that use LEDs, the additional noise produced by the ambient light focused onto the device cancels much of the gain advantage the APD might have had over a PIN. They are also typically 20 times more expensive than a good PIN photodiode. Finally, the high

bias voltage requirement and the temperature sensitivity of the APD cause the detector circuit to be much more complicated than those needed with a PIN.

APDs have an increase in sensitivity 5 to 15 dB over PIN photodiodes. Also they often provide a wider dynamic range. However APDs have some drawbacks like additional noise due to random gain, high bias requirements and it is wavelength dependent too, temperature sensitivity of gain requiring temperature compensation for stable operation, fabrication difficulties due to their complex structures, higher cost. Both Silicon, and germanium APDs are available.

The gain of APD is the result of carrier multiplication which introduces excess noise. To ensure carrier multiplications without excess noise, **silicon reach through APDs** are used. Silicon APDs have lower dark current. Germanium has also been used to fabricate fast and more sensitive APDs over the 0.8-1.6 micrometer wavelength. However, germanium APDs have larger excess nose factor compared to silicon APDs.

2.6 ATMOSPHERIC CHANNEL

For a free space channel if we consider a point source emitting Power P_t then the received power P_r can be given by[19]

$$P_r = P_t G_t L_p G_r \tag{2.4}$$

where G_t is the transmitter gain and can be expressed as

$$G_t = \frac{4\pi}{\Omega_t}$$

L_p is the propagation loss associated with the transmission of the laser beam and is given by

$$L_p = \left(\frac{\lambda}{4\pi z}\right)^2$$

G_r is the the receiver gain and can be written as

$$G_r = \frac{4\pi A_r}{\lambda^2}$$

When the propagating medium is not free space, additional effects must be taken into account. When propagating through atmosphere, the wave undergoes many effects that further alter the power level and phase of the field.

The atmosphere is composed of a collection of gases, atoms, water vapors, pollutants and other chemical particulates that are trapped by the earth's gravity field; it extends to approximately 400 miles altitude. The heaviest concentration of these particles is near earth in the troposphere level, with particle density decreasing with altitude up through the ionosphere. Actual particle distribution depends on the atmospheric conditions. Power loss and distortion are caused by the absorption and scattering of the optical beam by these particles. The clear air channel is the most benign one, characterized by long-range visibility, clear weather, and relatively low attenuation. The main effects on free-space optics (FSO), are geometric losses, absorption, scattering, and scintillation.

Geometrical Loss: This is the fraction of laser power that actually reaches the receiver in the absence of atmospheric losses. The divergence of the transmitter beam essentially sets this fraction assuming that the receive aperture is smaller than the spot size at the receiving end (a non-focusing system).

Absorption: As field radiation impinges on atmospheric particulates, a portion of its energy is absorbed, and the angle of the remainder is redirected. There are many types of gases in the atmosphere that can cause absorption, the dominant being water vapor in the wavelength region of interest. By staying out of the 'water' windows and keeping the path lengths short, absorption can largely be ignored as the particle size approaches the wavelength of the transmitted light.

Scattering: The scattering mechanism can be divided into three categories. The first one is Rayleigh scattering. It occurs when the atmospheric particles are much smaller than the wavelength. Rayleigh scattering occurs primarily off of the gaseous molecules in the atmosphere. The second type, Mie scattering occurs when the size of the particles approaches the wavelength of the transmitted light. The amount of scattering depends on the particle size distribution and the density of the particles. The third type of scattering

occurs when the atmospheric particles are much larger than the laser wavelength. This type of scattering is called geometric or non-selective scattering. This is called non-selective because there is no dependence of the attenuation coefficient on laser wavelength.

Scintillation: Scintillation is caused by small-scale fluctuations in the index of refraction of the atmosphere on small spatial scales. The major effect of scintillation is signal fading, due to phase changes in the wavefront of the signal arriving on the receiver causing both null and high signal receive levels. Unless the receiver has a very high dynamic range, or the aperture is large enough to average out the scintillation spots, this can have an extremely detrimental effect on the signal.

Background Light: The sun contains significant energy in its spectrum at all wavelengths of interest in OWC systems. Most OWC products use a combination of spatial and spectral (bandpass) filtering to reject this energy and help increase the SNR.

2.7 COMPARISON OF EXISTING SYSTEMS

Many OWC or often called freespace optics system (FSO) systems have been developed for establishing point to point, bidirectional and high speed telecommunications through the atmosphere. We can broadly classified commercially available links as short range links(link range below 2km) and long range links (link range above 2km) .

Short range links

LightPointe Communications, Inc. has introduced two short range products FlightLite FlightPath for up to 500m and 600m range and at 155mbps and 1.2 Gbps data rates respectively. Canobeam from canon is available for link ranges up to 2km at 622Mbps bit rates. For the speeds 155Mbps, GoC mbH has a Wireless optical links over 500m but at 850nm this is class 3A eyesafe.

While most products allow only point-to-point communication, companies such as AirFiber and Terabeam have brought out products that easily allow a mesh of links between nodes to be set up. AirFiber introduces a hybrid wireless system, enabling SONET or Gigabit Ethernet, with 99.999% availability at 155Mbps, 622Mbps, or

1.25Gbps at over a kilometer, in all-weather.[17]It's product range has 10Mbps link over 300m or 155Mbps over a 2km range[17].

Long range links

There are a number of long range products available for different datarates.for link ranges up to 4km there are products available from the companies like Data Communication export co.(DCEC) CBL, Gesellschaft for optische Communication mbH ,at various speed . For up to 5km link ranges GmbH product at 622Mbps, Laserbit Communications product laserbit at 155 are available. For higher link ranges LSA Photonics has introduced a product for relatively lower datarates (45Mbps) but longer ranges (up to 15km) ,it uses 780-920nm laser source.Terabeam elliptica free space optical transceiver provides high performance for fast Ethernet and oc-3/STM-1 networks. This is a class I eyesafe fSONA communication's product SONAbeam 155-M is designed for OC-3/STM-1 applications at 155.52 Mbps,or Fast Ethernet/FDDI applications with 125Mbps baud rate. Other members of this family has datarates from 34 to 1244Mbps. it employs 1550 nm semiconductor laser diode[6] . Table 2.2[18] compares all OWC product available in international market.

MANUFACTURER	PRODUCTNAME	BIT RATE	MAX. DISTANCE
Canon	Canobeam	Up to 622Mbps	Up to 2Km.
CBL GmbH-Communication by light	Laser-link xxx	Up to 622Mbps	Up to 5Km.
Data Communication export co.(DCEC)	Light station	Up to 155Mbps	Up to 4Km.
Gesellschaft for optische Communication mbH	CompactLink MonoLink MultiLink	Up to 10Mbps Up to 155Mbps Up to 155Mbps	Up to 4Km Up to 4Km Up to 4Km
Infrared Communication Systems Inc.	Skynet	Up to 622Mbps	Up to 6Km
Laserbit Communications	LaserBit	Up to 155Mbps	Up to 5Km
LightPointe Communications,Inc.	FlightLite FlightPath FlightSpectrum	Up to 155Mbps Up to 1.25Gbps Up to 2.5Gbps	Up to 500m Up to 600m Up to 4Km
LSA Photonics	Magnum45	45Mbps	Up to 15Km
Nbase-Xyplex	TereScope	Up to 155 Mbps	Upto 3.75Km
Optel GmbH	Opticomm	Up to 155 Mbps	Upto 5Km
Optical access Inc.	TereScope	Up to 1.25Gbps	Upto 4Km
PAV Datasystems Ltd.	SkyCom	1.5Mbps	Upto 4Km
AirFiber Inc.	OptiMesh	Up to 622Mbps	

Table 2.2 ***Comparision of Existing Systems***

CHAPTER 3

LASER BEAM PROPAGATION AND ATMOSPHERIC EFFECTS

3.1 LASER BEAM PROPAGATION

In general, laser-beam propagation can be approximated by assuming that the laser beam has an ideal Gaussian intensity profile, corresponding to the theoretical TEM_{00} mode. The TEM_{00} mode output of a laser is a spherical Gaussian beam. The wavefront normals (rays) of a plane wave are parallel to the direction of the wave so that there is no angular spread, but the energy extends spatially over the entire space. The spherical wave, on the other hand, originates from a single point, but its wavefront normals (rays) diverge in all directions. Waves with wavefront normals making small angles with the z axis are called paraxial waves. They must satisfy the paraxial Helmholtz equation. A solution of this equation is a wave called the Gaussian beam. The intensity distribution in any transverse plane is a Gaussian function centered about the beam axis. The width of this function is minimum at the beam waist and grows gradually in both directions. The wavefronts are approximately planar near the beam waist, but they gradually curve and become approximately spherical far from the waist.

The Gaussian Beam

A paraxial wave is a plane wave $\exp(-jkz)$ (with wavenumber $k = 2\pi / \lambda$ and wavelength λ) modulated by a complex envelope $A(r)$ that is a slowly varying function of position. The complex amplitude is [7]

$$U(r) = A(r)\exp(-jkz) \tag{3.1}$$

For the complex amplitude $U(r)$ to satisfy the Helmholtz equation, $V^2U + k^2U = 0$, the complex envelope $A(r)$ must satisfy the paraxial Helmholtz equation [7]

$$\Delta_T^2 A - j2k\frac{\partial A}{\partial z} = 0 \tag{3.2}$$

Where $\Delta_T^2 = \frac{\partial^2}{\partial x^2} + \frac{\partial^2}{\partial y2}$ is the transverse part of the Laplacian operator. One solution to the paraxial Helmholtz equation is paraboloidal wave for which

$$A(r) = \frac{A_1}{z}\exp(-jk\frac{\rho^2}{2z}) \ , \rho^2 = x^2 + y^2 \tag{3.3}$$

The paraboloidal wave is the paraxial approximation of the spherical wave $U(r) = (A/r)\exp(-jkr)$ when x and y are much smaller than z .Another solution of the paraxial Helmholtz equation provides the Gaussian beam. It is obtained from the paraboloidal wave by use of a simple transformation. Since the complex envelope of the paraboloidal wave (3.3) is a solution of the paraxial Helmholtz equation (3.2), a shifted version of it, with $z-\xi$ replacing z where ξ is a constant, and the solution is

$$A(r) = \frac{A_1}{q(z)}\exp\left[-jk\frac{\rho^2}{2q(z)}\right], \qquad q(z) = z-\xi \tag{3.4}$$

This provides a paraboloidal wave centered about the point $z = \xi$ instead of $z = 0$. When ξ is purely imaginary(ξ = -jz_0),where z_0 is real, (3.4) gives rise to the complex envelope of the Gaussian beam

$$A(r) = \frac{A_1}{q(z)}\exp\left[-jk\frac{\rho^2}{2q(z)}\right], q(z) = z + jz_0 \tag{3.5}$$

The parameter z_0 is known as the Rayleigh range.

We can write the complex function $1/q(z) = 1/(z + jz)$ in terms of its real and imaginary parts as

$$\frac{1}{q(z)} = \frac{1}{R(z)} - j\frac{\lambda}{\pi W^2(z)} \tag{3.6}$$

$W(z)$ and $R(z)$ are beam width and wavefront radius of curvature, respectively. An expression for the complex amplitude $U(r)$ of the Gaussian beam is obtained by Substituting Eqn. (3.6) into Eqn.(3.5) and using Eqn.(3.1) as

$$U(r) = A_0\frac{W_0}{W(z)}\exp\left[-\frac{\rho^2}{W^2(z)}\right]\exp\left[-jkz - jk\frac{\rho^2}{2R(z)} + j\xi(z)\right] \tag{3.7}$$

The beam parameters can be evaluated by following equations

$$W(z) = W_0\left[1+\left(\frac{z}{z_0}\right)^2\right]^{1/2} \tag{3.8}$$

$$R(z) = z\left[1+\left(\frac{z_0}{z}\right)^2\right] \tag{3.9}$$

$$\xi(z) = \tan^{-1}\left(\frac{z}{z_0}\right) \tag{3.10}$$

$$W_0 = \left(\frac{\lambda z_0}{\pi}\right)^{1/2} \tag{3.11}$$

Now consider a beam wave $U_0(r)$ propagating in the z direction in free space .At the transmitting aperture (z=0), the wave has a Gaussian amplitude distribution with beam size W_0 and a curved phase front with radius of curvature R_0.Then

$$U_0(0,\rho) = \exp\left[-\left(\frac{1}{W_0^2}+j\frac{k}{2R_0}\right)\rho^2\right] \tag{3.12}$$

where $k = \frac{2\pi}{\lambda}$ is wave number, λ is wavelength, ρ is the radial vector from the z axis.

We can also write Eqn. (3.12) as [8]

$$U_0(0,\rho) = \exp\left[-\frac{1}{2}k\alpha\rho^2\right] \tag{3.13}$$

where $\alpha = \alpha_1 + j\alpha_2 = \frac{\lambda}{\pi W_0^2} + j\frac{1}{R_0}$

at an arbitrary point (ρ, z) the beam in free space is given by

$$U_0(\rho,z) = \frac{1}{(1+j\alpha z)}\exp\left[jkz-\left(\frac{k\alpha}{2}\right)\frac{\rho^2}{(1+j\alpha z)}\right] \tag{3.14}$$

this is valid within a distance z [8] such that

$$z << \frac{\pi^3 W_0^4}{\lambda^3} \tag{3.15}$$

which covers almost all the laser propagation distances used in practice. The effect on the beam parameters as beam advances is described below.

Intensity

The optical intensity $I(r) = |U(r)^2|$ is a function of the axial and radial distances z and $\rho = \left(x^2+y^2\right)^{1/2}$,

$$I(\rho,z) = I_0\left[\frac{W_0}{W(z)}\right]^2 \exp\left[-\frac{2\rho^2}{W^2(z)}\right] \tag{3.16}$$

Where $I_0 = |U_0|^2$. At each value of z the intensity is a Gaussian function of the radial distance ρ. The Gaussian function has its peak at $\rho = 0$ (on axis) and drops monotonically with increasing ρ. The width $W(z)$ of the Gaussian distribution increases with the axial distance z as illustrated in Fig.3.1

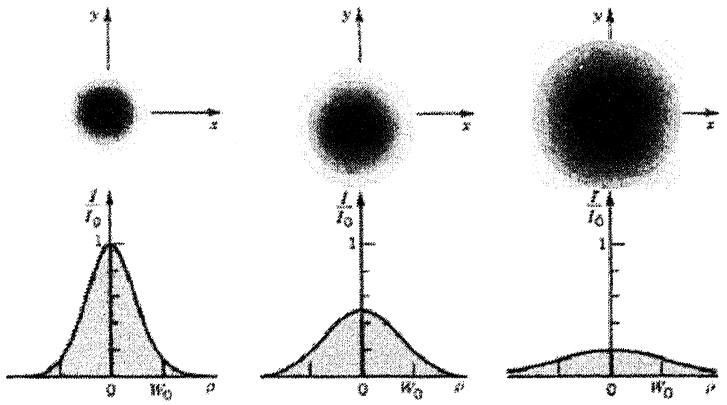

Figure 3.1 ***The normalized beam intensityI/I_0 as a function of the radial distance ρ at different axial distances: (a) $z = 0$ (b) $z = z_0$ (c) $z = 2z_0$*** [7]

On the beam axis ($\rho = 0$) the intensity can be given by[8]

$$I(0,z) = I_0\left[\frac{W_0}{W(z)}\right]^2 = \frac{I_0}{1+(z/z_0)^2} \tag{3.17}$$

It has maximum value I_O at $z = 0$ and drops gradually with increasing z, reaching half of its peak value at $z = +z_o$ (Fig. 3.2). When $|z| >> z_0$, $I(0,z) \approx I_0\, z_0^{\,2}/z$ so that the intensity decreases with the distance in accordance with an inverse-square law. The overall peak intensity $I\,(0, 0) = I_O$ occurs at the beam center ($z = 0$, $\rho = 0$).

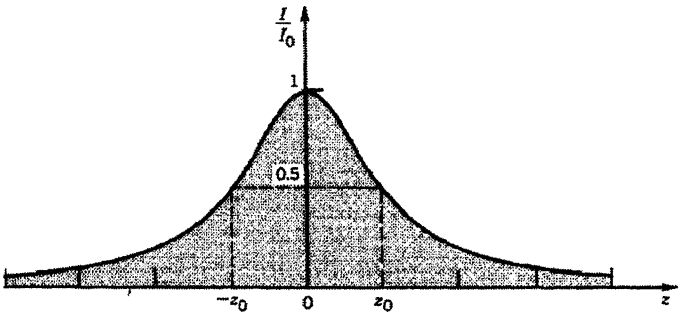

Figure 3.2 ***The normalized beam intensity I/I_0 at points on the beam axis ($\rho = 0$) as a function of z*** [7].

Power

The total optical power carried by the beam is the integral of the optical intensity over a transverse plane (at a distance z),

$$P = \int I(\rho, z) 2\pi\rho d\rho, \quad P = \frac{1}{2} I_0 (\pi W_0^2) \tag{3.18}$$

Since beams are often described by their power P, it is useful to express I, in terms of P as[8]

$$I(\rho, z) = \frac{2P}{\pi W^2(z)} \exp\left[-\frac{2\rho^2}{W^2(z)}\right] \tag{3.19}$$

The ratio of the power carried within a circle of radius ρ_0 in the transverse plane at position z to the total power is

$$\frac{1}{p} \int_0^{\rho_0} I(\rho, z) 2\pi\rho d\rho = 1 - \exp\left[-\frac{2\rho_0^2}{W^2(z)}\right] \tag{3.20}$$

Beam Radius

Within any transverse plane, the beam intensity assumes its peak value on the beam axis, and drops by the factor $1/e^2 = 0.135$ at the radial distance $\rho = W(z)$. Since 86% of the power is carried within a circle of radius $W(z)$, $W(z)$ is regarded as the beam radius (also called the beam width). The rms width of the intensity distribution is $\sigma = \frac{1}{2} W(z)$. The dependence of the beam radius on z is governed by

$$W(z) = W_0\left[1+\left(\frac{z}{z_0}\right)^2\right]^{1/2} \tag{3.21}$$

It assumes its minimum value W_0 in the plane $z = 0$, called the beam waist. Thus W_0 is the waist radius. The waist diameter $2W_0$ is called the spot size. The beam radius increases gradually with z, reaching $\sqrt{2}W_0$, at $z = z_0$, and continues increasing monotonically with z as shown in Fig. 3.3. For $z >> z_0$,

$$W(z) \approx \frac{W_0}{z_0} z = \theta_0 z \tag{3.22}$$

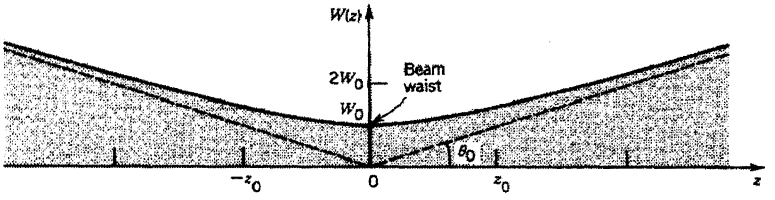

Figure 3.3 ***Beam radius as a function of propagation distance.*** **[7]**

where $\theta_0 = W_0/z_0$. Using Eqn.(3.22), we can also write

$$\theta_0 = \frac{\lambda}{\pi W_0} \tag{3.23}$$

Beam Divergence

when $z >> z_0$, the beam radius increases approximately linearly with z, defining a cone with half-angle θ_0.About 86% of the beam power is confined within this cone. The angular divergence of the beam is therefore defined by the angle

$$\theta_0 = \frac{2}{\pi}\frac{\lambda}{2W_0} \tag{3.24}$$

The beam divergence is directly proportional to the ratio between the wavelength λ and the beam-waist diameter $2W_0$.

Depth of Focus

The axial distance within which the beam radius lies within a factor $\sqrt{2}$ of its minimum value is known as the depth of focus. The depth of focus is twice the Rayleigh range.

Since the beam has its minimum width at $z = 0$, as shown in Fig. 3.3, it achieves its best focus at the plane $z = 0$. In either direction, the beam gradually grows "out of focus."

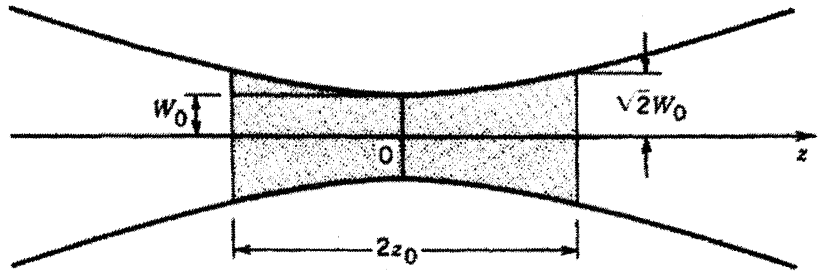

Fig. 3.4 ***The depth of focus of a Gaussian beam.***[7]

Hence depth of focus is given by

$$2z_0 = \frac{2\pi W_0^2}{\lambda} \tag{3.25}$$

Phase

The dependence of phase of the Gaussian beam on the distance is given by

$$\varphi(\rho, z) = kz - \xi(z) + \frac{k\rho^2}{2R(z)} \tag{3.26}$$

On the beam axis ($\rho = 0$) the phase is

$$\varphi(0, z) = kz - \xi(z) \tag{3.27}$$

Where kz phase of plan wave and $\xi(z)$ is phase retardation.

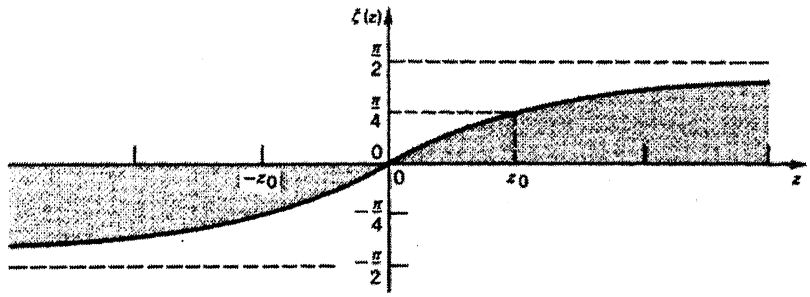

Figure 3.5 ***Phase retardation of the Gaussian beam relative to a uniform planewave at points on the beam axis.***[7]

Parameters Required for Characterizing a Gaussian Beam

Given the wavelength λ, the Gaussian beam is characterized by its peak amplitude, its direction (the beam axis), the location of its waist, and the waist radius W_0 or the Rayleigh range z_0. Thus, if the beam peak amplitude and the axis are known, two additional parameters are necessary. If the complex number $q(z) = z + jz_0$, is known, the distance z to the beam waist and the Rayleigh range z_0 are readily identified as the real and imaginary parts of $q(z)$. The q-parameter $q(z)$ is therefore sufficient for characterizing a Gaussian beam of known peak amplitude and beam axis. The linear dependence of the q-parameter on z permits us to readily determine q at all points, given q at a single point. If the beam width $W(z)$ and the radius of curvature $R(z)$ are known at an arbitrary point on the axis, the beam can be identified completely by solving Eqn.(3.8), Eqn.(3.9), and Eqn.(3.10) for z, z_0, and W_0. Alternatively, the q-parameter may be determined from $W(z)$ and $R(z)$ using the relation, $\frac{1}{q(z)} = \frac{1}{R(z)} - \frac{j\lambda}{\pi W^2(z)}$ from which the beam is identified.

In the clear atmosphere we can assume that there is no atmospheric attenuation. And also the absorption is negligible. The only loss in major role is due to the geometrical spreading that result in the mismatch of the aperture area of receiver and spot area.

3.2 OPTICAL PROPAGATION IN ATMOSPHERE UNDER VARIOUS WEATHER CONDITIONS

Free space optical communication is range and bit error limited by the atmospheric attenuation resulting from scattering during haze, rain, snow, and fog conditions in the atmospheric channel. Absorption plays a minor role while scattering is the main contributing factor which results in elastic collisions of light with atmospheric particles. In this section the effect of various weather conditions, such as Fog, Haze etc. on the optical propagation is described. To study these effects of atmosphere on the propagation of Laser light, we should be familiar with certain weather parameters discussed below.

3.2.1 Weather parameters

Visibility

This is an important parameter needed to calculate the optical attenuation due to Fog Haze, and clouds. Visibility is generally expressed as a distance. It is defined as the maximum distance at which the object contrast against its background is 2% using 550nm wavelength light that the human eye is most sensitive to. If the contrast at a distance z is C(z), then the relative contrast, defined as the ratio of C(z)/C(0) can be expressed as [20].

$$\frac{C(z)}{C(0)} = \left(\frac{L_{\max}(z) - L_{\min}(z)}{L_{\min}(z)}\right)\left(\frac{L_{\min}(0)}{L_{\max}(0) - L_{\min}(0)}\right) \tag{3.38}$$

where Lmax(z) refers to the object luminance and Lmin(z) is background luminance at distance z. The value of z for $\frac{C(z)}{C(0)} = 0.02$ is called the visual range (V). If we assume the background irradiance to be zero at z=0 and z=z, then Eqn.(3.28) reduces to

$$\frac{C(z)}{C(0)} = \frac{L_{\max}(z)}{L_{\max}(0)} \tag{3.29}$$

From Ref[20] we see that $L_{max}(z)$ can be approximated as

$$L_{\max}(z) = L_{\max}(0)\exp(-\alpha z)$$

where α is the attenuation coefficient.

Hence at visual range (i.e. at z=V) we get

$$\frac{C(V)}{C(0)} = \exp(-\alpha V) = 0.02$$

Hence

$$\alpha V = -\ln(0.02) = 3.912$$

Substituting, we get V in kilometers as

$$V = \frac{|\ln(0.02)|}{\alpha(\lambda = 550nm)} = \frac{3.912}{\alpha(\lambda = 550nm)} \text{ Km} \tag{3.30}$$

Saturation

Saturation is defined as the maximum possible amount of water vapor that can be held by air per unit volume. This parameter is a strong function of temperature. Higher the temperature, higher the maximum limit for water vapour.

Absolute humidity

Humidity is another important weather parameter if general interest. Absolute humidity is defined as the mass of water vapor in unit volume of air.

Relative humidity:

The absolute humidity parameter is rarely used to characterize humidity. Instead the parameter which is commonly used is Relative humidity, which is defined as the ratio of the absolute humidity to saturation.

Dew point

This the temperature at which saturation occurs. The air cannot hold any more water vapour at this temperature. If the temperature falls below dew point, condensation takes place.

3.2.2 Atmospheric attenuation

Atmospheric attenuation plays a big role in the performance of OWCS. However, it is difficult to fully characterize this effect. One The atmospheric attenuation is described by the Beer's law[20]

$$\tau(z) = \frac{P(z)}{P(0)} = \exp(-\alpha z) \tag{3.31}$$

$$\alpha = \alpha_{abs} + \alpha_{scat}$$

where $\tau(z)$ = transmittance at range z,

$P(z)$ = laser power at z,

$P(0)$ = laser power at the source, and

α = attenuation or total extinction coefficient (per unit length).

The total atmospheric attenuation coefficient (α) has two components, viz. α_{abs} and α_{scat}, corresponding to attenuation coefficient due to absorption and attenuation coefficient due to scattering, respectively.

Typical attenuation coefficients are for clear air, haze and fog are: clear air = 0.1 (0.43 dB/km), haze = 1 (4.3 dB/km), and fog = 10 (43 dB/km). The attenuation coefficient has contributions from the absorption and scattering of laser photons by different aerosols and gaseous molecules in the atmosphere. Main cause of atmospheric absorption is the molecules present in the atmosphere, the most important absorbing molecules being O_2 and CO_2. Depending on the weather conditions, altitude, and geographical location, the concentrations of those molecules vary. Therefore depending on the absorption band of those molecules, the transmittance reaches zero for some wavelengths. The wavelength intervals where the transmittance is relatively high are called atmospheric windows. Generally laser wavelengths (typically 785 nm, 850 nm, and 1550 nm) are chosen for outdoor transmission. The contributions of absorption to the total attenuation coefficient are very small at these wavelengths. Hence for these wavelengths, the scattering effects dominate the total attenuation coefficient.

The droplets in the atmosphere strike the photons in the laser beam and absorb their energy and reemit the light of a different kind. Depending on the size of the droplets, scattering can be divided into three types, viz. Rayleigh scattering, Mie scattering, and nonselective scattering. The type of scattering is determined by the size of the particular atmospheric particle with respect to the transmission laser wavelength.

The attenuation coefficient due to scattering can be calculated using a modified version of Eqn.3.30 [20]

$$\alpha_{scat} = \frac{3.91}{V}\left(\frac{\lambda}{550nm}\right)^{-q} \tag{3.32}$$

In the above expression, λ is the wavelength of light in nm, V is visibility in km and q is a factor which depends on V. Factor q = 1.6 for high visibility cases (i.e.V > 50 km). For

cases with average visibility (i.e. 6 km < V < 50 km), q = 1.3, while $q = 0.585\ V^{1/3}$ for low visibility cases(V < 6 km).

3.2.3 Effect of fog

One of the biggest challenges for an optical wireless link is the fog. As described earlier fog is the presence of water vapour in the atmosphere and is composed of water droplets between a few microns to a few hundred microns in diameter. The water molecules in the air absorb, scatter, and reflect any light passing through them. For short optical links, fog and heavy snow are the primary weather conditions which cause optical attenuation. Based on the visibility parameter different fog conditions can be classified into Dens fog, thick fog, moderate fog, light fog, thin fog or haze. Fig.3.6 illustrates this classification as well as the atmospheric attenuation as a function of visibility [20].

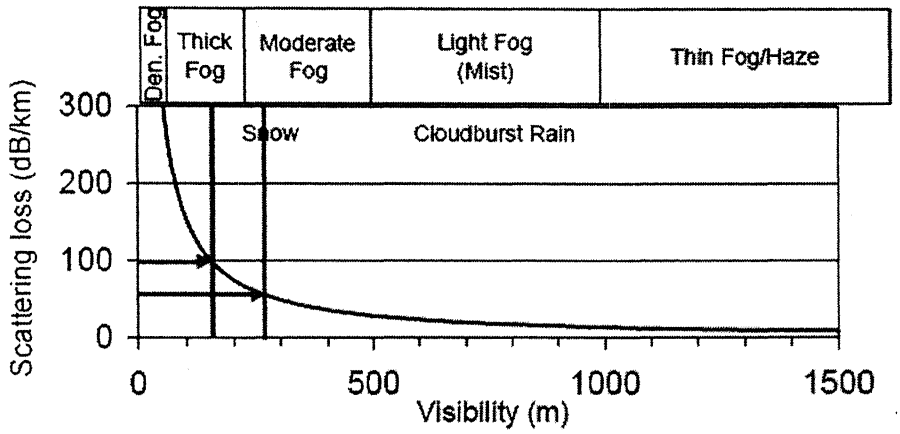

Fig 3.6 ***Scattering loss as a function of visibility***

For a practical link the power received at the receiver can be expressed as

$$P_r = P_t G_t L_p G_r \tau \tag{3.33}$$

where,

P_t is transmitted optical power,

$G_t \approx \left(\frac{2\pi W_0}{\lambda}\right)^2$ is the transmitter gain,

$L_p = \left(\frac{\lambda}{4\pi z}\right)^2$ gives the free space loss,

$G_r \approx \left(\frac{\pi D_r}{\lambda}\right)^2$ the receiver gain,

and τ the transmittance of laser beam propagating over the distance z. Now at the receiver the detector noise power can be written as [22]

$$P_d = \sqrt{F_d}(NEP) \tag{3.34}$$

where F_d is detector bandwidth and NEP is the noise equivalent power of the detector. These parameters are generally given in the detector datasheet. Here we have ignored the background light power. The current induced by the received signal, and detector noise current can be written as[22]

$$i_{sig} = \frac{MP_r\lambda q}{hc} \tag{3.35}$$

$$i_d = \frac{MP_d\lambda q}{hc} \tag{3.36}$$

where q is electronic charge, c is velocity of light, h is Plank's constant and M is the gain of the detector. For APD detectors M >>1, while for PIN photodiode M=1. Thus

$$i_{sig} = \frac{P_r\lambda q}{hc} \tag{3.37}$$

$$i_d = \frac{P_d\lambda q}{hc} \tag{3.38}$$

The number of photons generated in detector is proportional to the observation time interval and the number of photons generated in one time interval is independent of the number of photons generated in other interval. Also the detection process is a discrete process, with detector current variations around a certain average value. The detection process can be taken to be Poisson. In case of large signals this can be approximated to Gaussian.

The mean square fluctuation in the current due to the signal can be expressed by [22]

$$\overline{\sigma_{sig}^2} = 2qMFi_{sig}F_d \tag{3.39}$$

Similarly the mean square fluctuation in the current due to detector noise can be given by

$$\overline{\sigma_d^2} = 2qMFi_dF_d \tag{3.40}$$

where F is excess noise factor, which is applicable for APDs. Since we are using PIN photodiodes, F=1.

$$\overline{\sigma_{sig}^2} = 2qi_{sig}F_d \tag{3.41}$$

$$\overline{\sigma_d^2} = 2qi_dF_d \tag{3.42}$$

Since the mean square fluctuations in the photodetector current that are due to the signal and detector noise are uncorrelated and independent thus we can use the root sum of squares to calculate the total rms noise for transmission of a binary 1or 0.

$$\sigma_1 = \left(\overline{\sigma_{sig}^2(1)} + \overline{\sigma_d^2}\right)^{1/2} \tag{3.43}$$

$$\sigma_0 = \left(\overline{\sigma_{sig}^2(0)} + \overline{\sigma_d^2}\right)^{1/2} \tag{3.44}$$

where $\overline{\sigma_{sig}^2(1)}$ and $\overline{\sigma_{sig}^2(0)}$ are mean square fluctuation in current due to the signal for transmission of 1 and 0 respectively. Now we can calculate the probability distribution for each case (1 and 0) as

$$p_1(i) = \frac{\exp\left(-(i-I)^2 / 2\sigma_1^2\right)}{(2\pi\sigma_1^2)^{1/2}} \tag{3.45}$$

$$p_0(i) = \frac{\exp\left(-(i)^2 / 2\sigma_0^2\right)}{(2\pi\sigma_0^2)^{1/2}} \tag{3.46}$$

where I is the fixed signal level at a given range and atmospheric extinction. The threshold is taken as the point where the two distributions intersect. For large signal to noise ratios this point is usually one half of the signal level (i.e. 0.5I). Integrating each distribution from this point to the appropriate limits will give the probability of detecting either 1 or 0 in error thus

$$err_1 = \int_{-\infty}^{0.5I} \frac{\exp\left(-(i-I)^2 / 2\sigma_1^2\right)}{(2\pi\sigma_1^2)^{1/2}} di \tag{3.47}$$

$$err_0 = \int_{0.5I}^{\infty} \frac{\exp\left(-(i)^2 / 2\sigma_0^2\right)}{(2\pi\sigma_0^2)^{1/2}} di \tag{3.48}$$

The mean of these two probabilities is the overall BER.

$$BER = \frac{err_0 + err_1}{2} \tag{3.49}$$

Attenuation Characteristics under Different Fog Conditions

The attenuation vs visibility curves for various fog conditions are shown in Fig (3.7a and b).

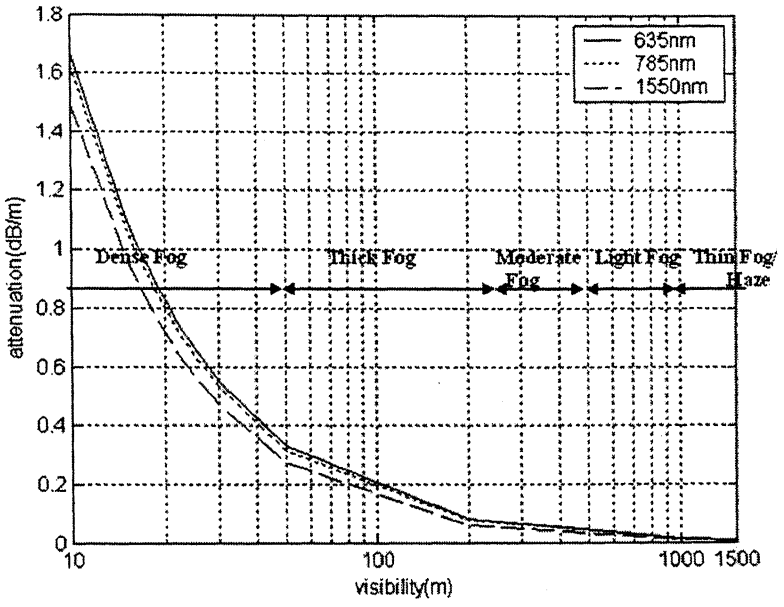

(a)

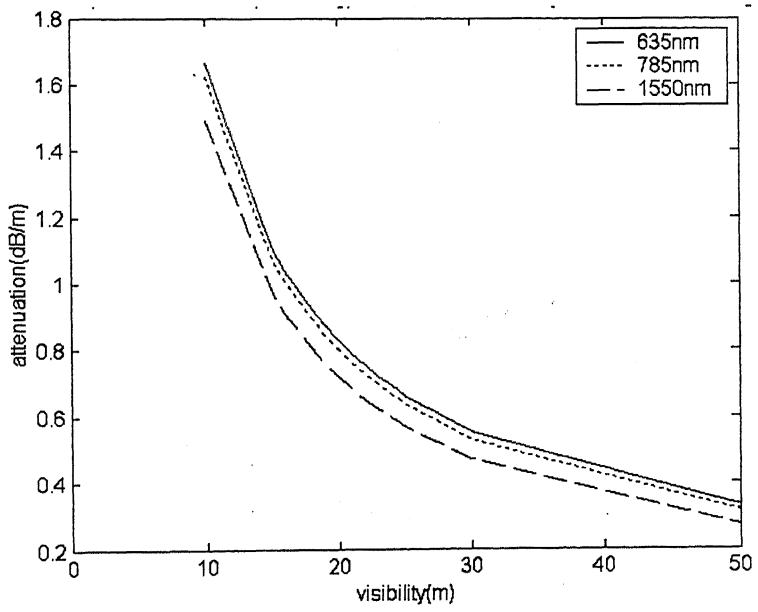

(b)

Fig.3.7 ***Atmospheric attenuation due to fog as a function of visibility***

These conditions are defined as per the visibilities as shown in Fig. (3.6). For example, thick fog is defined as the weather condition where the visibility is between 50 m and 250 m. it can be inferred from these curves that transmitting at 1550nm is advantageous in terms of atmospheric scattering losses in all weather. We see from the curves in Fig.3.7 that there is an inverse relationship between visibility and the amount of attenuation. The attenuation curve in Fig. 3.7(a) is expanded and redrawn in Fig. 3.7(b) for visible distances up to 50m.

3.3 OPTICAL PROPAGATION IN RANDOM MEDIA

When laser light propagates through the atmosphere its characteristics (amplitude, intensity, polarization and phase) get altered due to scattering and absorption. Another mechanism that influences the propagation of laser beam is small fluctuation in the refractive index of the air. These turbulent refractive index fluctuations in the atmosphere lead to intensity fluctuations, which are also known as scintillations. In most cases the atmosphere behaves turbulent. Turbulence is defined as air motions or eddies. These eddies transport heat and water vapour with refractive indices different from their surroundings. This results in refractive index fluctuations, since the refractive index of air is a function of temperature and humidity. It can be given approximately by[8]

$$n-1=77.6(1+0.00752\lambda^{-2})(P/T)10^{-6}$$

Atmospheric turbulence can degrade the performance of free-space optical links, particularly over ranges of the order of 1 km or longer. These fluctuations can lead to an increase in the link error probability, limiting the performance of the link. Atmospheric turbulence can be physically described by Kolmogorov theory. The energy of large eddies is redistributed without loss to eddies of decreasing size until finally dissipated by viscosity. The size of turbulence eddies normally ranges from a few millimeters to a few meters, denoted as the inner scale l_0 *and* the outer scale L_0, respectively. We can express the refractive index as,[13]

$$n(\vec{r},\ t) = n_0 + n_1(\vec{r},\ t)$$

where n_0 is the average index and $n_1(\vec{r},\ t)$ is the fluctuation component induced by spatial variations of temperature and pressure in the atmosphere. The correlation function of n_1 is defined as

$$\Gamma_{n_1}(\vec{r_1},\ t_1;\vec{r_2},\ t_2) = E\left[n_1(\vec{r_1},\ t_1)n_1(\vec{r_2},\ t_2)\right]$$

Putting $t_1 = t_2$ we can get $\Gamma_{n_1}(\vec{r_1},\ \vec{r_2})$, which is the spatial coherence of the refractive index. Mutual coherence function (MCF) is widely used to describe spatial coherence of optical waves [9]. An optical field can be written as

$$u(\vec{r}) = A(\vec{r})\exp\left(j\phi(\vec{r})\right) = u_0(\vec{r})\exp[\phi_1]$$

where $u_0(\vec{r}) = A_0(\vec{r})\exp\left[j\phi_0(\vec{r})\right]$ is the field amplitude without air turbulence. The exponent of the perturbation factor can be given by [13].

$$\phi_1 = \log\left[\frac{A(\vec{r})}{A_0(\vec{r})}\right] + j\left[\phi(\vec{r}) - \phi_0(\vec{r})\right] = X + jS$$

where X is the log-amplitude fluctuation and S is the phase fluctuation. These fluctuations can be assumed independent Gaussian random variables. This assumption is valid for long propagation distances through turbulence. The marginal distribution of the log-amplitude is given by

$$f_X(X) = \frac{1}{(2\pi\sigma_X^2)^{1/2}}\exp\left[-\frac{(X - E[X])^2}{2\sigma_X^2}\right]$$

The intensity can be related with X as

$$I = I_0\exp(2X - E[X])$$

where $E[X]$ is the ensemble average of log-amplitude X. From the above two equations the average light intensity can be calculated

as $E[I] = E[I_0\exp(2X - 2E[X])] = I_0\exp(2\sigma_X^2)$

$$\sigma_x^2 = 0.56\left(\frac{2\pi}{\lambda}\right)^{7/6}\int_0^z C_n^2(x)(z-x)^{5/6}dx$$

$$\phi_n(\vec{k}) = 0.033C_n^2k^{-11/3}$$

$$C_n^2(h) = K_0 h^{-1/3} \exp\left(\frac{-h}{h_0}\right)$$

Here, C_n is the wave number spectrum structure parameter, Here K_0 is a parameter describing the strength of the turbulence and h_0 is the effective height of the turbulent atmosphere. For atmospheric channels near the ground (h<18.5m), C_n^2 can vary from 10^{-13} $m^{-2/3}$ for strong turbulence to 10^{-17} $m^{-2/3}$ for weak turbulence, with 10^{-15} $m^{-2/3}$ often quoted as a typical "average" value .The distribution of light intensity fading induced by turbulence is log-normal [13] and can be given by:

$$f_I(I) = \frac{1}{2I(2\pi\sigma_X^2)^{1/2}} \exp\left[-\frac{[\ln(I) - \ln(I_0)]^2}{8\sigma_X^2}\right] \tag{3.50}$$

3.4 GAUSSIAN BEAM OPTICS

In many applications it is necessary to focus, modify, or shape the laser beam by using lenses and other optical elements. This is especially true in the case of semiconductor laser diodes, which have very large divergence angles (typically >30 degrees).

3.4.1 Transmission through a Thin Lens

If a Gaussian beam is transmitted through a set of circularly symmetric optical components aligned with the beam axis, the Gaussian beam gets transformed to another Gaussian beam as long as the overall system maintains the paraxial nature of the wave. As a result of the transformation the beam waist and curvature are altered so that the beam is reshaped.

The complex amplitude transmittance of a thin lens of focal length f is proportional to $\exp(jk\rho^2/2f)$. When a Gaussian beam crosses the lens its complex amplitude, given in Eqn.3-7, is multiplied by this phase factor. As a result, its wavefront is bent, but the beam radius is not altered. A Gaussian beam centered at z = 0 with waist radius W_0 is transmitted through a thin lens located at a distance z, as illustrated in Fig. 3.8. The phase

at the plane of the lens is $kz + k\rho^2/2R - \xi$, where $R = R(z)$ and $\xi = \xi(z)$ are given by (3.9) and (3.10), respectively. The phase of the transmitted wave is altered to

$$kz + k\rho^2/2R - \xi - k\frac{\rho^2}{2R'} = kz + k\frac{\rho^2}{2R'} \tag{3.51}$$

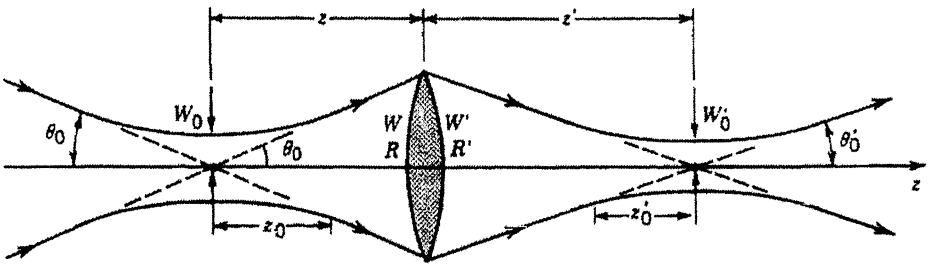

Fig. 3.8 ***Transmission of a Gaussian beam through a thin lens.[7]***

where

$$\frac{1}{R'} = \frac{1}{R} - \frac{1}{f} \tag{3.52}$$

The transmitted wave is itself a Gaussian beam with width $W' = W$ and radius of curvature R', where R' satisfies the imaging equation $\frac{1}{R'} = \frac{1}{R} - \frac{1}{f}$. Note that R is positive since the wavefront of the incident beam is diverging and R' is negative since the wavefront of the transmitted beam is converging. The waist radius of the new beam is

$$W_0' = \frac{W}{\left[1 + (\pi W^2/\lambda R')^2\right]^{1/2}} \tag{3.53}$$

And the center is located a distance

$$-z' = \frac{R'}{1 + (\lambda R'/\pi W^2)^2} \tag{3.54}$$

Parameters of the two beams are related by following equations

Waist radius $$W_0' = MW_0 \tag{3.55}$$

Waist location $$(z' - f) = M^2(z - f) \tag{3.56}$$

Depth of focus $$2z_0' = M^2(2z_0) \tag{3.57}$$

Divergence $$2\theta_0' = \frac{2\theta_0}{M} \tag{3.58}$$

Magnification $$M = \frac{M_r}{(1+r^2)^{1/2}} \tag{3.59}$$

Where $$r = \frac{z_0}{z-f} \text{ and } M_r = \left|\frac{f}{z-f}\right| \tag{3.60}$$

3.4.2 Focusing of LASER beam

If a lens is placed at the waist of a Gaussian beam, as shown in Fig. 3.9, the parameters of the transmitted Gaussian beam are determined by substituting z = 0 in equations

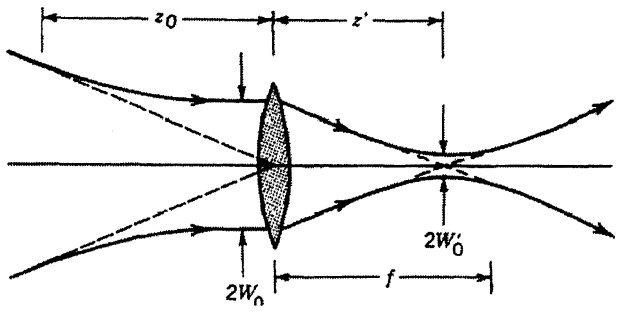

Fig. 3.9 ***Focusing a beam with a lens at the beam waist[7].***

(3.55) to (3.60). The transmitted beam is then focused to a waist radius W_0' at a distance z' given by

$$W_0' = \frac{W_0}{\left[1+(z_0/f)^2\right]^{1/2}} \tag{3.61}$$

$$z' = \frac{f}{1+(f/z_0)^2} \tag{3.62}$$

If the depth of focus of the incident beam $2z_0$ longer than the focal length f of the lens, then $W_0' \approx (f/z_0)W_0$. Using $z_0 = \pi W_0^2/\lambda$ we can obtain

$$W_0' \approx \frac{\lambda}{\pi W_0'} f = \theta_0 f \tag{3.63}$$

$$z' \approx f \tag{3.64}$$

The transmitted beam is then focused at the lens's focal plane as would be expected for parallel rays incident on a lens. This occurs because the incident Gaussian beam is well approximated by a plane wave at its waist. The spot size expected from ray optics is, of course, zero. In wave optics, however, the focused waist radius W_0' is directly proportional to the wavelength and the focal length, and inversely proportional to the radius of the incident beam. In the limit $\lambda \to 0$, the spot size does indeed approach zero in accordance with ray optics. The diameter of focused spot is given by

$$2W_0' \approx \frac{4}{\pi}\lambda F_{\#} \tag{3.65}$$

where, $F_{\#} = \frac{f}{D}$ is F number of the lens.

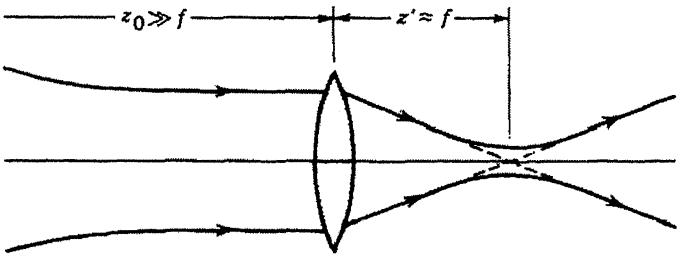

Fig. 3.10 ***Focusing a collimated beam.***[7]

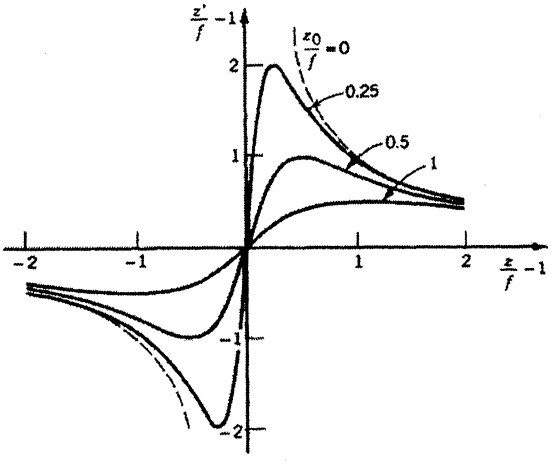

Figure 3.11 ***Relation between the waist locations of the incident and transmitted beams.***[7]

When a Gaussian beam is transmitted through a thin lens of focal length f, the locations of the waists of the incident and transmitted beams z and z' are related by

$$\frac{z'}{f} - 1 = \frac{z/f - 1}{(z/f - 1)^2 + (z_0/f)^2} \tag{3.66}$$

3.4.3 Optimum Collimation

We can use the standard expression for $W(z)$ given below to calculate beam radius for any value of z.

$$W(z) = W_0\left[1 + \left(\frac{\lambda z}{\pi W_0^2}\right)^2\right]^{1/2}$$

We can also utilize this equation to see how final beam radius varies with z for a given starting beam radius. It can be shown that for $\lambda = 632.8$ nm and $z = 100$ m, the beam radius at 100 m reaches a minimum value for a starting beam radius of about 4.5 mm. Therefore, if we want to achieve the best combination of minimum beam diameter and minimum beam spread (or best collimation) over a distance of 100 m, our optimum starting beam radius would be 4.5 mm. Any other starting value would result in a larger beam at $z = 100$ m.

We can find the general expression (approximate expression) for the optimum starting beam radius for a given distance, z as

$$W_0(opt) = \left(\frac{\lambda z}{\pi}\right)^{1/2}$$

Using this optimum value of W_0 will provide the best combination of minimum starting beam diameter and minimum beam spread (ratio of W(z) to W(0) over the distance z). For $z = 100$ m and $\lambda = 632.8$ nm, W_0(optimum) = 4.48 mm. If we put this value for W_0 (optimum) back into the expression for $W(z)$,

$$W(z) = \sqrt{2}(W_0)$$

Thus, for this example, $W(100) = \sqrt{2}(4.48)$

If we use beam-expanding optics that allows us to adjust the position of the beam waist, we can actually double the distance over which beam divergence is minimized. By focusing the beam-expanding optics to place the beam waist at the midpoint, we can restrict beam spread to a factor of the square root of 2 over a distance of 2 z_0, as opposed to just z_0.

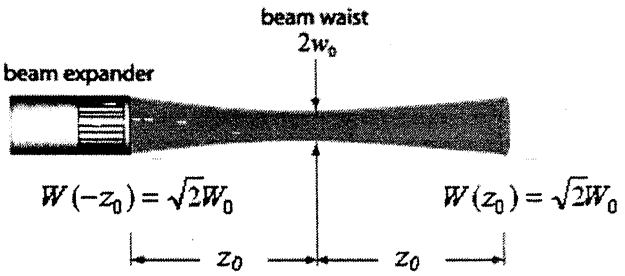

Figure 3.12 ***Focusing a beam expander to minimize beam radius and spread over a specified distance*** [23]

This result can now be used in the problem of finding the starting beam radius that yields the minimum beam diameter and beam spread over 100 m. Using 2(z_0) = 100, or z_0 = 50m, and λ = 632.8 nm, we get a value of W(z_0) = $(2\lambda/\pi)^{1/2}$ = 4.5 mm, and W_0 = 3.2 mm. Thus, the optimum starting beam radius is the same as previously calculated. However, by focusing the expander we achieve a final beam radius that is no larger than our starting beam radius, while still maintaining the $\sqrt{2}$ factor in overall variation. Alternately, if we started off with a beam radius of 6.3 mm, we could focus the expander to provide a beam waist of W_0 = 4.5 mm at 100 m, and a final beam radius of 6.3 mm at 200 m.

CHAPTER 4

DESIGN OF SUBSYSTEMS FOR THE EXPERIMENTAL OWCS

Design of an optical communication system is mostly dictated by the basic requirement of the system and also the availability of the components and cost. The system designer has many choices when selecting components for an outdoor optical communication system. The typical requirement of the system for our experiments are shown in Table 4.1.Designing fiber optic transmitters and receivers for wireless applications presents unique design challenges that are different from those found in long-distance regulated telecommunications applications. The transmitter in an OWCS communications transceiver generally consists of a driver and an optical emitting device. This device can be an LED or a laser. The driver must convert digital data into current pulses that cause the source to generate light. For outdoor applications the power requirements are high and LED cannot provide the necessary power. This rules out the use of LEDs for outdoor applications. So only lasers are used for outdoor applications. Hence the points to keep in mind while designing an outdoor optical wireless link are

- **Source:** Source must be a Laser. The key factors to be considered are optical power launched into the medium, rise and fall time, stability etc.
- **Transmitter configuration:** According to the nature of transmission (Digital or analog transmission) the transmitter may be designed. The main deciding factors in the transmitter design are input impedance, supply voltage, dynamic range, optical feedback etc.
- **Detector:** p-n, p-i-n, or avalanche photodiode can be chosen according to the application. Responsivity, response time, active area, bias voltage, dark current etc. are the important specifications of a detector.

- **Receiver configuration**: various components of the receiver like Preamplifier (low impedance, high impedance or trans-impedance front-end), post amplifier etc. has to be designed according to the need of application. The important characteristics of a receiver are BER or SNR, dynamic range etc.
- **Modulation and coding:** intensity modulation, pulse modulation techniques for either digital (e.g. PCM, Adaptive delta modulation) or analog (PAM, pulse frequency modulation, PWM, PPM) transmission cab be used. Various encoding schemes for digital transmission such as biphase (Manchester) and delay modulation (Miller) codes also can be used. For analog transmission, direct intensity modulation or frequency of the electrical sub-carrier can be used.

4.1 TRANSMITTER DESIGN

The specifications for the transmitter were formulated as shown in Table 4.1. In transmitter design perspective the important thing is selection of an optical source. The following are major Performance Requirements of optical source

S.No.	Specification	Value
1	Data rate	20 Mbps
2	Link range	100m
3	Transmission type	Digital
4	Acceptable BER	10^{-9}
5	Cost	Low
6	Reliability	High

Table 4.1 ***Link specifications***

- The light output should be highly directional.
- Should emit light at wavelengths where the detectors are efficient and atmospheric losses are low.
- Capable of simple signal modulation (i.e. direct) over a wide bandwidth extending from audio frequencies to beyond the gigahertz range.

- Must be capable of maintaining a stable optical output which is largely unaffected by changes in ambient conditions (e.g. temperature)
- It is essential that the source is comparatively cheap and highly reliable in order to compete with conventional transmission techniques.
- A semiconductor laser should be very compact in size.
- The spatial and spectral characteristics of a semiconductor laser are strongly influenced by the properties of the junction medium. (such as band gap and refractive index variations).
- Modulation at high frequencies should be achieved.

4.1.1 Design considerations for transmitter

As discussed in chapter 2 for outdoor optical link, the laser diode is the best choice, and hence the transmitter specifications are laid down accordingly. The specifications for the transmitter based on the important transmitter parameters are as follows

- ***Optical power output:*** - In an outdoor optical link, one of the most important transmitter parameter is the amount of optical power that the transmitter can emit in to air with respect to the dc drive current supplied. From the optical power budgeting considerations [4,14], we can find the minimum average optical power required at the transmitter end as

  $$P_T = P_R + C_L + M_a \text{ dBm} \quad \text{.....(4.1)}$$

  where, P_T : minimum average power required at the transmitter to give full modulation depth , P_R : minimum average power required at the receiver, C_L : total losses in dBm, and M_a the safety margin.

- ***Speed of response*:** The response of an optical source to a current step input is often specified in terms of rise time, which is reciprocally related to the device frequency response. The rise time of many available LEDs lie between 2 and 50 ns and give 3 dB bandwidth of around 7 to at least 175 MHz. Rise times for laser

diodes are generally of the order of 0.1-1 ns, thus allowing large bandwidth. However, injection laser performance is limited by the device switching time. Hence to achieve higher speeds it is necessary to minimize the switch on delay. Total rise time can be given by[14]

$$t_{sys} = 1.1\left(t_s^2 + t_d^2\right)^{1/2} \tag{4.2}$$

where

t_{sys} :total rise time of the link in ns,

t_s :rise time of the transmitter source in ns

t_d :rise time of the detector in ns

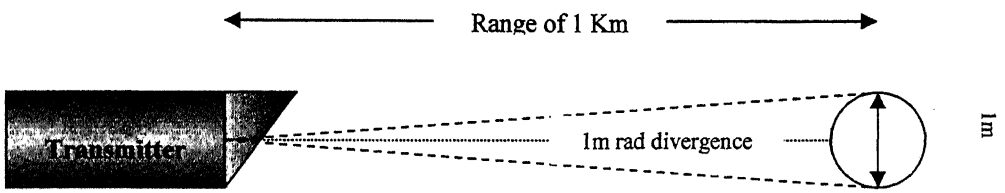

Fig. 4.1 ***Beam divergence***

- ***Beam divergence*: -** Transmit beam spreads constantly with increasing range at a rate determined by the far-field diffraction angle, as shown in Fig. 4.1. This gives rise to geometrical spreading of the beam [4].

$$\text{Geometrical spreading loss} = 10\log\left[\frac{A_R}{A_T + \frac{\pi}{4}(\theta z)^2}\right] \tag{4.3}$$

where, A_R is Surface area of receive aperture, A_T is Surface area of the transmit aperture divergence, θ is Angle in radiance, z is Link Range in meters.

- ***Thermal behavior***: - The thermal behavior of optical source can limit their operation within the optical transmitter. Threshold currents of AlGaAs devices for example, increases by approximately by 1% per degree centigrade increase in junction temperature. Hence any significant increase in junction temperature of the injection laser may cause loss of biasing and a reduction in the optical output power. Hence an optical feedback circuitry is required to maintain a constant optical output level from the device.

- ***Extinction ratio penalty***: - This is the ratio of the optical energy transmitted in the '0' bit period to that transmitted during the '1' bit period. For an ideal system it should be zero. But since injection lasers are pre-biased during a '0' bit period, some optical power may be emitted during the pulse. Typical extinction ratios are 0.05-0.1 and such non-zero values give rise to noise penalty, called extinction ratio penalty within the optical link. In practice it is found to be in the range of 1-2 dB.

- ***Eye safety***: The maximum optical power out put of the transmitter is limited by the eye safety considerations as given in Table 2.1. Out door point-to-point systems generally use high power lasers that operate in the class 3B (2.5-500mW) to achieve a good power budget. Hence the optical power output of the transmitter source can be from 1.28-500 mW for wavelength of 0.8-0.9 nm ranges. The safety standards recommend that these systems should be located where the beam cannot be interrupted or viewed inadvertently by a person. Roof top locations or high walls are the right places to install the link.

- ***Cost***: - The cost of the transmitter should be as low as possible and should use readily available components. The circuit should be simple and easy to design and fabricate.

4.1.2 Wavelength selection

Optical wireless communication is now becoming very popular, robust optical transmitters and receivers are the gift of this technology for establishing point to point communication through the atmosphere despite of there advantages these systems are also having challenges. The selection of wavelength is a crucial issue. Mainly Two factors should be considered while specifying the operating wavelength. First is Eyesafety. The system must not pose any danger to the people who encounter the beam. Light from Lasers in 400-1400nm wavelength range is passed through and lens and is focused on to a small spot on the retina hence it is more dangerous. In contrast the beams at wavelength larger than 1400 nm are absorbed by the cornea and lens and do not focus on the retina. Currently two categories of the optical wireless systems are coming in the market- systems operating near 800nm and near 1550nm. It may be noted that the allowable safe power at 1550nm is about 50 times higher than that at 800nm.[24].

The second point to keep in mind is Performance of the system. Some performance related factors should also be considered. Atmosphere poses several challenges to the OWC systems. Some optical attenuation processes are wavelength dependent, such as Rayleigh scattering from air molecules which varies as the fourth power of wavelength. The other attenuation process is Mie-scattering which causes more attenuation than Rayleigh scattering. The wavelength dependence of Mie scattering is sensitive to the nature of fog droplets; it is stronger when the size of the droplet is nearly equal to the wavelength of light. But in light fog and haze the attenuation due to mie scattering is less. The wavelength dependence of scattering attenuation coefficient is given by [20]

$$\alpha = \frac{3.91}{V}\left(\frac{\lambda}{550nm}\right)^{-q}$$

where V is visibility in Km, and $q = 0.585V^{1/3}$, for V<6 Km.

Hence for OWC inks used in high fog situations, lower wavelength source will be the right choice.

Another factor affecting the wavelength selection is beam spreading due to diffraction which is linearly proportional to the wavelength. The resulting attenuation can be given by $(4\pi A_t / \lambda^2)$ where A_t is the transmitting area.

For terrestrial OWC links the other challenging issue is Background radiation (sunlight).The solar background radiation is four times less effective for 1550nm than for 800nm .The performance of receiver is also wavelength dependent. Generally the photodiodes near 800nm and near 1550nm achieve comparable quantum efficiency. The output response of the detector depends on the energy of the photon. A photon at 800nm has roughly double the energy of that at 1550nm. Hence for same noise conditions the optical energy will be at 1550nm will be approximately 3dB less. This necessitates higher sensitivity of a 1550nm system. Also the capacitance and gain of the APD are also wavelength dependent quantities. Hence the selection of wavelength for an OWC system should be done in the light of above discussed factors.

4.1.3 Transmitter Design

The transmitter circuit basically consists of a pre-biasing circuit and a driver circuit as shown in Fig.4.2. Due to the non-availability of laser diodes, a low cost laser pointer was used in our design. A 47 K ohms resistance is included in series with the laser to avoid switch-on and switch-off surges. Biasing circuit is designed such that it allows a dc current of value just below the threshold current of the laser to flow when the data input is a '0'. Driver circuit is designed such that it allows a dc current of maximum permissible value to flow through the laser, when the data input is a '1'. Details of the circuit will be given in next chapter.

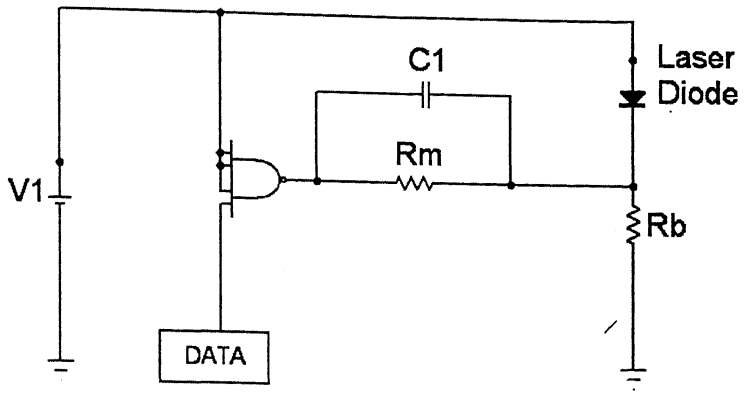

Fig. 4.2. ***Transmitter circuit***

4.2RECEIVER DESIGN

In the design of an outdoor optical wireless link, one of the important elements of the system is the receiver. Any optical communication system requires a defined range of optical power into the receiver for proper operation. In practice, the received power must be higher than the minimum level. The difference between these two power levels is the optical margin. When an optical wireless communication system is designed, consideration is given to expected transmitter power, receiver sensitivity, and atmospheric losses. The link loss budget is then planned so that there is some extra optical power at the receiver (e.g. optical margin) to allow for degradation of optical components and atmospheric losses.

4.2.1 Performance Requirements of Photodetector

The fundamental goal in the design of an optical receiver is to minimize the amount of optical power that must reach the receiver in order to achieve a given BER or SNR. This power commonly referred to as sensitivity, depends upon the detector type and characteristics as well as the design of the amplifier. The important element to be selected

is photodetector. The following criteria define the important performance and compatibility requirements for detectors:

- The photodetector should have high quantum efficiency, i.e. produce a maximum electrical signal for a given amount of optical power.
- The sensitivity of the photodetector at operating wavelengths should be high enough.
- Response time should be small to obtain a suitable bandwidth.
- The detector should have High fidelity to reproduce the received signal waveform with fidelity over a wide range. A minimum noise should be introduced by the detector. The gain mechanism within the detector or associated circuitry must also be of low noise.
- Dark currents, leakage currents and shunt conductance should be low.
- Stable performance characteristics (sensitivity, noise, internal gain). Variation of performance characteristics vary with temperature and other ambient conditions should be small or necessary compensation should be provided.
- Low Power consumption. Ideally the detector should not require excessive bias voltages or currents.
- High reliability.
- Low cost.

The choice of detector depends on the application. A photoconductor is an attractive device, considering its simplicity of fabrication and ease of operation. However, its high dark current and the associated Johnson noise make it unsuitable for high-performance communication applications. The best combination of bandwidth and sensitivity is obtained by the p-i-n diode and the APD. Fig. 4.3[1] shows a comparison of the minimum detectable optical power in photoconductors, p-i-n diodes and APDs [14]. Avalanche photodiodes are advantageous over PIN photodiodes in applications where electrical noise in the preamplifier is dominant, and not the shot noise. They are very useful where the signal is weak, and the only

source of noise is the shot noise of the photodetector dark current. In optical wireless systems, however, the background light is generally large resulting in high shot noise, even with PIN diode, thus limiting the usefulness of APDs. Hence we decided to use a PIN photodiode as the detector.

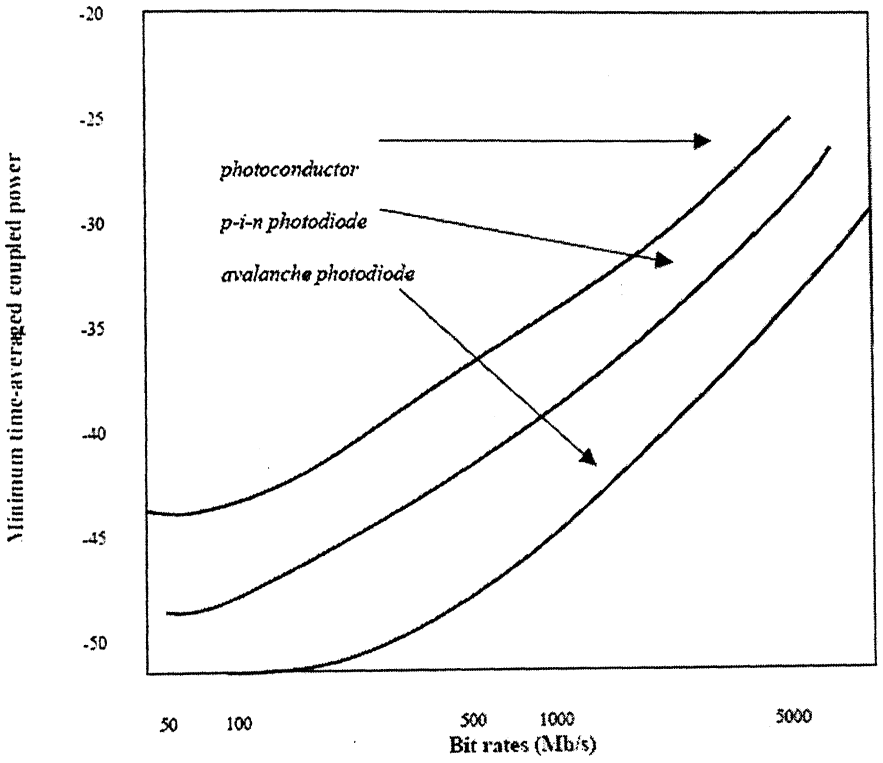

Fig4.3 ***Comparison of the minimum detectable optical power in photoconductors, p-i-n diodes and APDs***

4.2.2 Receiver Front End Circuits

The input optical power required at the receiver depends on the detector type and the electrical components within the receiver structure. It is strongly dependent upon the Noise (i.e. quantum, dark, and thermal) associated with the receiver.

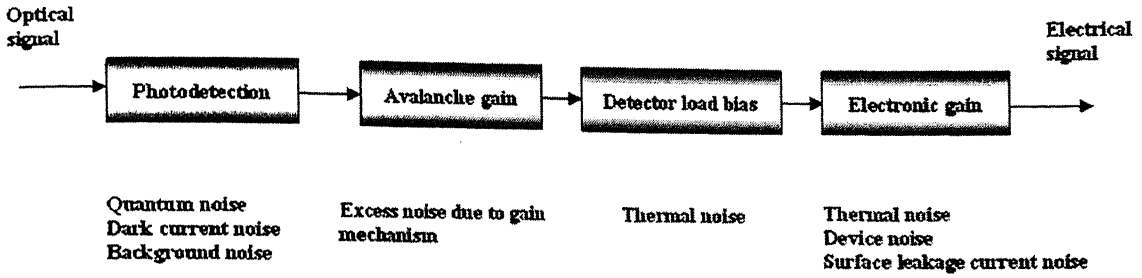

Fig. 4.4 ***Various noises sources encountered in the detection process***

Fig. 4.4 shows a block diagram of the front end (detector and pre-amplifier) of an optical receiver and the various noise sources associated with it [14].

There are basically three types of receiver front-end configurations, viz. low impedance, high impedance, and transimpedance front ends. Each one has its own merits and demerits. Selection of a front end depends upon the requirements of sensitivity, bandwidth and dynamic range. **Sensitivity** is defined as the minimum average optical power required at the receiver for a specified performance and data rate. **Dynamic range** specifies the range of power over which the receiver is able to function as per specifications. It is generally expressed in decibels as the ratio of the maximum optical power to the minimum optical power incident on the receiver giving the specified performance.

4.2.3 Design Considerations for Receiver

***Bandwidth*:** Bandwidth of the receiver should be at least 10 MHz to be able to receive a bit rate of 20 Mbps as per the Nyquist criteria. But since this is a point-to-point outdoor link the transmitter power can be up to several milliwatts and also the full transmitter power is concentrated on to the receiver. Hence the selection of bandwidth for the receiver should be a safe choice. For an installed point-to-point link the dynamic range requirement has to cater to the environmental and ageing margins and the range of link length that the receiver is expected to accommodate.

Sensitivity: As far as the sensitivity of the receiver is concerned, one always tries to make the most sensitive receiver. But considering limitations set by the quantum limit and compromises required in a practical receiver due to various factors like dynamic range, thermal noise, dark current, inter symbol interferences and degradation due to the optical source, a practical receiver can achieve around 10-15dB of the fundamental limit set by the quantum theory, which is –38.9dBm for a p-i-n diode [2,15].

Cost: The cost should be as little as possible using components available in the laboratory and the circuit should be simple, reliable and stable.

4.2.4 Transimpedance amplifier Design

Of most importance to the optical receiver are the photodetector and the following low noise preamplifier. Together these two elements dictate many of the receiver's characteristics as well as its performance. We decided to choose the popular transimpedance (TZ) preamplifier design with a FET front end [15]. TZ amplifier is shown in Fig. 4.5.

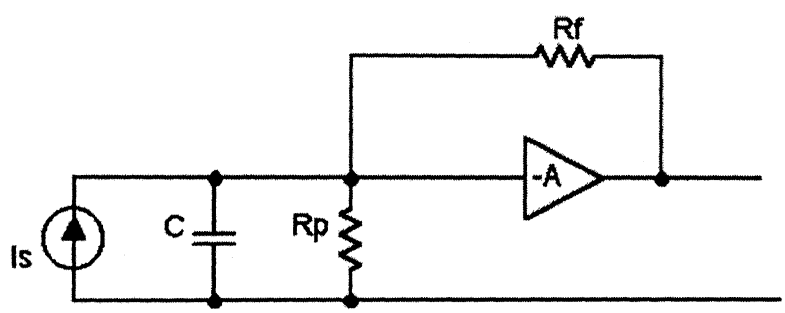

Fig. 4.5 ***Feed back (TZ) amplifier.***

The TZ preamplifier design is a popular approach to avoid the dynamic range problem. In addition, it is normally designed to take advantage of the negative feedback effect so that the amplifier bandwidth is extended to the desired value. Thus no equalizing circuitry is

required. However because of the thermal noise of the feedback resistor, the receiver noise level is higher and the receiver sensitivity is somewhat less than that of a high impedance design.

In principle, the receiver sensitivity degradation of the transimpedance design can be kept to negligible value by keeping the feedback resistance as large as possible. For a desired bandwidth value this can be achieved by increasing the amplifier open-loop gain. However the maximum open loop gain is ultimately limited by the propagation delay and phase shift of the amplifying stages inside the feed back loop. A certain gain and phase margin is desirable to assure stability and acceptable pulse response. Thus as the bit rate increases, the number of amplifying stages and the open loop gain is necessarily reduced. As a result the thermal noise of the feedback resistance in a transimpedance amplifier is normally a significant portion of the total noise.

It should be noted that a receiver amplifier can be designed to have transimpedance structure but with the feedback resistance increased so that its thermal noise contribution to the receiver noise is negligible. Such an amplifier is still classified as a high impedance design because it usually requires further equalization.

The receiver amplifier noise level is often characterized by an input equivalent noise current power at a given operating bit rate. For a FET front-end amplifier, the input equivalent noise current power is given by[15]

$$\left\langle i_{na}^2 \right\rangle = \frac{4KT}{R_f} I_2 B + 2eI_L I_2 B + \frac{4KT\Gamma}{g_m}(2\pi C_T)^2 f_c I_f B^2 + \frac{4KT\Gamma}{g_m}(2\pi C_T)^2 I_3 B^3 \qquad (4.4)$$

where, B is operating bit rate, R_f is feedback resistance in TZ design, I_L is total leakage current (FET gate current and un-multiplied dark current component of the photodiode), g_m is FET transconductance, C_T is total input capacitance (including photodiode and stray capacitance), f_c is the 1/f noise corner frequency of the FET, Γ is numerical constant, K is Boltzman constant, and T is absolute temperature.

where , η is photodetector quantum efficiency, $\overline{P}$ is average optical power required for a desired BER , $h\Omega = hc/\lambda$ is the photon energy, Q = a parameter relating to the desired error rate (6 for BER of 10^{-9}), For the case of a simple p-i-n photodiode, we have $G = F(G) = 1$ and $I_{dm} = 0$. In addition, the amplifier noise term $\langle i_{na}^2 \rangle$ normally dominates the signal shot noise term $QeBI_1$ in Eqn.4.7. Thus the receiver sensitivity expression for a p-i-n photodiode becomes

$$\eta \overline{P} = Q \frac{h\Omega}{e} \sqrt{\langle i_{na}^2 \rangle} \tag{4.8}$$

Thus we see that for a p-i-n photodiode, the receiver sensitivity is proportional to $\langle i_{na}^2 \rangle$. The effect of dark current on the receiver sensitivity is such that, higher the bit rate, the less important the noise effect of the dark current. Other receiver sensitivity degradation sources are inter-symbol interference, optical source extinction ratio and optical source bandwidth.

Dynamic range: - The receiver dynamic range is the difference (in decibels) between the minimum detectable power level (receiver sensitivity) and the maximum allowable input power levels. As the received optical power increases, from its minimum level, the receiver bit error rate decreases because a higher signal to noise ratio is obtained. This improved performance continues until saturation or overloading occurs at the receiver. At this point (i.e. end of linear operation), the received signal waveform becomes distorted and the error rate starts to increase due to inter-symbol interference. The dynamic range is a function of the feedback resistor of the front-end receiver amplifier. As the feedback resistor decreases, the maximum allowable received optical power increases. Thus the dynamic range is increased. However, reduction in the feedback resistor, results in an increase in the amplifier noise level. Thus there is a trade-off between high receiver sensitivity and wide dynamic range.

***Bandwidth*:** - Let us now consider the current to voltage transfer functions of two amplifiers, one without feed back (HZ) and the other with feedback (TZ). For the non-feed back case this transfer function $H(\omega)$ is given by [16]

$$H(\omega) = \frac{AR_p}{1 + j\omega R_p C_T} \tag{4.9}$$

where A is open loop voltage gain ,R_p is and $C_T = C_d + C_i$,R_b is bias resistor, R_i is input resistance of the amplifier, C_d is detector capacitance, C_i is input capacitance of the amplifier. For the feedback case the transfer function $H_F(\omega)$ is,

$$H(\omega) = \frac{R_f}{1 + (j\omega R_f C_T / A)} \tag{4.10}$$

Comparing Eqn. 4.9 and Eqn. 4.10 it can be seen that the feed back amplifier has a much greater bandwidth than the non-feedback amplifier, particularly if A is large. This greatly facilitates subsequent equalization and makes the feedback configuration, in the medium frequency range. At high frequencies the propagation delay existing in the closed loop of the feedback amplifier reduces the phase margin and becomes a significant design factor.

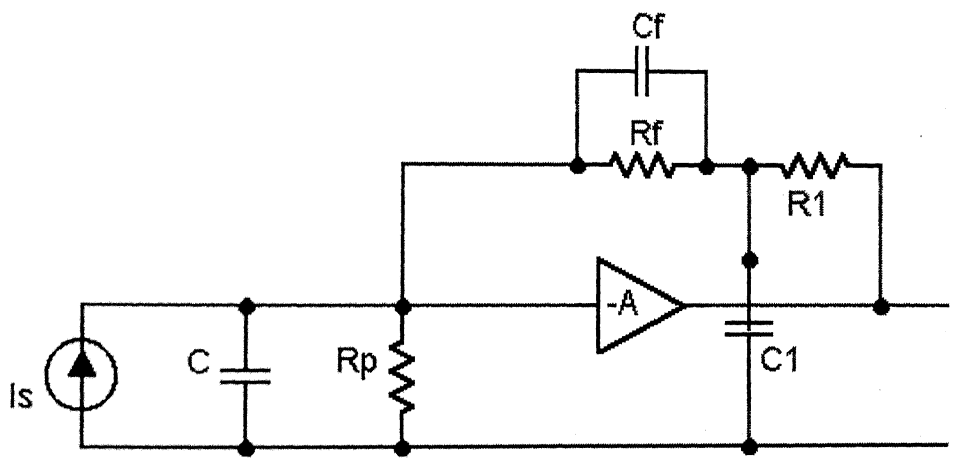

Fig. 4.6. ***Feed back amplifier with compensating network.***

A feedback amplifier is shown in simplified form in Fig. 4.6. From Eqn 4.4 we see that a low output noise level requires the use of a high value of R_f and a small value of C_T. The amplifier however has a pole at an angular frequency of $A/R_f C_T$, so that by increasing R_f

the bandwidth would be reduced necessitating more equalization. To overcome this one makes A as large as the stability of the closed loop will allow.

Another factor, which serves to reduce the amplifier bandwidth, is the stray capacitance that must necessarily be associated with the feedback resistor R_f. We denote this capacitance C_f. Taking C_f into account the closed loop response becomes [16]

$$H(\omega) = \frac{R_f}{1 + j\omega R_f \left(\frac{C_T}{A} + C_f \right)} \tag{4.11}$$

The usual means of canceling the effect of C_f is to employ a compensating network as shown in Fig. 4.6. With this network the feedback factor β_F is [16]

$$\beta_F = \frac{1 + R_{fs}}{R_f + R_1 + (C_f + C_1) R_f R_{1s}} \tag{4.12}$$

with R_1 and C_1 being the elements of the compensating network. If $R_f C_f = R_1 C_1$, the feedback factor becomes

$$\beta_F = \frac{1}{R_f + R_1} \tag{4.13}$$

With respect to the noise level, as long as $R_1 << R_f$,its contribution to the output noise is negligible.

This configuration largely overcomes the drawbacks of the high impedance front end by utilizing a low noise, high input impedance amplifier with negative feedback. No equalizing circuitry is required. However, because of the thermal noise of the feedback resistor, the receiver noise level is higher and the receiver sensitivity is somewhat less than that of a high impedance design. In principle, this receiver sensitivity degradation can be kept to negligible value by keeping the feedback resistance as large as possible. For a desired bandwidth value, this can be achieved by increasing the amplifier open-loop gain. Characteristics illustrating the variation in received power level against the value of the feedback resistor R_f is shown in Fig. 4.7[14].

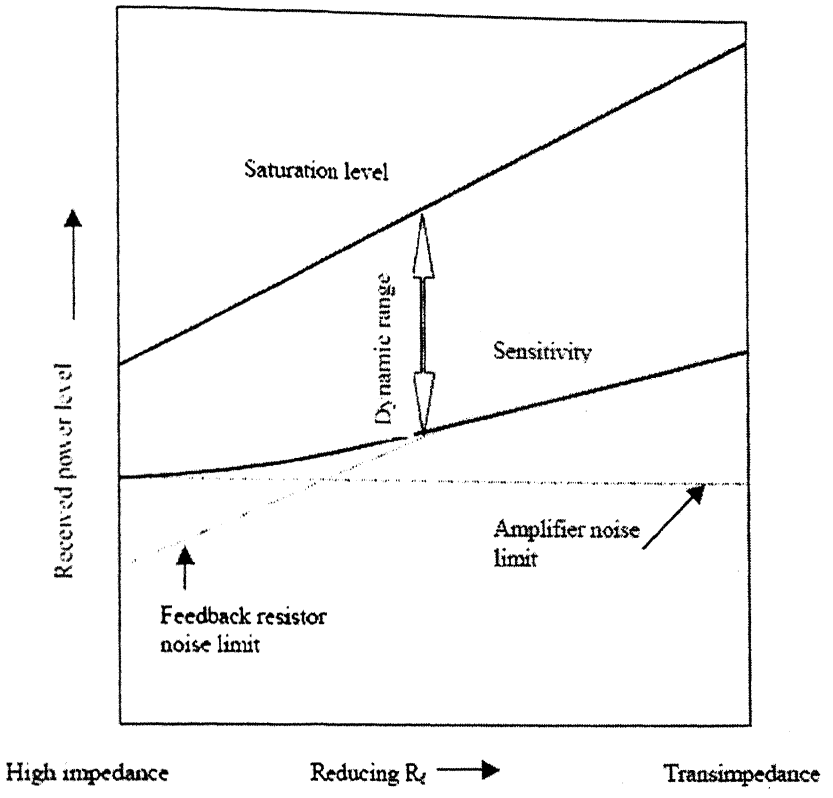

Fig. 4..7 ***Characteristics illustrating the variation in received power level against the value of the feedback resistor*** R_f **[14]**

4.2.5 FET vs. BJT for the Front-end

Unlike the BJT, the FET has extremely high input impedance, low noise and low capacitance, which make the FET, appear as an ideal choice for the front end. However it has a very low transconductance. Hence at low bit rates the FET is superior whereas at higher bit rates (>50MHz) the bipolar devices produce superior performance. Fig. 4.8 shows the noise performance of various preamplifiers over a range of bandwidths [2]. We have used an FET as front-end amplifier device.

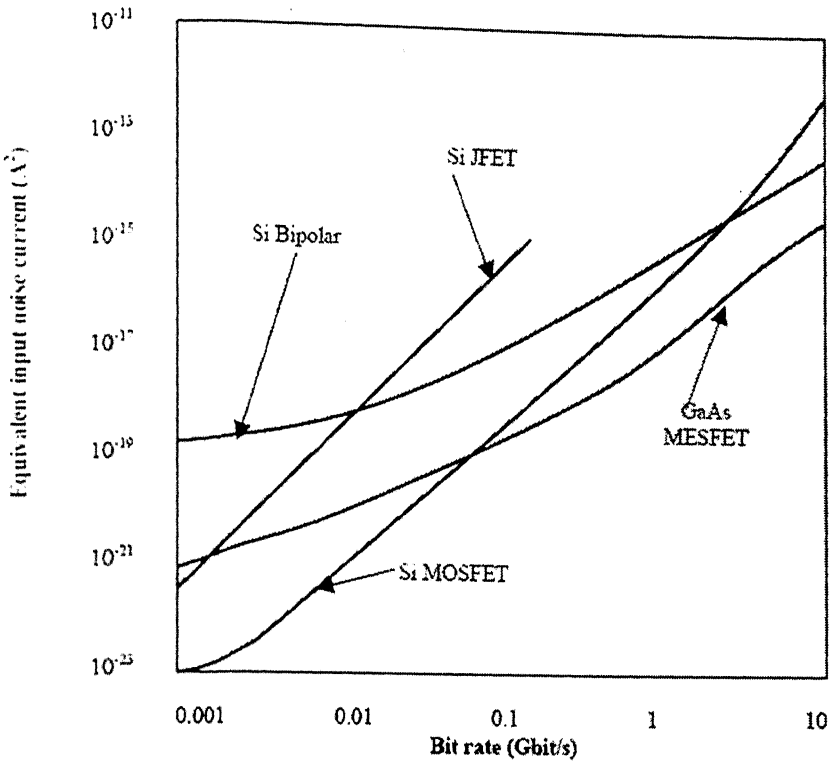

Fig.4.8 ***Noise performance of various preamplifiers***

4.2.6 Preamplifier design

The design of the preamplifier requires particular attention since it may be expected to contribute most of the amplifier noise. The FET in the preamplifier stage is operated optimally in common source mode. In this mode the input impedance, the power gain and the output impedance are high. In this case the input capacitance C_i comprises the parallel combination of the gate to source capacitance C_{gs} and the miller capacitance associated with the gate to drain capacitance C_{gd}. Therefore to minimize C_i one must overcome the miller effect by reducing the voltage gain of the FET. This can be achieved by following the common source stage with a stage having low input impedance. This is realized using a shunt feedback stage using BJT, to ensure good bandwidth. The common source FET with shunt feedback stage is shown in Fig. 4.9. shunt feed back stage offers very good noise rejection from succeeding stages without introducing more noise itself and also because of its low output impedance, it reduces the effect of loading from the next stage.

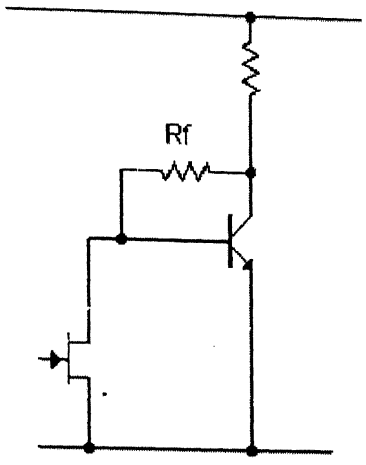

Fig 4.9 ***Common source FET with shunt feedback***

with R_1 and C_1 being the elements of the compensating network. If $R_fC_f = R_1C_1$, the feedback factor becomes

$$\beta_F = \frac{1}{R_f + R_1} \tag{4.14}$$

As long as $R_1 << R_f$ it's contribution to the output noise is negligible.

4.3 OPTICAL SUB-SYSTEMS DESIGN

Design of optical sub-systems is dictated by the type and characteristics of the optical source used at the transmitter. In our design, we are using a low cost laser diode (LD) which is removed from a laser pointer readily available. The characteristics of the LD such as P-I characteristics and Far-field intensity pattern yield important parameters for the optical subsystem design.

4.3.1 P-I Characteristics of Laser diode

This characteristic shows the relation between optical output power and the LD drive current. PI characteristic can provide:

- The value of the threshold current below which the laser gives very little output light.

- The slope efficiency of the LD, that is the rate of change of optical power with drive current. Ideally slope efficiency should be a constant above threshold up to a saturation point.
- Evidence of undesirable "kinks" or non-linearities in the LD characteristic that can point to inherent problems that will mean rejection of the device.

Results of the experimental P-I characteristics obtained for the LD used in our experiment is later given in chapter 5, Fig 5.15.

4.3.2 Far-field characteristics

Unlike conventional light beams, Gaussian beams do not diverge linearly. Near the laser, the divergence angle is extremely small; far from the laser, the divergence angle approaches the asymptotic limit. $W(z) = \frac{\lambda z}{\pi W_o}$. The Raleigh range ($z_0$), defined as the distance over which the beam radius spreads by a factor of the square-root of 2, is given by

$$z_o = \frac{\pi W_o^2}{\lambda}$$

At the beam waist ($z = 0$), the wavefront is planar (i.e. $R(0) = \infty$). Likewise, at $z = \infty$, the wavefront is planar ($R(\infty) = \infty$). As the beam propagates from the waist, the wavefront curvature, therefore, must increase to a maximum and then begin to decrease, as shown in the above figure. The Raleigh range, considered to be the dividing line between near-field divergence and mid-range divergence, is the distance from the waist at which the wavefront curvature is a maximum. Far-field divergence (the number quoted in laser specifications) must be measured at a distance much greater than z_0. This is a very important distinction because calculations for spot size and other parameters will be inaccurate if near- or mid-field divergence values are used. For a tightly focused beam, the distance from the waist (the focal point) to the far field can be beyond a few millimeters or less. For beams coming directly from the laser, the far-field distance can be measured in meters.

A typical far-field radiation pattern is shown in Fig. 4.11 . From the width of the beam, generally full-width at Half-maximum or FWHM, the waist spotsize of the LD can be

computed. Measurement details of the Far-field radiation are discussed in chapter 5, Sec.5.5.1. Waist spotsize calculation from the beam width is shown below.

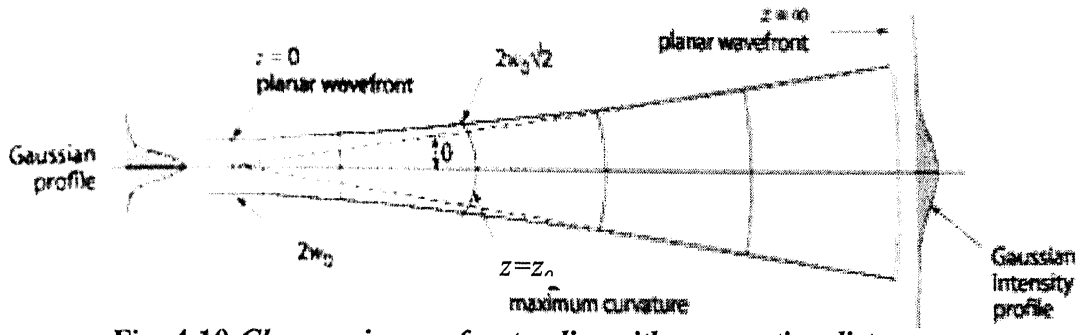

Fig. 4.10 ***Changes in wavefront radius with propagation distance***

As we have seen in Eqn.3.21, the beam radius is a function of distance z. We can rewrite Eqn.3.21 as

$$W^2(z) = W_0^2\left[1+\left(\frac{\lambda z}{\pi W_0^2}\right)^2\right]$$

The Far Field diffraction angle of the fundamental Gaussian beam is given by [3]

$$\theta_{beam} = \tan^{-1}\left(\frac{\lambda}{\pi W_0}\right) \text{ for } \theta_{beam} << \pi \qquad (4.14)$$

θ_{beam} Corresponds to the half angle at $1/e^2$ (approximately 13.5 %) of the maximum intensity. Generally $\theta_{½}$,which is the half of the FWHM (Full Width at Half Maximum) angle, is used in the calculation of spot sizes, instead of θ_{beam} . $\theta_{½}$ in terms of θ_{beam} can be shown to be

$$\theta_{½} = \tan^{-1}\left(\frac{\lambda\sqrt{\ln(2)/2}}{\pi W_0}\right) \qquad (4.15)$$

From the above relations we can write W_0 as

$$W_0 = \frac{\lambda\sqrt{\ln(2)/2}}{\pi\tan(\theta_{½})} \qquad (4.16)$$

The FWHM value obtained for our LD was 0.2792 radians .For our laser the value of beam waist comes out to be 0.8469μm. Hence the beam divergence can be calculated as

$$\theta_0 = \frac{\lambda}{\pi W_0}$$

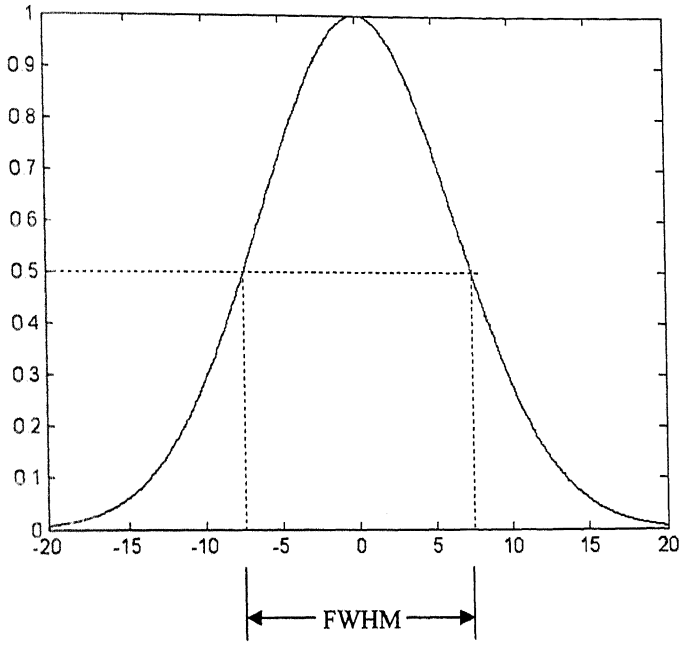

Fig.4.11 ***A typical Far-field radiation pattern of a Laser beam***

The divergence angle without lens is calculated as 0.2387 radians, whereas with lens it is 0.1 milli radians.

The laser which we used for experiment had a miniature aspheric lens packaged along with the LD. From beam radius measurements, the beam waist of the transformed beam (i.e. LD beam along with the aspheric lens) was worked out and found to be 1.26 mm. The variation of beam radius with respect to distance for without lens and with lens are shown in the below Fig.4.12 and Fig 4.13. It is very much clear that the beam with a smaller waist spotsize will diverges more. In the case of the LD (without lens) W_0=0.83μm and the spot size at 12m is more than 3m. However, after the lens, the waist spotsize changes to W_{0T}= 1.26 mm, which gives a spot size of 2.3mm at z=12m around 2.3mm. The measured variation in w(z) are shown in chapter5, Fig 5.19.

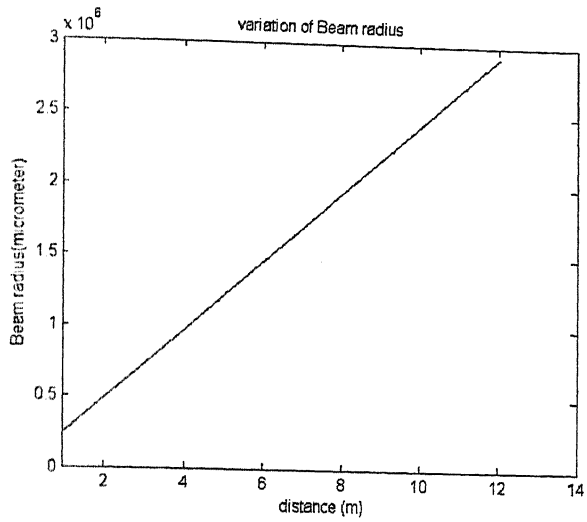

Fig. 4.12 ***Variation of Beam radius without lens***

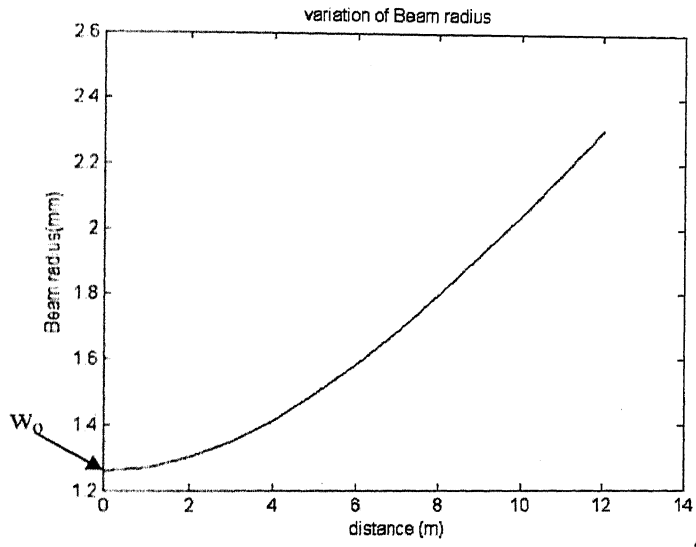

Fig. 4.13 ***Variation of Beam radius with lens***

4.3.3 Additional Optical Subsystems at Transmitter and Receiver

Depending on the required specifications of the outdoor link, it may be necessary to have further optics both at the transmitter and the receiver. The aim of adding another lens is to achieve further collimation of the beam. Similarly, it may be necessary to use a Receiver lens at the receiver side, just in front of the photodetector to focus the beam.

CHAPTER 5

SYSTEM IMPLEMENTATION AND RESULTS

For our experiments an outdoor optical wireless link was implemented using discrete components available in the laboratory. The transmitter and receiver circuits are simulated using Microcap circuit simulation software. Details of the implementation of various subsystems, the overall system as well as results are discussed in this chapter.

5.1 IMPLEMENTATION OF TRANSMITTER CIRCUIT

A simple circuit using one of the TTL 50 ohm driver IC (74S140) was used for implementing the LD transmitter circuit. The transmitter circuit shown in Fig. 5.1. We have used a laser source removed from a low cost laser pointer readily available in the campus. The laser package was taken out from the metal casing of the Pointer by carefully cutting and opening the casing. The switch of the pointer was shorted. The package already has a 75 ohms resistor in series with the LD. The measured P-I characteristic of the LD is shown in Fig.5.2. From this characteristic the threshold current was found to be 18mA. It is extremely important to avoid loose connections in the circuit, as there is a danger of the laser getting damaged due to transients. In our transmitter a modulation current of 28 mA was used, corresponding to an optical power of 690 μW.

5.2 IMPLEMENTATION OF RECEIVER CIRCUIT

A PIN diode with JFET as the front end amplifying device and a shunt feedback stage with BJT formed the preamplifier stage of the receiver. N-type silicon p-i-n photodetector BPX65 is used .The JFET used was BFW10, (N-channel silicon field effect

transistor). The BJTs used were from the high frequency N-P-N transistor array CA3127E. The preamplifier stage of the receiver circuit is shown in Fig. 5.3. The preamplifier output is fed to NE529 high-speed comparator to obtain a TTL compatible signal. The reference input to the comparator was fine tuned using a resistor network. Most part of the implemented preamplifier circuit was that of an earlier work [12] in the Fibre Optics Lab. However, some minor modifications were made to the circuit. One of the major changes is the photodetector. We used BPX65 p-i-n photodiode which has smaller active area, instead of the C30808 p-i-n photodiode used earlier.

5.3 CIRCUIT SIMULATION AND ANALYSIS

The preamplifier circuit was simulated on Micro-cap (7.2.4.0 evaluation version) simulator package. Equivalent circuit of the detector consists of a current source with a shunt capacitor C_d , representing the depletion capacitance of the detector. Series resistance and shunt conductance both being small, will have negligible effect on performance so they were omitted from the equivalent circuit for convenience. Dark current flowing in the detector in laboratory conditions was measured using the circuit shown in Fig. 5.4. It was found to be 6.3nA.

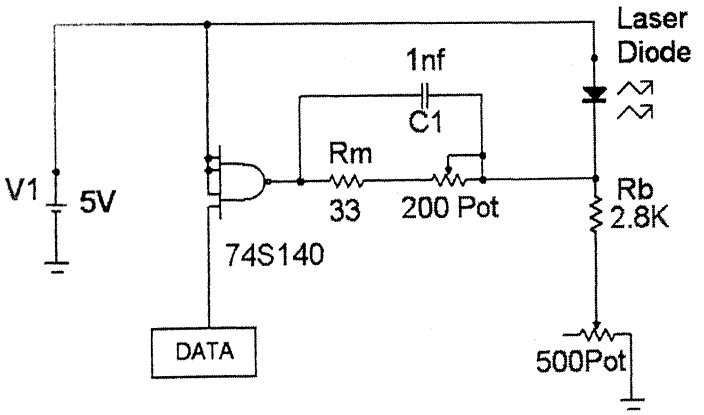

Fig 5.1 ***Implementation of transmitter circuit***

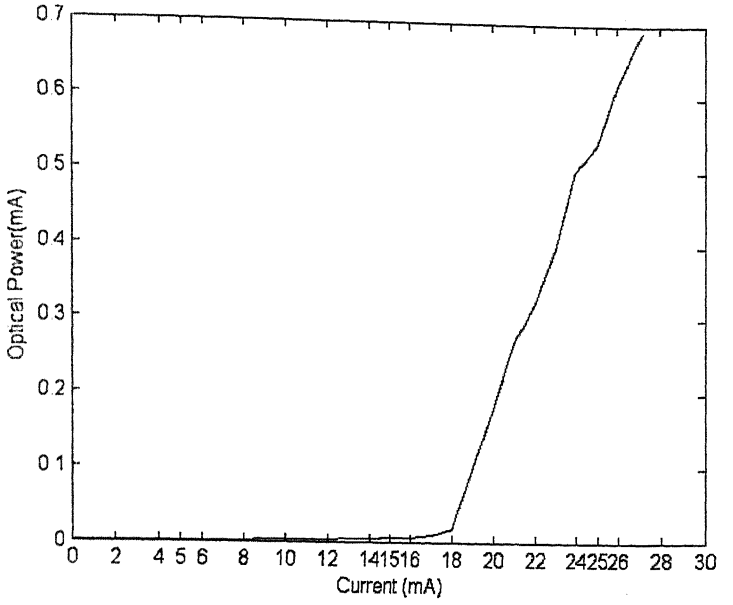

Fig 5.2 ***P-I Characteristics of Laser diode***

This measured value of dark current was used as the dc value of the current source. The magnitude of peak current flowing through the detector when light falls on it is 1.542 μA. The computational model of the photodetector as shown in Fig. 5.5 (a) and (b) were used for Transient analysis and AC analysis.

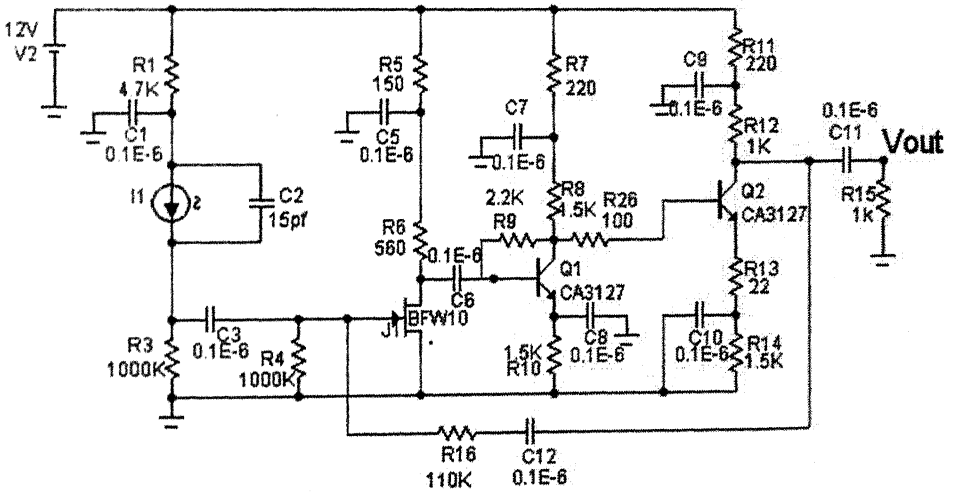

Fig. 5.3 ***Preamplifier circuit***

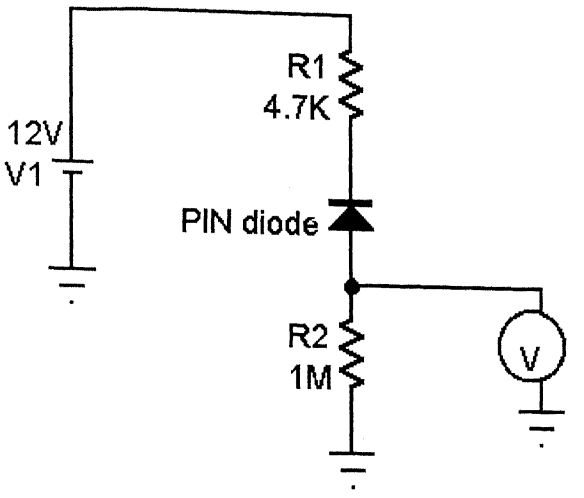

Fig. 5.4 ***Set up for measuring the dark current under lab conditions***

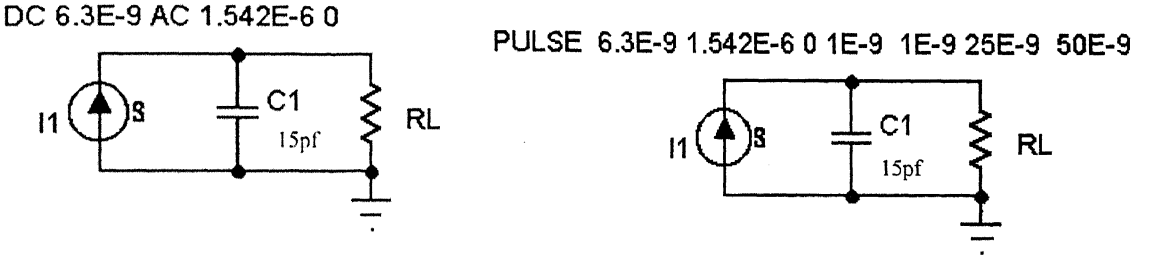

(a) ***AC analysis model*** **(b)** ***Transient analysis model***

Fig. 5.5. ***Computational model of photodetector used for circuit simulation***

For transient analysis, the current source was a PULSE source with i_1 =6.3 nA, i_2 = 1.542 μA, t_d = 0, t_r = 1E-9, t_f = 1E-9, pw = 25E-9, per = 50E-9, assuming ON/OFF keying (1010... data pattern)with t_r = t_f =1 ns In AC analysis, the current source was represented as an AC source with DC value equal to 6.3 nA (dark current) and the magnitude of AC equal to 1.542 μA (I_p).

The model parameters used for the N-channel silicon JFET (BFW10) and the BJT (CA3127) for circuit simulation and their values are given in Table 5.1 and 5.2.These parameters were taken from manufacturer's website. The preamplifier circuit used for simulation is shown in Fig. 5.3. The frequency response of the preamplifier circuit is

shown in Fig. 5.6. The 3 dB bandwidth was found to be 14.32 MHz with a flat response up to a frequency of 10 MHz. The ***transient analysis*** was done to evaluate the response of the circuit to 500Kbps, 1 Mbps, 5 Mbps, 10Mbps, and 20Mbps On/Off pulse. The simulation plots are shown in Fig. 5.7 to Fig. 5.11. From this we can infer that beyond 20 Mbps the performance of the circuit will deteriorate drastically due to the capacitive effect of the photodetector and the BER will increase rapidly.

PARAMETERS	EXTRACTED VALUE
BETA	8E-4
LAMBDA	6.7E-3
VTO	-3.53
CGD	10PF
CGS	4.5PF

Table 4.2 ***model parameters of JFET BFW 10***

PARAMETERS	EXTRACTED VALUE	PARAMETERS	EXTRACTED VALUE
IS	1.33E-16	CJC	0.4PF
BF	96	VJC	750M
NF	1	MJC	330M
VAF	20	PTF	0
IKF	0	TR	1.34ns
ISE	0	EG	1.11
NE	1.5	XTB	0
BR	1	XTI	3
NR	1	TRE1	0
VAR	0	TRE2	0
IKR	0	XCJC	1
ISC	0	CJS	2.175PF
NC	2	VJS	750M
NK	500M	MJS	0.33
ISS	0	FC	134PS
NS	1	TF	500M
RE	4	XTF	0
RB	15	VTF	0
RB	15	ITF	0
RBM	0	TRM1	0
IRB	0	TRM2	0
RC	21	TRC1	0
CJE	0.6PF	TRC2	0
VJE	750M	KF	0
MJE	330M	AF	1

Table 4.3 *Model parameters of CA3127*

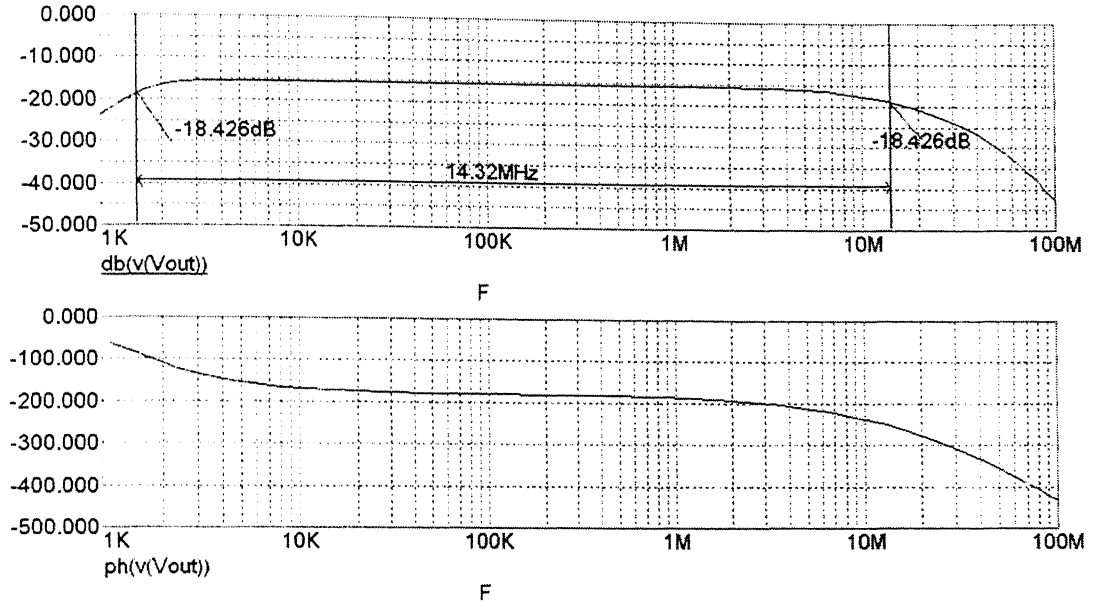

Fig. 5.6 ***Frequency response of preamplifier***

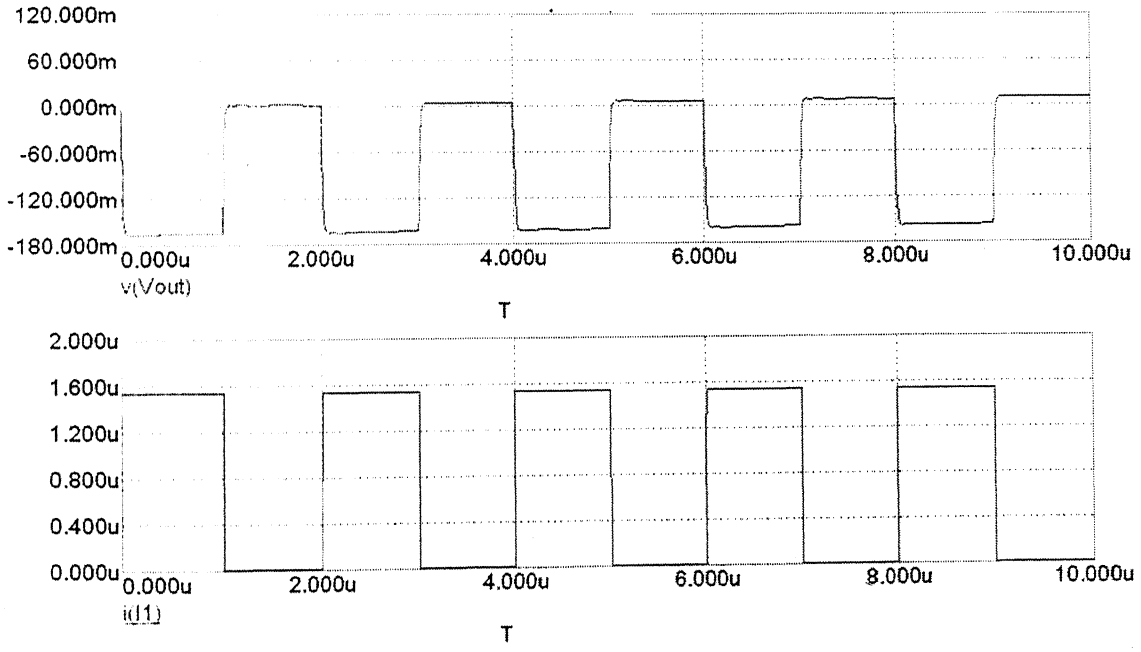

Fig. 5.7 Transient response of preamplifier at 500Kbps

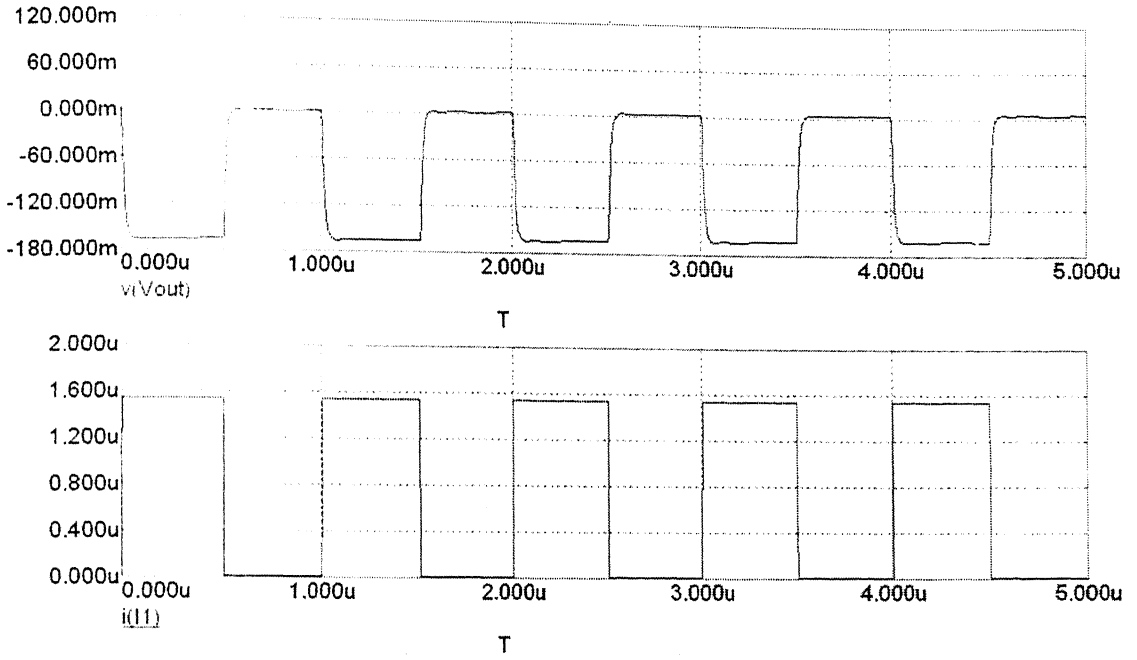

Fig. 5.8. Transient response of preamplifier at 1Mbps

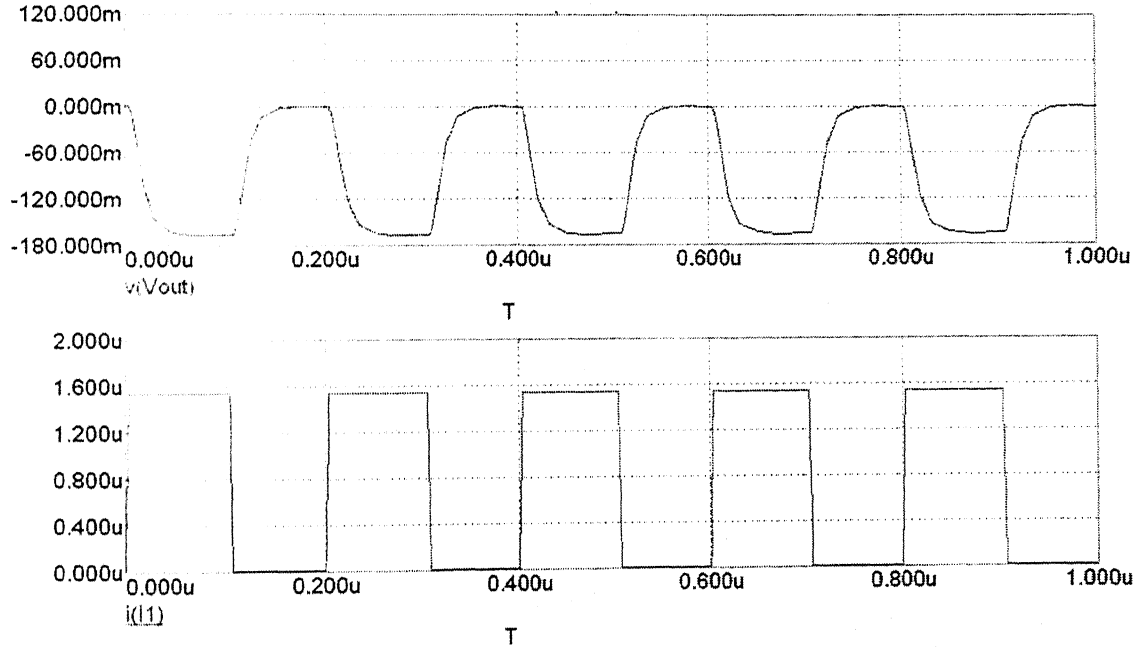

Fig. 5.9 Transient response of preamplifier at 5Mbps

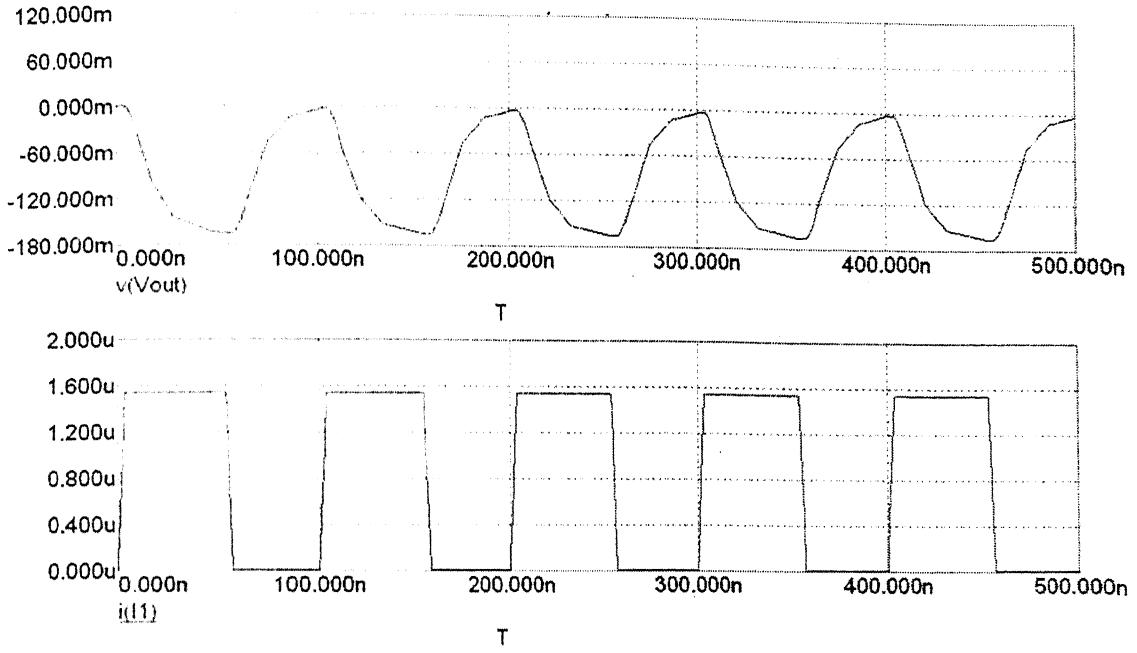

Fig. 5.10 Transient response of preamplifier at 10Mbps

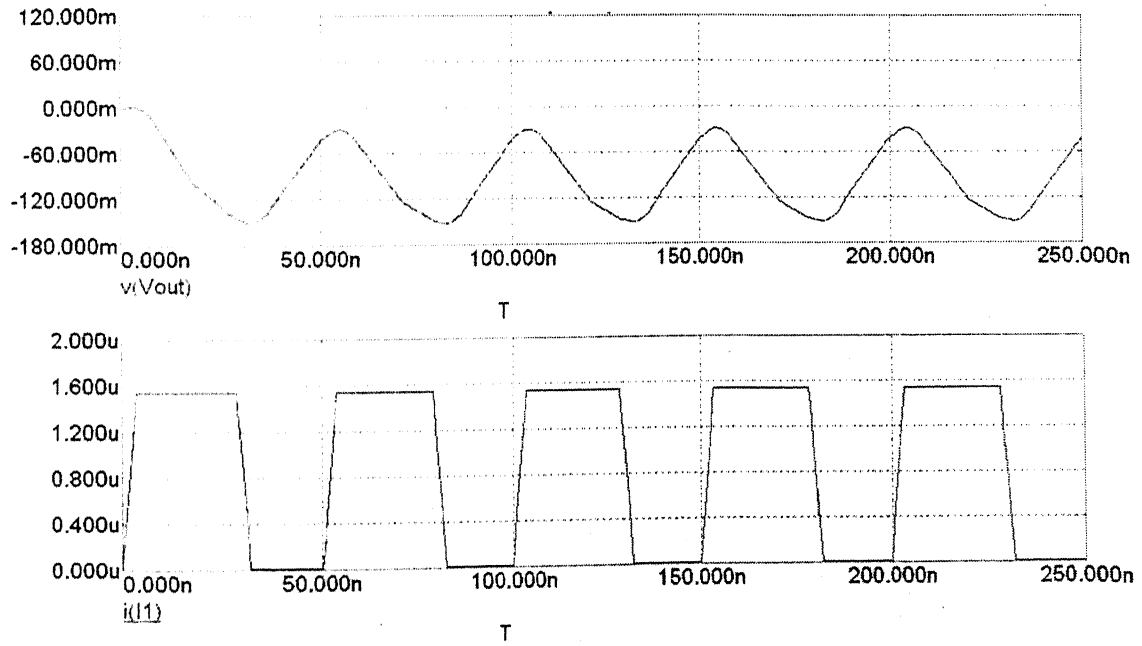

Fig. 5.11 Transient response of preamplifier at 20Mbps

5.4 PRINTED CIRCUIT BOARD DESIGN AND FABRICATION

The transmitter and the receiver circuit designed were wired up on a breadboard and the values verified with the simulated results. Then printed circuit board (PCB) was designed.

The following high frequency design rules were kept in mind while preparing the layout of the PCB.

- Length and width of signal conductor should be as small as possible.
- The signal and ground conductors should not be too close as their capacitance along with the output resistance acts as Low Pass Filter.
- Cross talk can occur if two signal lines run parallel to each other for.

- Measures to reduce ground and supply line noise are to have low impedance between the supply line and the ground line by having broad conductors close to each other. Also by providing an electro magnetically stable ground by having large copper surface for ground, we can reduce the noise.

The whole assembly was shielded using an aluminium box, which enhanced the performance of the receiver by at least 2 dB, and also the output was much more stable.

PCB and component layout are shown in Fig 5.12, and 5.13 below.

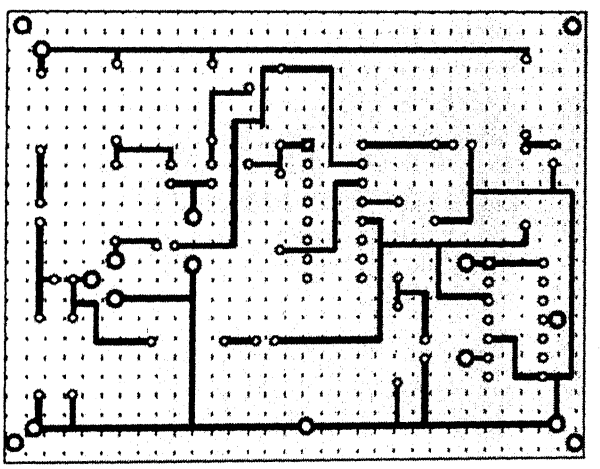

Fig 5.12 ***PCB layout of Receiver***

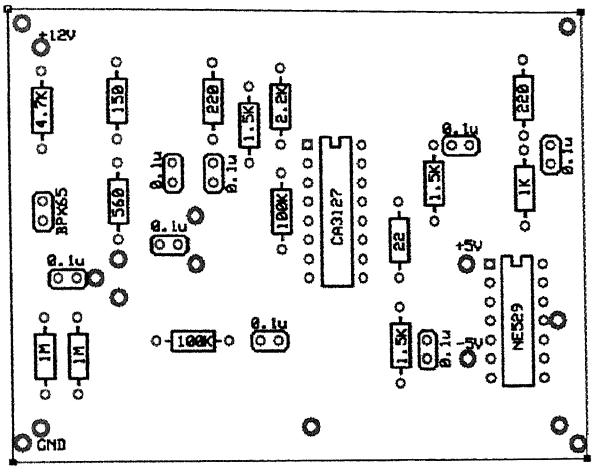

Fig 5.13 ***component layout for Receiver PCB***

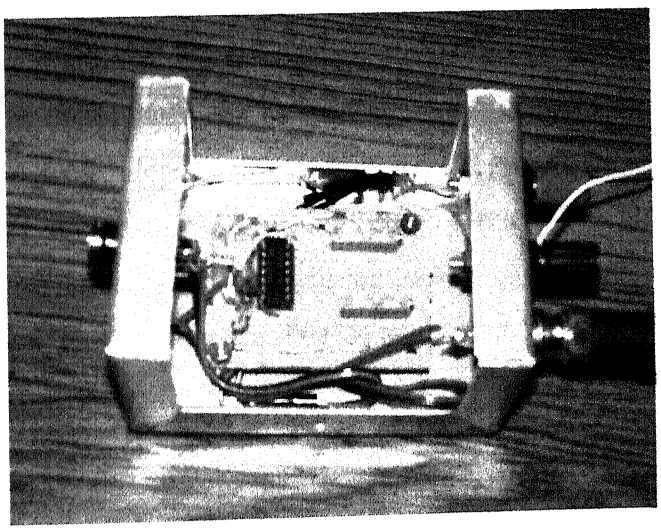

Fig 5.14 ***Implemented Transmitter***

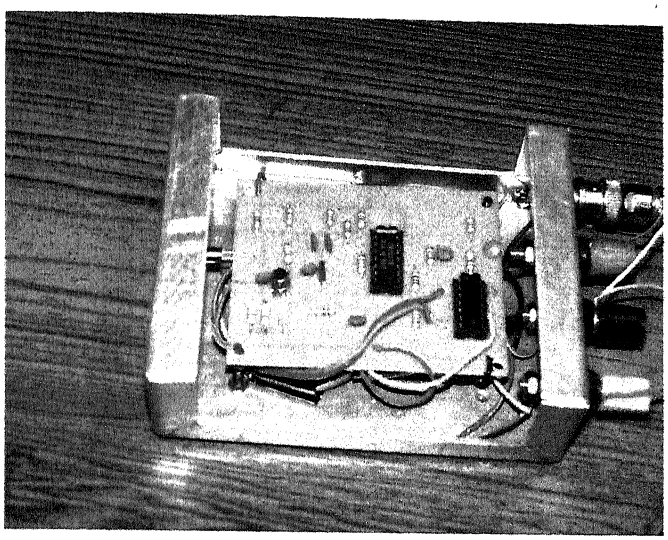

Fig 5.15 ***Implementation of Reciever***

5.5 EXPERIMENTS (INDOOR)

5.5.1 Radiation pattern

To measure the radiation pattern of laser, setup shown in Fig.5.16 is used. Laser is placed on the turn table and the power meter is placed on the mount .the laser and the power meter open aperture is aligned. The turn table has a 360 degree protractor attached so that the angular position of the laser can be read out. Measurements are taken at different angles between -20 to 20 degrees. Fig5.17 shows the radiation pattern. Experimental points (shown *) are fitted with the Gaussian beam pattern (dotted curve) which seemed to fit best (as per visual check). Accordingly, we took the curve corresponding to Fit-4 as the one for our case. This curve has a FWHM angle of 0.2796 radians (or 16 degrees). This corresponds to a waist spot size of 0.8469 μm.

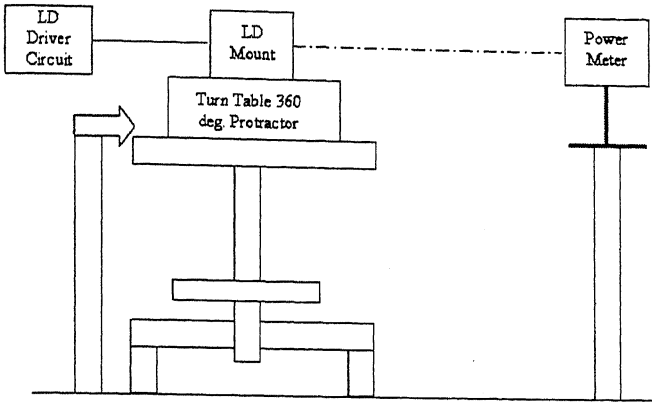

Fig 5.16 ***Experimental setup for the measurement of Radiation pattern of laser***

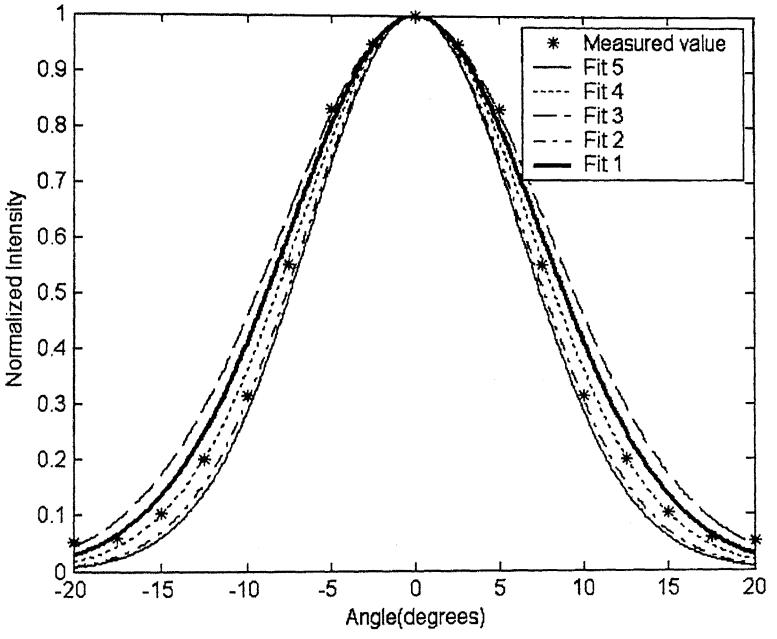

Fig 5.17 ***Radiation pattern of laser (Measured and Gaussian fits)***

5.5.2 Indoor Power Measurements

The high-speed optical wireless link was set up as shown in Fig.5.18. Alignment of the laser beam was done visually by observing it on a white background and then bringing the detector slit on the receiver to the centre of the beam. The receiver and transmitter were set up at 12m apart. The receiver had to be placed in such a way to prevent direct any light falling on it. Also, a simple red filter (red cellophane sheet) was

used in front of the photo detector to avoid the effect of ambient light. Batteries of 6V and 12V are used for Power supply which reduced the supply noise considerably. In order to prevent damage of the laser transmitter the following precautions were taken. Since lasers are highly sensitive to static and other surges, all forms of transient should be prevented from reaching laser. This was ensured right from cutting open the key chain laser cover to the stage when the laser is soldered on to the circuitry. A diode was connected across the laser to bypass reverse bias transients. A 75 Ω resistor, which already existed in the PCB of the key chain laser, was allowed to be in series with the laser. This gave protection against over biasing. The switching-on/off procedures given below were strictly followed:

a) All cable connections made before switching on the power supply.
b) Ensure that 47 K ohms potentiometer is in the maximum resistance position before switching-on.
c) Turn-on the power supply and slowly bring the voltage up to 5V.
d) Slowly vary the 47 K pot from maximum resistance position to minimum resistance position keeping an eye on the laser output.
e) Check the power output of the laser with a power meter.
f) While switching-off, first increase the 47 K pot position from minimum resistance position to maximum resistance position.
g) Slowly reduce the power supply voltage to zero voltage.
h) Switch off the power supply after waiting for two minutes.

Power received at the aperture of the detector in power meter at every one meter point from the receiver is measured. The variation of the received power with respect to distance is shown in Fig.5.19. From this data the power loss is calculated and plotted with respect to distance in Fig.5.20. Fig.5.21 is the plot of the spot radius at every one meter distance.

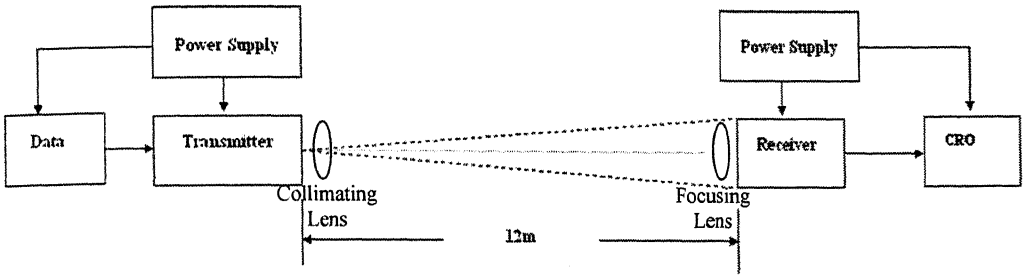

Fig 5.18 Experimental Link setup

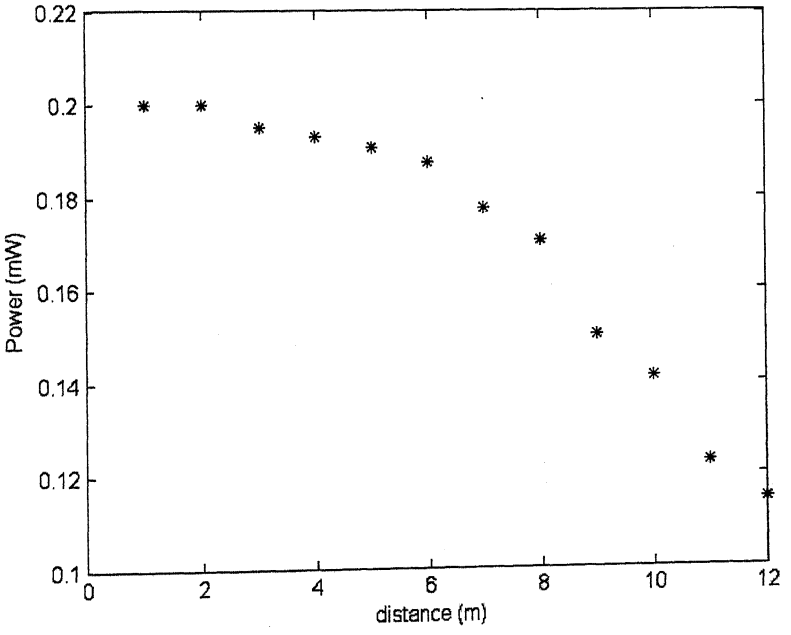

Fig5.19 ***Power received over the detector aperture***

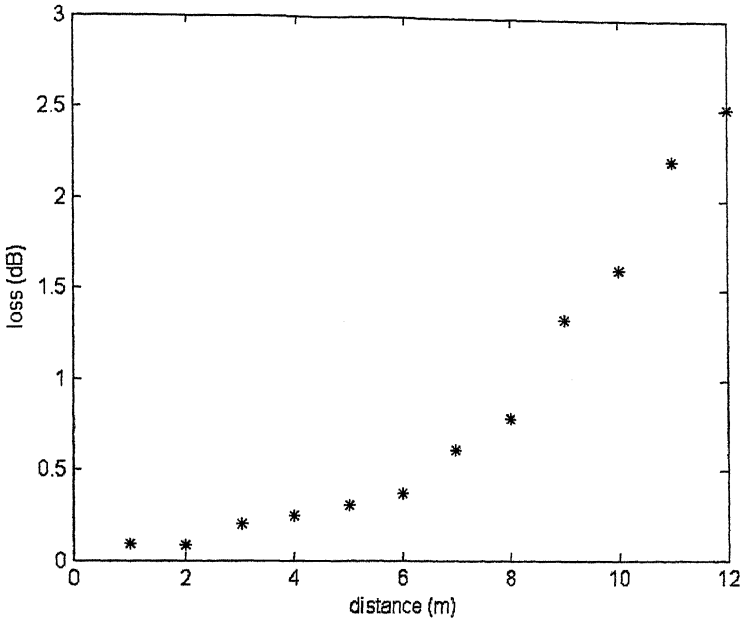

Fig5.20. ***Power loss vs. distance in indoor situation***

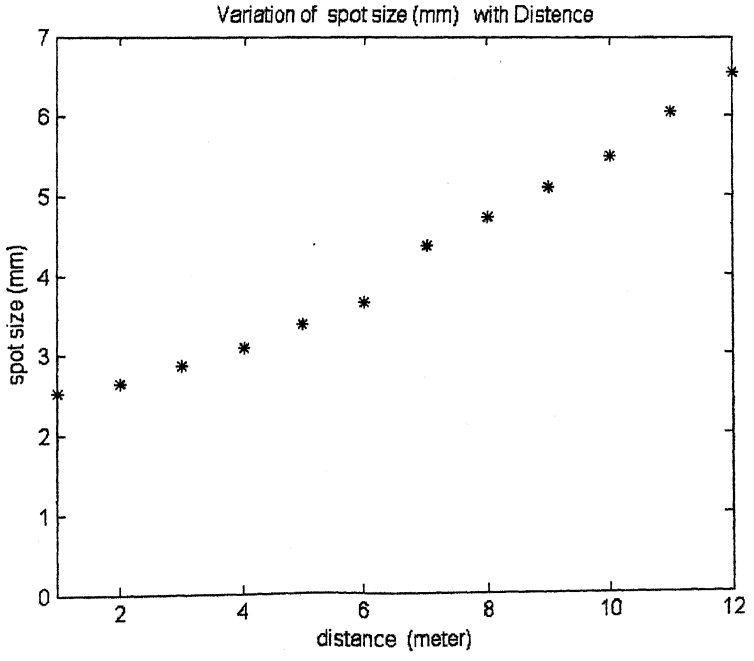

Fig5.21 ***Measured values of spot radius at different distances***

5.6 Outdoor Power Measurements

The outdoor link is set up using the transmitter and receiver circuits discussed earlier. The link range was initially kept as 20 meters, and the power received at every one meter distance from the transmitter, was measured. These power measurements were carried out in different fog conditions. Atmospheric attenuation in fog is calculated theoretically (using Eqn.3.31) at different distances for different visibility conditions and the results are plotted in Fig.5.22 to Fig.5.26, for visibilities of 16m, 16.5m, 17m, 21m and 29 m, respectively. The measured attenuation for the above visibilities are also plotted in the above graphs for comparison. From the graphs it may be observed that the agreement between theory and experiment are good up to a distance of about 10m. The disagreement for larger distances may be due the geometrical spreading losses, in addition to the attenuation.

The attenuation in dB (as calculated by Eqn.3.31) is linear with distance for a given and distance is linear for a particular visibility condition. It is clear from the plots in Fig.5.22 to Fig.5.26 that the slope of the curve is increasing as visibility reduces.

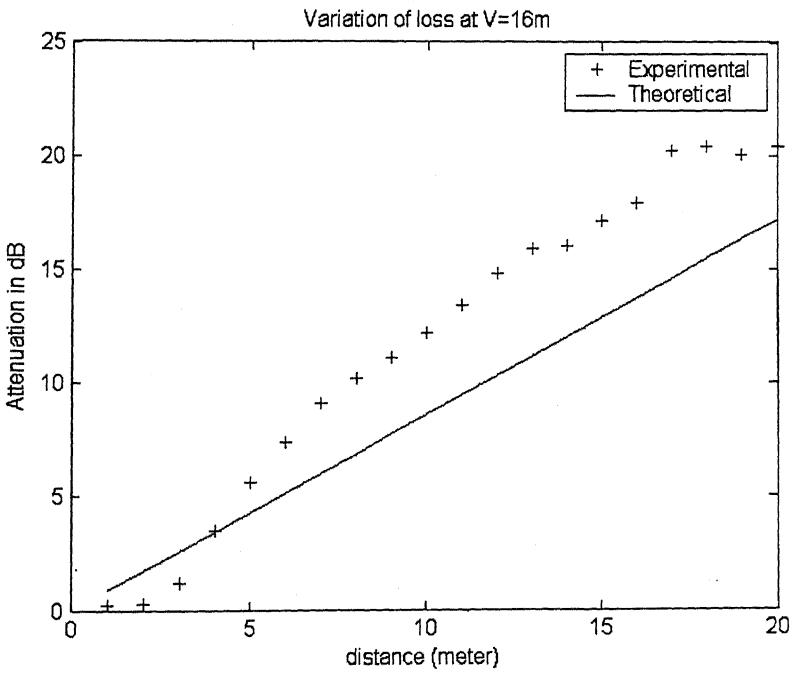

Fig 5.22 ***Atmospheric attenuation calculated in Fog at different distances for visibility=16m***

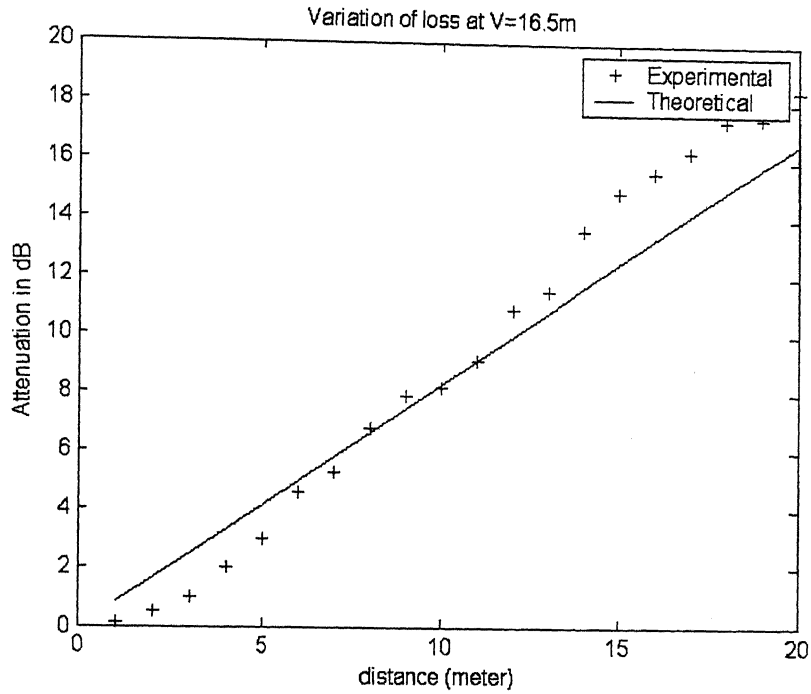

Fig 5.23 ***Atmospheric attenuation calculated in Fog at different distances for visibility=16.5m***

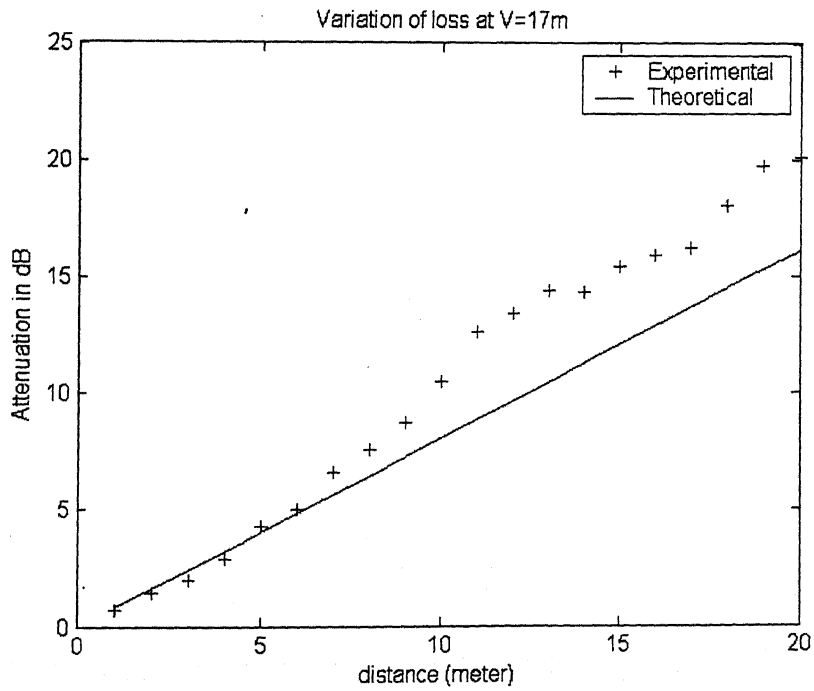

Fig 5.24 ***Atmospheric attenuation calculated in Fog at different distances for visibility=17m***

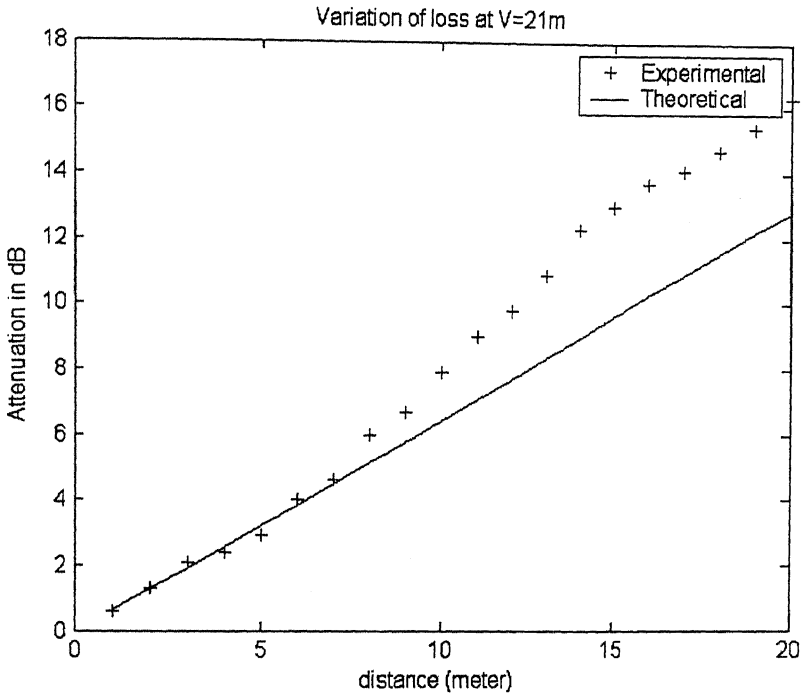

Fig 5.25 ***Atmospheric attenuation calculated in Fog at different distances for visibility=21m***

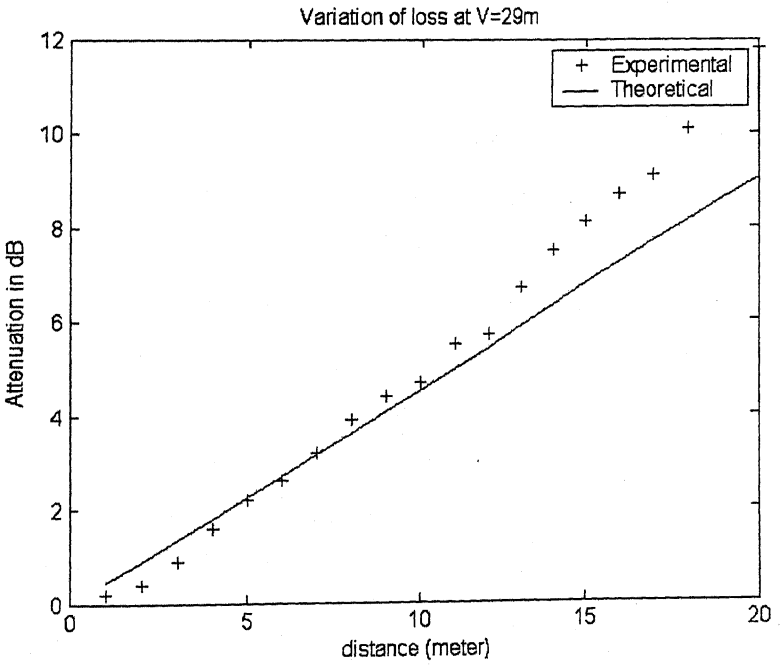

Fig 5.26 ***Atmospheric attenuation calculated in Fog at different distances for visibility=29m***

From the data of Fig.5.22-Fig.5.26, the attenuation per unit length was arrived at for various visibility conditions and is plotted in Fig.5.27. Experimental results

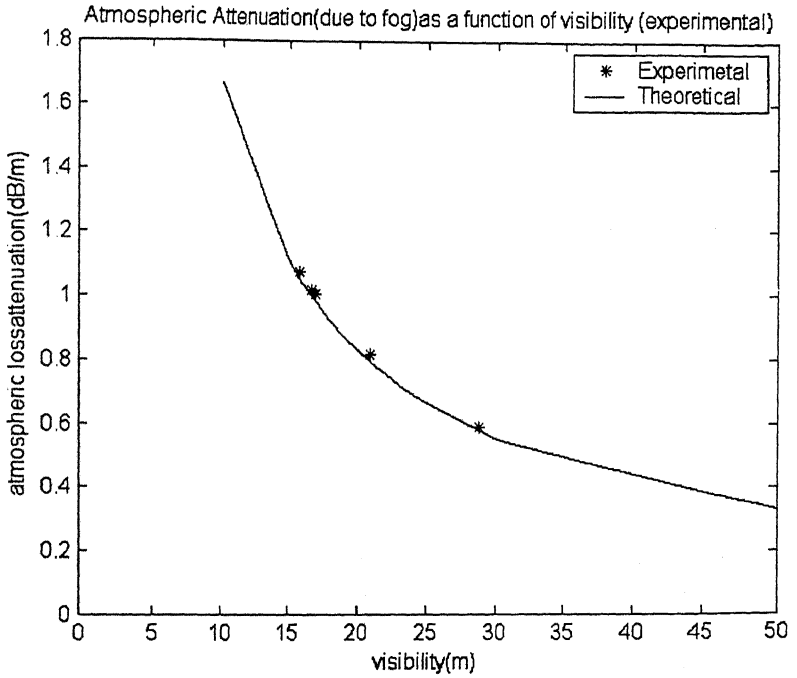

Fig 5.27 ***Atmospheric attenuation in Fog (dB/m) as a function of visibility***

In order to get experimental data on the atmospheric losses, power measurements were taken under clear weather conditions. Measurements were taken with an without focusing lens in front of the receiver (receiver lens). A plot on the power received as a function of the distance from the transmitter (with no receiver lens) is shown in Fig.5.28. From this data, atmospheric losses in clear weather as a function of distance was obtained. The derived attenuation data is compared with the geometric spreading losses in Fig.5.29. It is seen that the trend of the losses follows the geometrical spreading losses.

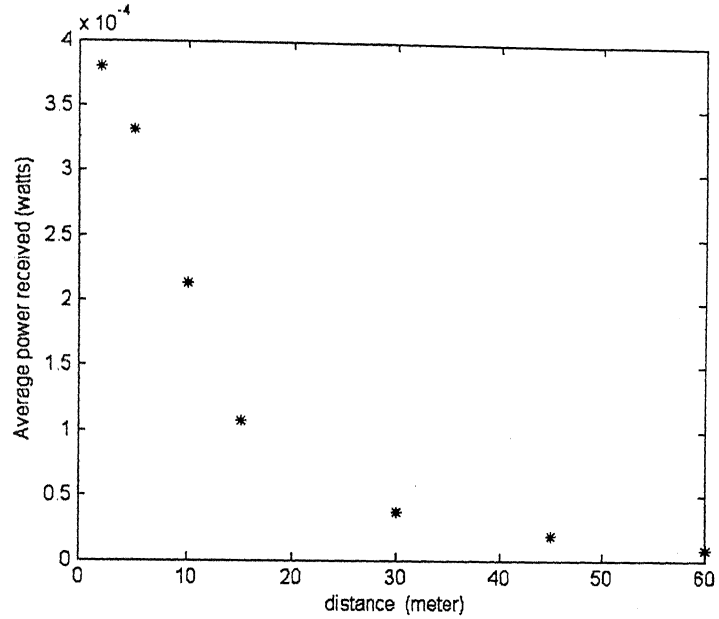

Fig 5.28 Power received on the detector aperture on different distances from the transmitter in clear Weather without receiver lens

However, the total losses are found to be much more than that of geometrical losses. In general, under clear weather conditions the main contribution to the loss is expected to be due to due to geometric spreading. Other effects contributing to the losses are absorption and scattering.

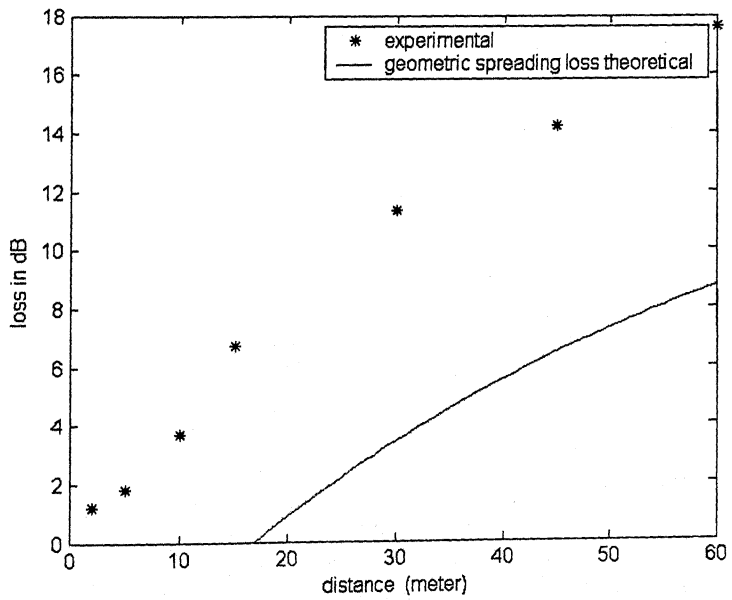

Fig 5.29 ***Loss vs. distance without receiver lens***

Fig.5.30 shows the power received at the receiver with the receiver lens in front of the receiver. The corresponding losses are plotted in Fig. 5.31.

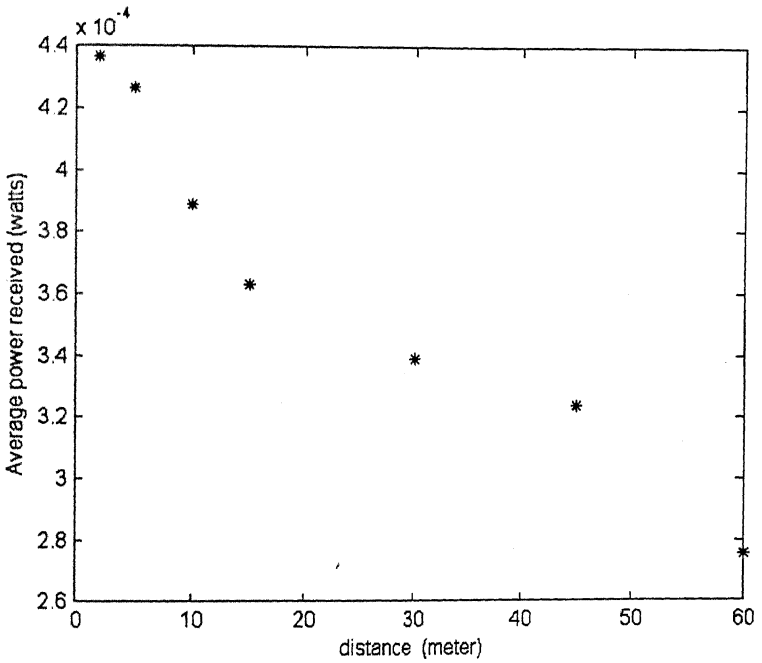

Fig 5.30 ***Power received on the detector aperture vs. distances in clear Weather (using receiver lens)***

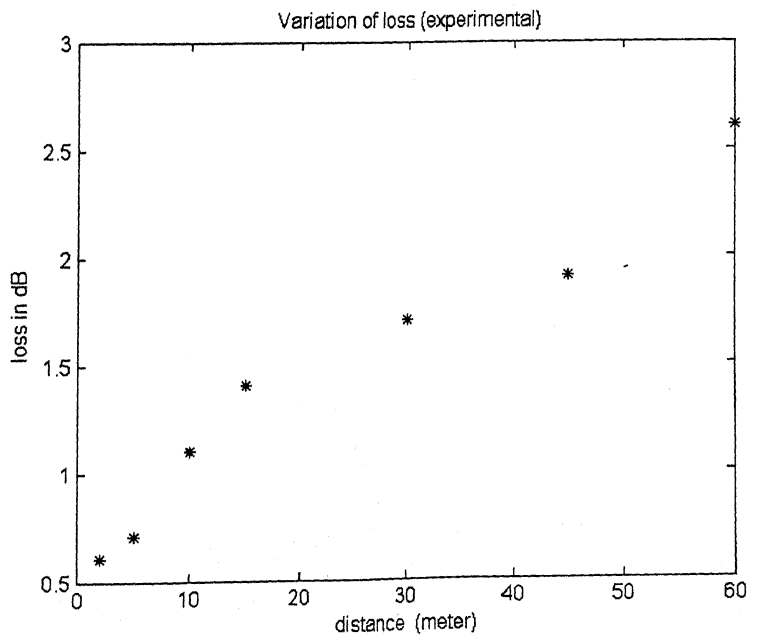

Fig 5.31 Power ***loss (dB) vs. distances in clear atmosphere (using Receiver lens)***

From the above plots it can be seen that the losses are decreased drastically due to the reduction in the geometric spreading loss contribution due to the use of the receiver lens.

5.7 PERFORMNACE OF THE OUTDOOR LINK

With Receiver Lens

The outdoor link was successfully established in clear weather for a link range of 60m. Data was transmitted at 10Mbps (101010..... pattern). A receiver lens (focal length=5cm) was kept at 5cm in front of the receiver. The implemented receiver had a sensitivity of -20dbm and 15dB dynamic range. The power received in front of the lens was -20.6 dBm. After focusing the beam by the above lens, the power at the photodetector point was measured to be -5.6 dBm.

For dense fog conditions at a visibility of 16m the link range is expected to be19m, while and for a visibility of 29m the predicted link range is35m.

Without Receiver Lens

From the loss/m data we see that under dense fog conditions, at a visibility of 16m the link range obtainable is about 14m, while for a visibility of 29m the predicted link range is 24m.

CHAPTER 6

RESULTS, CONCLUSIONS AND SUGGESTIONS FOR FURTHER WORK

The main aim of the present work was to study the effect of atmospheric conditions on the performance of an outdoor optical wireless communication system. Basic outdoor optical wireless systems were reviewed. Various aspects of Gaussian beam propagation were reviewed. Effect of atmosphere on Gaussian beam was studied. An outdoor optical wireless link was designed and implemented.

Experiments were conducted in fog and the optical powers were measured up to 20m at intervals of 1m for five different visibility conditions. The atmospheric attenuation as per the existing models was compared with the measured data. The theory and experiment had reasonable agreement.

On the basis of our studies it can be concluded that outdoor optical wireless communication is an attractive, reliable and cost effective method of transmitting high speed data. However, the performance of the outdoor optical communication system is greatly influenced by atmospheric conditions. The attenuation offered to an outdoor optical link depends on various atmospheric conditions, viz. fog, haze, etc. It was found from our studies that the attenuation due to fog and haze varies inversely with visibility. These theoretical results based on existing models agreed reasonably well with our experimental results.

An outdoor wireless optical link has been successfully implemented using discrete components available in laboratory. This link is capable of communicating at a distance

up to 60 m under clear weather. The experimental link had optics at the transmitter and receiver ends. Under dense fog conditions, the link is expected to work up to about 20m.

Data was successfully transmitted at 10Mbps over a distance of 60m in clear weather. The laser transmitter gave a power output of -3 dBm at the transmitter end. The receiver sensitivity was –20 dBm at 10Mbps. The losses were mainly due to the atmospheric attenuations. The use of a collimating lens at the transmitter minimized the spreading loss up to a certain level. At the receiver, a lens to focus the beam reduced the losses substantially.

6.1 SUGGESTIONS FOR FURTHER WORK

Experiments and system design were carried out as per the availability of components and measuring instruments. Many modifications can be incorporated to enhance the accuracy of the experiments and performance of the system.

- Our experimental studies focused only on clear weather and different types of Fog(Dens thick,moderate,light etc.). The effect of other weather conditions, such as rain, snow and clouds as well as turbulence induced atmospheric scintillation, may also be studied.
- Outdoor experiments for larger lengths up to 1 km may be conducted by fixing transmitter and receiver on the roof of tall buildings in the campus. Over a period of time data can then be collected to study the effect of various atmospheric conditions over a period of time.
- In our studies we have not considerd the absorption losses as they are expected to be low for distances up to 500m. The effect of absorption losses may also be studied.
- It is very important to have good and lasting alignment between the transmitter and the receiver. Use of good quality mounts can help very much, which in turn will enhance the accuracy of measurements.
- The power output of the laser beam was less than what was specified. Use of a better source or concentrators at the receiver end to concentrate the beam on to the

detector, can help in improving the overall receiver performance. Concentrators at the receiver end can nullify the effect of beam divergence and thus reduce the geometrical spreading loss.

- The effect of various noises is one of the important considerations in the preamplifier design. Use of low noise, high frequency devices, as well as careful design will reduce noise and thereby improve the system performance.
- Passive components and devices should be preferably surface mount type to improve the high frequency response.
- To reduce the effect of ambient light, some optical filters can be used at the receiver end to further improve the system performance.

REFERENCES

1. David J.T. Heatley et.al., "*Optical Wireless: The story so far*",IEEE communication magazine, pp 72-82,1998.
2. S. D. Personick, "Receiver design for optical fiber systems", *Proc. IEEE,* vol. 65, pp 1670 – 1678, 1977.
3. Joseph John "*Semiconductor Laser Diode to Single-Mode Fibre Coupling using Discrete and Micro-Lenses*", PhD thesis School of Electronic and Electrical Engineering, Faculty of Engineering, University of Bermingham,1993.
4. I.I. Klm et al., "*Wireless optical transmission of fast Ethernet, FDDI, ATM, and ESCON protocol data using the TerraLink laser communication system*", Optical Engineering, vol. 37, pp 3143-3155, 1998.
5. Ron Stieger and Eddie Kaetz. "*Product Testing of Free-space Optical Transceivers*", Optical Wireless communications V, Proceedings Of SPIE, vol. 4873, pp 111-120, 2002.
6. Robert T. et al. "*Environmental Qualification and field Test results for the SONAbeam 155-M*", Optical Wireless communications IV, Proceedings Of SPIE, vol. 4530, pp 72-83, 2001.
7. B.E.A. Saleh and M.C. Teich. "*Fundamentals of Photonics*", John Wiley & sons, inc., New York.
8. J.W. strohbehn "*Topics in Applied Physics*",vol.25,Springer-Verlag ,Berlin Heidelberg New York.
9. J. W. Goodman, "*Statistical Optics*". New York: Wiley, 1985.
10. Chinlon Lin (Ed), "*Optoelectronic Technology and Lightwave Communication Systems*". New York: Van Nostrand Reinhold, 1989.
11. David A. Johnson,P.E. "*Handbook of optical through the air communication*".
12. Major Saju Thomas "*Design and implementation of an outdoor high-speed optical wireless link*" M.Tech thesis IIT Kanpur 2002.
13. Xiaoming Zhu, *"Free-Space Optical Communication through Atmospheric Turbulence Channels"* IEEE Transactions On Communications, Vol. 50, NO. 8, pp 4285-4294 August 2002.
14. John. M. Senior, *Optical Fiber Communications*, 2nd ed.. New Delhi: Prentice-Hall of India, 1994.
15. T. V. Muoi, "*Receiver design for high speed optical fiber systems*", Journal of light wave technology, LT-2, pp 243-267, 1984.
16. J. L. Hullett and T. V. Muoi, "*A feedback receive amplifier for optical transmission systems",* IEEE Trans. Commun., vol. 24, pp 1180-1185, 1976.

Silicon Photodetector BPX65 Series

HIGH SPEED

The BPX65 family of detectors feature Centronic's 1mm² high speed, high sensitivity chip already successful in a wide variety of applications. The chip can be packaged in various forms suitable for fibre-optic communication, such as the AX65-RF (precisely centred, isolated, low chip to window spacing) a standard 2 or 3 lead TO18 or even epoxy encapsulated. It has also been used for encoder designs and with MIL SPEC release at the heart of advanced laser warning systems.

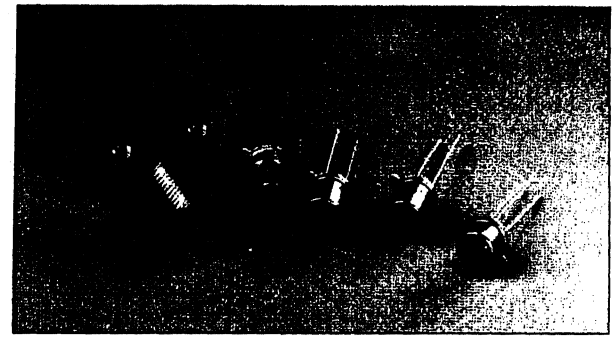

ABSOLUTE MAXIMUM RATINGS

	Max. Rating
DC Reverse Voltage	50V
Peak Pulse Current (10 µs, 1% duty cycle)	200mA
Peak DC Current	10mA
Irradiance (CW level for extended periods)	5W/cm²
Storage Temperature Range	-55°C + 125°C
Operating Temperature Range	-55°C + 120°C
Soldering Temperature Range	200°C

Series BPX65 - Typical Spectral Response

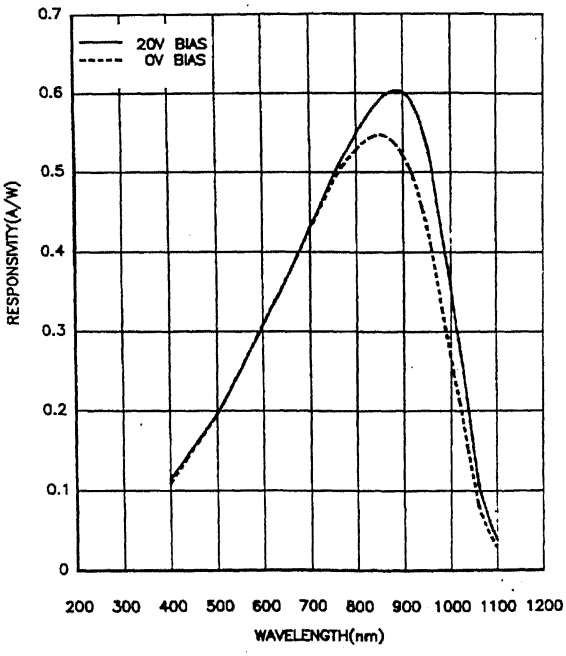

Series BPX65 - Typical Capacitance versus Bias Voltage

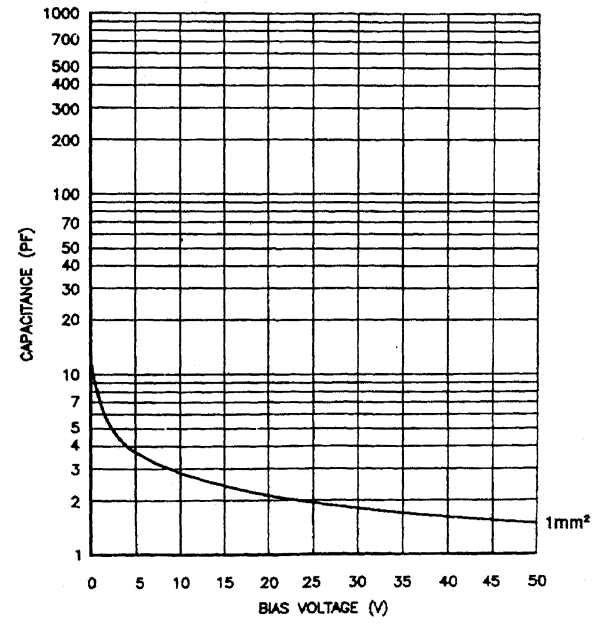

Silicon Photodetector BPX65 Series

Electrical / Optical Specifications

Characteristics measured at 22°C (±2) ambient, and a reverse bias of 20 volts, unless otherwise stated.

Single Elements

Type No.	Active Area		Responsivity A/W λ = 900 nm		Dark Current nA		NEP W/Hz$^{1/2}$ λ = 900nm	Capacitance pF		Rise time ns λ = 830 nm R_L = 50Ω	Package
	mm^2	mm	Min.	Typ.	Max.	Typ.	Typ.	V_R = 0V Max.	V_R = 20V Max.	Typ.	
BPX65	1	1 x 1 mm	0.52	0.55	5	1	3.3×10^{-14}	15	3.5	3.5	1
AX65R2F	1	1 x 1 mm	0.52	0.55	5	1	3.3×10^{-14}	15	3.5	3.5	2A
X65EB	1	1 x 1 mm	0.52	0.55	5	1	3.3×10^{-14}	15	3.5	3.5	1B

Highlighted items are Centronic standard products generally available from stock

Package Dimensions - mm (inches)

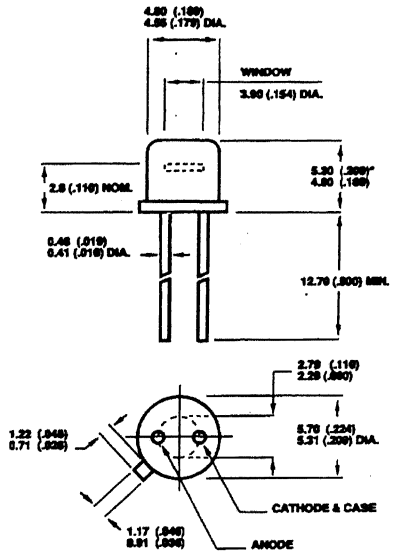

1 (TO18)

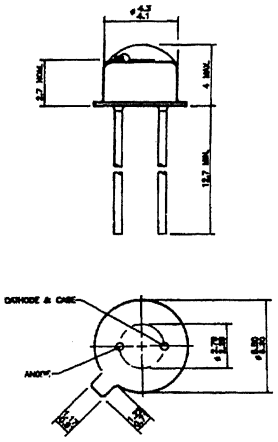

1b

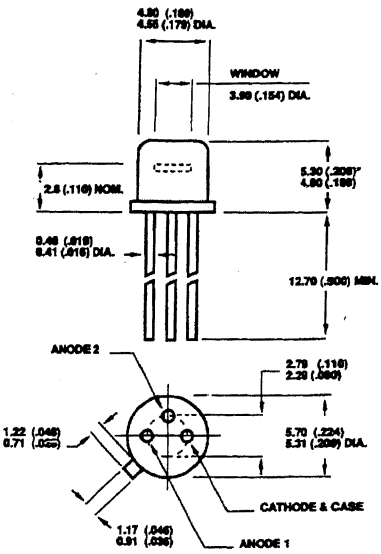

2 (TO18)

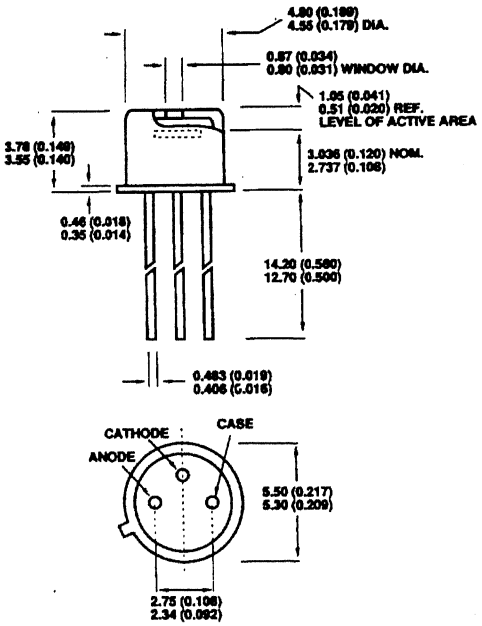

2a (T046)

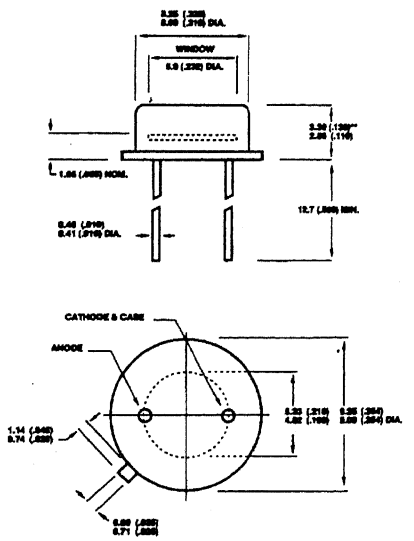

3 (TO5)

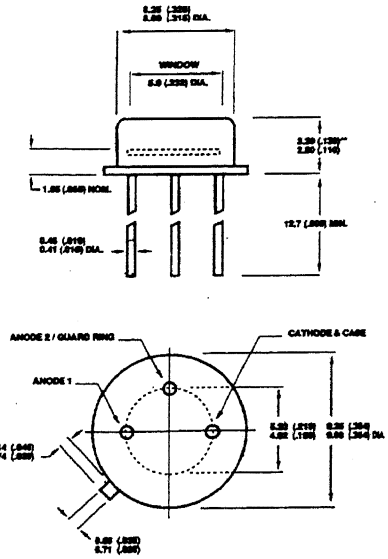

4 (TO5)

* (TO18) Window glass climb 0.15 (.006) MAX. ** (TO5) Window glass climb 0.3 (.012) MAX.

Voltage comparator NE529

DESCRIPTION

The NE529 is a high-speed analog voltage comparator which, for the first time, mates state-of-the-art Schottky diode technology with the conventional linear process. This allows simultaneous fabrication of high-speed TTL gates with a precision linear amplifier on a single monolithic chip.

FEATURES

- 10 ns propagation delay
- Complementary output gates
- TTL or ECL compatible outputs
- Wide common-mode and differential voltage range
- Typical gain 5000

APPLICATIONS

- A/D conversion
- ECL-to-TTL interface
- TTL-to-ECL interface
- Memory sensing
- Optical data coupling

PIN CONFIGURATIONS

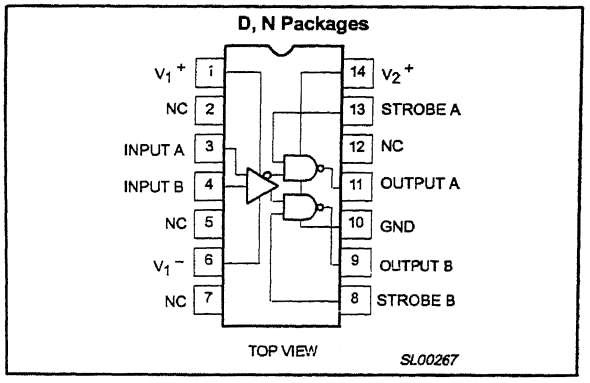

Figure 1. Pin Configuration

BLOCK DIAGRAM

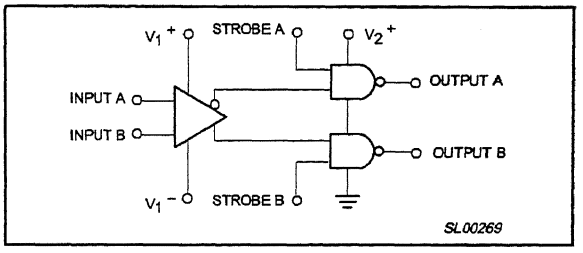

Figure 2. Block Diagram

ORDERING INFORMATION

DESCRIPTION	TEMPERATURE RANGE	ORDER CODE	DWG #
14-Pin Plastic Dual In-Line Package (DIP)	0 °C to +70 °C	NE529N	SOT27-1
14-Pin Small Outline (SO) Package	0 °C to +70 °C	NE529D	SOT108-1

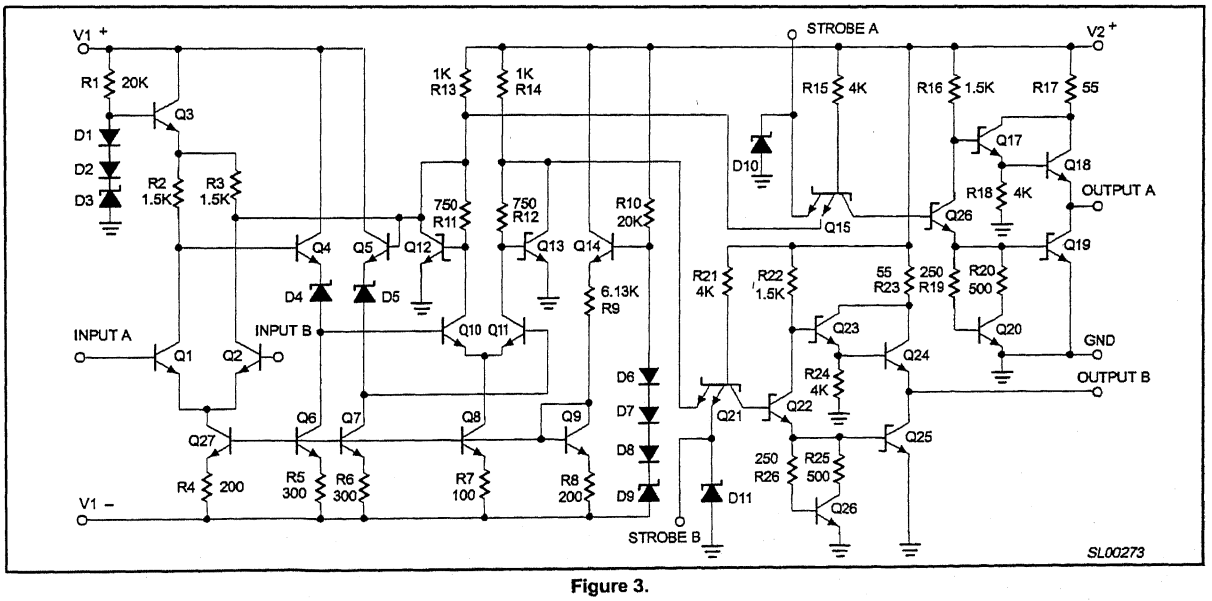

Figure 3.

ABSOLUTE MAXIMUM RATINGS

SYMBOL	PARAMETER	RATING	UNIT
V_1+	Positive supply voltage	+15	V
V_1-	Negative supply voltage	–15	V
V_2+	Gate supply voltage	+7	V
V_{OUT}	Output voltage	+7	V
V_{IN}	Differential input voltage	±5	V
V_{CM}	Input common mode voltage	±6	V
P_D	Maximum power dissipation[1] T_{amb} = 25 °C (still-air) N package D package	 1420 1040	 mW mW
T_{amb}	Operating temperature range	0 to +70	°C
T_{stg}	Storage temperature range	–65 to +150	°C
T_{sld}	Lead soldering temperature (10 sec max)	 +230	 °C

NOTES:
1. Derate above 25 °C at the following rates:
   N package at 11.5 mW/°C
   D package at 8.3 mW/°C

DC ELECTRICAL CHARACTERISTICS

$V_1+ = +10$ V; $V_2+ = +5.0$ V; $V_1- = -10$ V; unless otherwise specified.

SYMBOL	PARAMETER	TEST CONDITIONS	LIMITS			UNIT
			Min	Typ	Max	
Input characteristics						
V_{OS}	Input offset voltage @ 25 °C				6	mV
	Over temperature range				10	mV
I_{BIAS}	Input bias current @ 25 °C			5	20	µA
	Over temperature range	$V_{IN} = 0$ V			50	µA
I_{OS}	Input offset current @ 25 °C			2	5	µA
	Over temperature range	$V_{IN} = 0$ V			15	µA
V_{CM}	Common-mode voltage range		–5	0		V
Gate characteristics						
V_{OUT}	Output voltage					
	"1" state	$V_2+ = 4.75$ V; $I_{SOURCE} = -1$ mA	2.7	3.3		V
	"0" state	$V_2+ = 4.75$ V; $I_{SINK} = 10$ mA			0.5	V
	Strobe inputs					
	"0" Input current[1]	$V_2+ = 5.25$ V; $V_{STROBE} = 0.5$ V			–2	mA
	"1" Input current @ 25 °C[1]	$V_2+ = 5.25$ V; $V_{STROBE} = 2.7$ V			100	µA
	Over temperature range	$V_2+ = 5.25$ V; $V_{STROBE} = 2.7$ V			200	µA
	"0" input voltage	$V_2+ = 4.75$ V			0.8	V
	"1" input voltage	$V_2+ = 4.75$ V	2.0			V
I_{SC}	Short-circuit output current	$V_2+ = 5.25$ V; $V_{OUT} = 0$ V	–18		–70	mA
Power supply requirements						
	Supply voltage					
V_1+			5		10	V
V_1-			–6		–10	V
V_2+			4.75	5	5.25	V
	Supply current	$V_1+ = 10$ V; $V_1- = -10$ V				
		$V_2+ = 5.25$ V				
I_1+		Over temp.			5	mA
I_1-		Over temp.			10	mA
I_2+		Over temp.			20	mA

NOTE:
1. See logic function table.

AC ELECTRICAL CHARACTERISTICS

$T_{amb} = 25$ °C (See AC test circuit).

SYMBOL	PARAMETER	TEST CONDITIONS	LIMITS			UNIT
			Min	Typ	Max	
t_R	Transient response	$V_{IN} = \pm 100$ mV step				
	Propagation delay time					
t_{PLH}	Low-to-high			12	22	ns
t_{PHL}	High-to-low			10	20	ns
	Delay between output A and B			2	5	ns
	Strobe delay time					
t_{ON}	turn-on time			6		ns
t_{OFF}	turn-off time			6		ns

HARRIS Semiconductor

CA3127

August 1996

High Frequency NPN Transistor Array

Features

- Gain Bandwidth Product (f_T) . . . . . >1GHz
- Power Gain . . . . . 30dB (Typ) at 100MHz
- Noise Figure . . . . . 3.5dB (Typ) at 100MHz
- Five Independent Transistors on a Common Substrate

Applications

- VHF Amplifiers
- Multifunction Combinations - RF/Mixer/Oscillator
- Sense Amplifiers
- Synchronous Detectors
- VHF Mixers
- IF Converter
- IF Amplifiers
- Synthesizers
- Cascade Amplifiers

Description

The CA3127 consists of five general purpose silicon NPN transistors on a common monolithic substrate. Each of the completely isolated transistors exhibits low 1/f noise and a value of f_T in excess of 1GHz, making the CA3127 useful from DC to 500MHz. Access is provided to each of the terminals for the individual transistors and a separate substrate connection has been provided for maximum application flexibility. The monolithic construction of the CA3127 provides close electrical and thermal matching of the five transistors.

Ordering Information

PART NUMBER (BRAND)	TEMP. RANGE (°C)	PACKAGE	PKG. NO.
CA3127E	-55 to 125	16 Ld PDIP	E16.3
CA3127M (3127)	-55 to 125	16 Ld SOIC	M16.15
CA3127M96 (3127)	-55 to 125	16 Ld SOIC Tape and Reel	M16.15

Pinout

CA3127
(PDIP, SOIC)
TOP VIEW

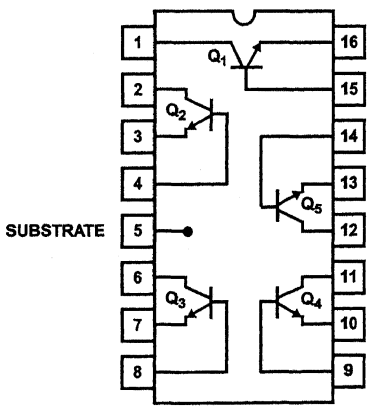

File Number 662.3

Absolute Maximum Ratings

The following ratings apply for each transistor in the device

Collector-to-Emitter Voltage, V_{CEO} 15V
Collector-to-Base Voltage, V_{CBO} 20V
Collector-to-Substrate Voltage, V_{CIO} (Note 1) 20V
Collector Current, I_C 20mA

Operating Conditions

Temperature Range . . . . . -55°C to 125°C

Thermal Information

Thermal Resistance (Typical, Note 2) θ_{JA} (°C/W)
PDIP Package 90
SOIC Package 175
Maximum Power Dissipation, P_D (Any One Transistor) 85mW
Maximum Junction Temperature (Die) . . . . . 175°C
Maximum Junction Temperature (Plastic Packages) . . . . . 150°C
Maximum Storage Temperature Range . . . . . -65°C to 150°C
Maximum Lead Temperature (Soldering 10s) . . . . . 300°C
(SOIC - Lead Tips Only)

CAUTION: Stresses above those listed in "Absolute Maximum Ratings" may cause permanent damage to the device. This is a stress only rating and operation of the device at these or any other conditions above those indicated in the operational sections of this specification is not implied.

NOTES:

1. The collector of each transistor of the CA3127 is isolated from the substrate by an integral diode. The substrate (Terminal 5) must be connected to the most negative point in the external circuit to maintain isolation between transistors and to provide for normal transistor action.
2. θ_{JA} is measured with the component mounted on an evaluation PC board in free air.

Electrical Specifications $T_A = 25°C$

PARAMETER	TEST CONDITIONS		MIN	TYP	MAX	UNITS
DC CHARACTERISTICS (For Each Transistor)						
Collector-to-Base Breakdown Voltage	$I_C = 10\mu A$, $I_E = 0$		20	32	-	V
Collector-to-Emitter Breakdown Voltage	$I_C = 1mA$, $I_B = 0$		15	24	-	V
Collector-to-Substrate Breakdown-Voltage	$I_{C1} = 10\mu A$, $I_B = 0$, $I_E = 0$		20	60	-	V
Emitter-to-Base Breakdown Voltage (Note 3)	$I_E = 10\mu A$, $I_C = 0$		4	5.7	-	V
Collector-Cutoff-Current	$V_{CE} = 10V$ $I_B = 0$		-	-	0.5	µA
Collector-Cutoff-Current	$V_{CB} = 10V$, $I_E = 0$		-	-	40	nA
DC Forward-Current Transfer Ratio	$V_{CE} = 6V$	$I_C = 5mA$	35	88	-	
		$I_C = 1mA$	40	90	-	
		$I_C = 0.1mA$	35	85	-	
Base-to-Emitter Voltage	$V_{CE} = 6V$	$I_C = 5mA$	0.71	0.81	0.91	V
		$I_C = 1mA$	0.66	0.76	0.86	V
		$I_C = 0.1mA$	0.60	0.70	0.80	V
Collector-to-Emitter Saturation Voltage	$I_C = 10mA$, $I_B = 1mA$		-	0.26	0.50	V
Magnitude of Difference in V_{BE}	Q_1 and Q_2 Matched $V_{CE} = 6V$, $I_C = 1mA$		-	0.5	5	mV
Magnitude of Difference in I_B			-	0.2	3	µA
DYNAMIC CHARACTERISTICS						
Noise Figure	$f = 100kHz$, $R_S = 500\Omega$, $I_C = 1mA$		-	2.2	-	dB
Gain-Bandwidth Product	$V_{CE} = 6V$, $I_C = 5mA$		-	1.15	-	GHz
Collector-to-Base Capacitance	$V_{CB} = 6V$, $f = 1MHz$		-	See Fig. 5	-	pF
Collector-to-Substrate Capacitance	$V_{CI} = 6V$, $f = 1MHz$		-		-	pF
Emitter-to-Base Capacitance	$V_{BE} = 4V$, $f = 1MHz$		-		-	pF
Voltage Gain	$V_{CE} = 6V$, $f = 10MHz$, $R_L = 1k\Omega$, $I_C = 1mA$		-	28	-	dB
Power Gain	Cascode Configuration $f = 100MHz$, $V+ = 12V$, $I_C = 1mA$		27	30	-	dB
Noise Figure			-	3.5	-	dB
Input Resistance	Common-Emitter Configuration $V_{CE} = 6V$, $I_C = 1mA$, $f = 200$ MHz		-	400	-	Ω
Output Resistance			-	4.6	-	kΩ
Input Capacitance			-	3.7	-	pF
Output Capacitance			-	2	-	pF
Magnitude of Forward Transadmittance			-	24	-	mS

NOTE:

3. When used as a zener for reference voltage, the device must not be subjected to more than 0.1mJ of energy from any possible capacitance or electrostatic discharge in order to prevent degradation of the junction. Maximum operating zener current should be less than 10mA.